Power Quality Improvement for Distribution Systems Under Non-Linear Conditions

by

Ehab El-Sadaany

A thesis

presented to the University of Waterloo

in fulfilment of the

thesis requirement for the degree of

Doctor of Philosophy

in

Electrical Engineering

Waterloo, Ontario, Canada, 1998

©Ehab El-Sadaany 1998

National Library of Canada
Bibliothèque nationale du Canada

Acquisitions and Bibliographic Services
Acquisitions et services bibliographiques

395 Wellington Street
Ottawa ON K1A 0N4
Canada

395, rue Wellington
Ottawa ON K1A 0N4
Canada

Your file Votre référence

Our file Notre référence

The author has granted a non-exclusive licence allowing the National Library of Canada to reproduce, loan, distribute or sell copies of this thesis in microform, paper or electronic formats.

L'auteur a accordé une licence non exclusive permettant à la Bibliothèque nationale du Canada de reproduire, prêter, distribuer ou vendre des copies de cette thèse sous la forme de microfiche/film, de reproduction sur papier ou sur format électronique.

The author retains ownership of the copyright in this thesis. Neither the thesis nor substantial extracts from it may be printed or otherwise reproduced without the author's permission.

L'auteur conserve la propriété du droit d'auteur qui protège cette thèse. Ni la thèse ni des extraits substantiels de celle-ci ne doivent être imprimés ou autrement reproduits sans son autorisation.

0-612-30605-4

Canada

The University of Waterloo requires the signatures of all persons using or photocopying this thesis. Please sign below, and give address and date.

Abstract

The proliferation of non-linear and electronically switched devices has increased the presence of nonsinusoidal currents and voltages in electrical distribution systems. The analysis of harmonics on the distribution systems has been described as being essential to understanding the nature of harmonic performance. One of the basic reasons for conducting a harmonic study is to analyze the effectiveness of proposed remedies to any existing harmonic problem. The analysis and design of any mitigation equipment requires precise calculation of both voltage and current waveforms. Moreover, the parameters that affect the harmonic performance have to be accurately identified and examined.

This thesis offers a new time-domain based approach for the determination of both voltage and current waveforms in non-linear distribution systems taking into account the interaction between both voltage and current harmonics (attenuation effect). In addition, the parameters that control the generation and propagation of harmonics into the distribution systems have been identified and investigated. A simple but efficient time-domain based technique has been developed and employed in order to estimate the combined non-linear load susceptance at different harmonic frequencies based on the previously calculated voltage and current waveforms and with the attenuation phenomenon considered. A novel design and implementation of reactance one-port compensators has been applied to reduce both voltage and current harmonic distortion levels in non-linear distribution systems. This application represents a significant contribution to distribution systems analysis as it successfully limits the system distortion. The performance of the proposed compensator is assessed by both simulation and experimental testing.

Acknowledgements

First and foremost, I would like to thank and praise *Allah* almighty, the only One *God*, for enlightening my way and directing me through each and every success I have or may reach.

I would like to express my heartfelt gratitude to my supervisor Professor *Magdy Salama* for his constant encouragement, support and invaluable guidance. He has shaped my view of what constitutes valuable research. He was always there when I needed him, not only at the research level, but also at the personal level.

I would also like to gratefully recognize the contribution of Professor *Aziz Chikhani* for his valuable comments on my work and his confidence in my abilities. I feel very fortunate to have worked with him.

To Professors *Abdel Rahim Badr*, *Ali Al-Kharashi* and *Metwaly Al-Sharkawy* (of Ain Shams University, Egypt), I would like to extend my sincere thanks for their wisdom and vision for encouraging and pushing me to travel and seek knowledge. They always treated me as a son, rather than just a student. May *Allah* reward them in this world and in the hereafter.

My thanks also go to members of the Electrical and Computer Engineering department, especially *Wendy Boles* for her endless support and help in solving my problems and *Gini Ivan-Roth* for her everlasting help. as well as *Cathy Seitz* and *Lynda Lang* for their support, and co-operation.

To my friends I would like to express my sincere appreciation, especially *Mohamed Khalil*, *Colleen Tcker* and Dr. *Gasser Auda* for reviewing several drafts of this dissertation and providing suggestions which helped in enhancing its presentation. I would also like to thank my friend *Ayman Elsayed* for attending many dry runs in preparation for the defense presentation of this thesis and for the fruitful discussions we had together. I would like to extend my sincere thanks to my friends Dr. *Mahmoud El-Sakka* for his support with LaTeX; his willingness to take the time to thoroughly answer my questions was greatly appreciated, Dr. *Tarek Hegazy* for his great ideas and help in preparing the defense presentation and *Mohamed Badran* for his support.

To my mother, I would like to extend my profound thanks and appreciation for her deep understanding and moral support. May *Allah* reward her in this world and in the hereafter. My wholehearted thanks go to my beloved wife *Samar Mohamed* for her love, patience, encouragement, caring and understanding. Finally, I would like to thank my beloved daughters *Mennat Allah*, *Hajar* and *Reem* for filling my life with fun and pleasantness ever since they were born.

To

my mother and the memory of my father,

my wife and my daughters,

my brother,

my parents in law,

my sister in law,

my nephews and my niece,

the rest of my family and the rest of my wife's family,

and finally

to whom it may concern.

Contents

Acknowledgements v

Dedication vi

1 Introduction 1

1.1 Thesis layout 3

2 Background 4

2.1 Basic concepts 5

2.1.1 Periodic functions 5

2.1.2 Orthogonal functions 5

2.2 Fourier series 5

2.3 Harmonic distortion indices 7

2.4 Harmonic sources 8

2.4.1 Devices with non-linear voltage and current relationship 8

2.4.2 Devices involving electronic switching 9

2.5 Harmonic effects 10

2.6 Harmonic distortion evaluation 12

2.6.1 Models for network components 15

2.6.2 Techniques for harmonic analysis 19
2.7 Summary 23

3 Power Definitions and Harmonic Mitigation **24**
3.1 Preamble 24
3.2 Powers in sinusoidal situations 25
3.3 Powers under non-sinusoidal conditions 26
3.3.1 Frequency-domain approach 27
3.3.2 Time-domain approach 31
3.3.3 Discussion 33
3.4 Harmonic mitigation 34
3.4.1 Power electronic solutions 35
3.4.2 Passive solutions 36
3.4.3 Discussion 39
3.5 Assessment 40

4 Attenuation Phenomenon **42**
4.1 Introduction 42
4.2 Motivation 43
4.3 Proposed methodology 45
4.3.1 Approach 46
4.4 Work strategy 50
4.5 Harmonic sources models 51
4.5.1 Group #1 load model 51
4.5.2 Group #2 load model 52
4.5.3 Group #3 load model 54
4.6 Method of analysis 56

4.7 Simulation results 58
4.8 Experimental verification 62
4.9 Assessment 63

5 Effect of Different System Parameters on Distribution System Harmonic Levels 65

5.1 Introduction 66
5.2 Secondary distribution feeder description 67
5.3 Simulation method 69
5.4 Simulation results 70
5.4.1 Diversity due to phase angle dispersion 70
5.4.2 Effect of changing the source impedance X/R ratio 75
5.4.3 Effect of changing the loading level 76
5.4.4 Effect of load combination 85
5.4.5 Effect of changing the load position 87
5.5 Physical experiment 88
5.5.1 Loading level effect 89
5.5.2 Combination effect 89
5.6 Assessment 92

6 Neutral Current Harmonics in Three-Phase Four-Wire Distribution System 96

6.1 Introduction 96
6.2 Three-phase four-wire system 99
6.3 Simulation method 100
6.4 Simulation results 101
6.4.1 Attenuation effect 101

6.4.2 Effect of loading level 103
6.4.3 Effect of load combination 108
6.4.4 Effect of system unbalance 110
6.5 Assessment 113

7 Harmonic Mitigation Using Reactance One-Port Networks 116
7.1 Introduction 117
7.2 Equivalent load susceptance calculation 121
7.3 Reactive power compensation 123
7.3.1 One-port network synthesis 125
7.4 Simulation results 129
7.4.1 Numerical example 130
7.4.2 PAVC load 131
7.4.3 Three-phase four-wire circuit 134
7.4.4 Test distribution system 137
7.5 Experimental verification 143
7.6 Sensitivity analysis 147
7.6.1 Sensitivity to filter elements variation 151
7.6.2 Sensitivity to load level variation 152
7.7 Assessment 154

8 Conclusions and Future Research 156
8.1 Contributions 159
8.2 Future investigations 160

A Instantaneous Power Components 161

B Experimental Setup 164

C IEEE Recommended Standreds (IEEEstd-519) **167**

C.1 Current distortion limits 168

C.2 Limits on commutation notches 168

C.3 Voltage distortion limits 169

D FILTER COMPONENTS **170**

Bibliography **172**

List of Tables

4.1 THDI with and without attenuation effect for different loads 62

4.2 Net harmonic currents for different non-linear loads 63

5.1 Secondary distribution feeder data 67

5.2 Net harmonic currents for different system conditions 73

5.3 System distortion level as affected by the source impedance X/R ratio . . 78

5.4 Current harmonics variation as affected by constant loading level DBR units 83

5.5 Current harmonics variation as affected by variable loading level DBR units 84

5.6 Current harmonics variation as affected by constant loading level DBR units 85

5.7 Current harmonics variation as affected by variable loading level DBR units 86

5.8 Different system configuration for load position interchanging study . . . 87

5.9 Effect of interchanging load position on the distribution system distortion level 88

5.10 Simulation and experimental net harmonic currents generated by DBR loads 90

6.1 Phase and neutral current harmonics without attenuation effect 102

6.2 Phase and neutral current harmonics with attenuation effect 102

6.3 Effect of changing the loading level of DBR units arranged in three-phase balanced configuration on neutral current 105

6.4 Effect of varying the number of DBR units on the neutral current, NEV and phase current harmonic contents 106
6.5 Effect of combining different loads on both neutral current and system THD 109
6.6 Phase and neutral current harmonics in balanced and unbalanced three-phase four-wire system 112
6.7 Neutral triplen and non-triplen harmonic currents share in the total neutral current in balanced and unbalanced cases 113

7.1 RMS and THD values for phase voltage, phase current and neutral current in 3-phase system having DBR and CFL load combination before and after compensation 138
7.2 Current and voltage THD values corresponding to compensator inductive and capacitive elements variation of 3%. 152
7.3 Current and voltage THD values corresponding to compensator inductive and capacitive elements variation of 5%. 153
7.4 Current and voltage THD values corresponding to loading level variation 154

C.1 Basis for harmonic current limits 167
C.2 Current distortion limits for general distribution systems (120 V $\rightarrow$ 69 KV) 168
C.3 Low-Voltage system classification and distortion limits 169
C.4 Voltage distortion limits 169

D.1 Components ratings and manufacturer 170

List of Figures

2.1 Single-phase power converter equivalent circuit 10

2.2 Three-phase power converter equivalent circuit 11

2.3 General passive load model 16

2.4 General transformer model for harmonic studies 18

2.5 Overhead and underground lines model 19

3.1 Application of an active filter at a non-linear load 36

3.2 Common tuned passive filter configurations 38

4.1 Different linear and non-linear loads sharing the same supply impedance . 47

4.2 Iterative approach flow chart 49

4.3 Voltage-Current characteristics for CFL load 52

4.4 Single-phase, magnetic ballast CFL load model 53

4.5 The current waveform for CFL load 53

4.6 The harmonic contents for CFL load 53

4.7 Single-phase DBR load model 55

4.8 The current waveform for DBR load 55

4.9 The harmonic contents for DBR load 55

4.10 Single-phase PAVC load model 57

4.11 The current waveform for PAVC load 57
4.12 The harmonic contents for PAVC load 57
4.13 Load voltage waveform with and without attenuation for CFL load 59
4.14 Supply current waveform with and without attenuation for CFL load . . . 59
4.15 Reduction in current harmonics due to attenuation effect in CFL loads . . 59
4.16 Load voltage waveform with and without attenuation for DBR load . . . 60
4.17 Supply current waveform with and without attenuation for DBR load . . 60
4.18 Reduction in current harmonics due to attenuation effect in DBR loads . 60
4.19 Load voltage waveform with and without attenuation for PAVC load . . . 61
4.20 Supply current waveform with and without attenuation for PAVC load . . 61
4.21 Reduction in current harmonics due to attenuation effect in PAVC loads . 61

5.1 The secondary distribution feeder under study 68
5.2 N identical loads sharing the same supply 72
5.3 Diversity factors for different current harmonics 73
5.4 3rd, 5th, 7th, and 9th harmonic currents for different condition 74
5.5 11th, 13th, and 15th harmonic currents for different condition 74
5.6 3rd, 5th, 7th, and 9th harmonic currents for different X/R ratios 77
5.7 11th, 13th, and 15th harmonic currents for different X/R ratios 77
5.8 Current and voltage total harmonic distortion factors for different X/R ratios 78
5.9 Variation of a DBR unit input current waveform with the change of percentage loading 80
5.10 3rd, 5th, $and 7^{th}$ harmonic currents for different loading levels of single DBR unit 81
5.11 9th, 11th, 13th, and 15th harmonic currents for different loading levels of single DBR unit 81

5.12 Variation of current THD as affected by increasing the number of DBR load units 82
5.13 Variation of voltage THD as affected by increasing the number of DBR load units 82
5.14 Current and voltage total harmonic distortion factors as affected by combining different loads 86
5.15 Voltage waveform for different CFL load percentage obtained experimentally 90
5.16 Current waveform for different CFL load percentage obtained experimentally 91
5.17 Reduction in current harmonics due to varying the loading level of CFL load; experimental results 91
5.18 Reduction in the system THDI due to combining different loads; experimental result 93
5.19 Reduction in current harmonics due to changing the percentage sharing among load combination; experimental result 93

6.1 Three-phase four-wire balanced system 99
6.2 Neutral current waveform with and without attenuation effect 103
6.3 Variation of neutral current magnitude with the change in the DBR unit loading level 104
6.4 The variation of the 3rd, 5th, and 7th harmonic currents with the number of DBR units 107
6.5 The variation of the 9th, 11th *and* 13th harmonic currents with the number of DBR units 107
6.6 Neutral to earth voltage variation with changing the number of DBR units 108
6.7 3rd, 5th, and 7th harmonic currents contents due to different combination percentages 110

6.8 9th, 11th, 13th, and 15th harmonic contents due to different combination percentages 111
6.9 Different harmonic currents contribution to the neutral current in both balanced and unbalanced case 114

7.1 Flow chart describing the non-linear load susceptance calculation 124
7.2 Plot of the compensator susceptance locus for 1st, 3rd *and* 5th harmonic reactive power compensation 126
7.3 One-port compensator for inductive loads harmonic reactive power compensation 127
7.4 One-port compensator for capacitive loads harmonic reactive power compensation 129
7.5 One-port compensator for DBR load reactive power compensation 132
7.6 Supply current of circuit having DBR load before and after compensation 132
7.7 Load voltage of circuit having DBR load before and after compensation . 133
7.8 Net harmonic currents for DBR load with and without reactance one-port compensator 133
7.9 One-port compensator for PAVC load reactive power compensation 135
7.10 Supply current of circuit having PAVC load before and after compensation 135
7.11 Load voltage of circuit having PAVC load before and after compensation . 136
7.12 Net harmonic currents for PAVC load with and without reactance one-port compensator 136
7.13 One-port compensator for three-phase four-wire system loaded with DBR and CFL load combination reactive power compensation 138
7.14 Phase current of 3-phase system having DBR and CFL load combination before and after compensation 139

7.15 Phase voltage of 3-phase system having DBR and CFL load combination before and after compensation 139
7.16 Neutral current of 3-phase system having DBR and CFL load combination before and after compensation 140
7.17 Phase current harmonic contents for 3-phase system having DBR and CFL load combination with and without reactance one-port compensator . . . 140
7.18 Test secondary distribution system to examine the reactance one-port compensator performance 141
7.19 1st stage One-port compensator for test system reactive power compensation 142
7.20 2nd stage One-port compensator for test system reactive power compensation 143
7.21 Combined reactance one-port compensator for test system reactive power compensation 144
7.22 Supply current of the test distribution system before and after compensation 145
7.23 Load voltage of the test distribution system before and after compensation 145
7.24 Supply current harmonic contents for the test distribution system before and after compensation 146
7.25 Test distribution system point of common coupling voltage harmonic contents before and after compensation 146
7.26 Supply current of circuit having DBR load before and after compensation, as obtained experimentally 148
7.27 Load voltage of circuit having DBR load before and after compensation, as obtained experimentally 148
7.28 Phase current of three-phase circuit having DBR and CFL combination before and after compensation, as obtained experimentally 149
7.29 Phase voltage of three-phase circuit having DBR and CFL combination before and after compensation, as obtained experimentally 149

7.30 Neutral current of three-phase circuit having DBR and CFL combination before and after compensation, as obtained experimentally 150

A.1 In-phase current and the unidirectional power P_p 163

A.2 Reactive current and the double frequency power oscillations 163

Chapter 1

Introduction

Power quality has become an important concern for utility, facility and electric engineers in recent years. Power quality variations fall into two basic categories: the first is disturbances that include transient voltages, voltage sags and interruptions; the second is the steady state variations which include voltage variations and harmonics. To some, harmonic distortion is still considered to be the most significant power quality problem.

Harmonic studies have become an important component of distribution systems analysis and design [1], given the ever-growing presence of harmonic producing devices. These studies are used to quantify the distortion levels in voltage and current waveforms at various points within distribution systems and to study how these levels might be reduced. The current emphasis on power quality [2] has reinforced the need for harmonic studies as a standard component of distribution systems analysis.

Supply authorities, who are responsible for the integrity of the supply, are concerned with this harmonic distortion, and have developed various harmonic standards [3, 4] to limit the distortion at the point of common coupling PCC between the load and the supply system. If both voltage and current harmonic distortion levels are not within these limits, the system performance can be improved by installing harmonic filters.

Until recently, electrical engineers involved in research on distribution systems harmonic analysis have differed substantionally in their approach to the evaluation of the system harmonic distortion levels. The difficulties in performing this task include the non-linearity of harmonics [5], the voltage and frequency dependency of distribution system loads [6, 7] and the diversity between harmonic currents injected by different non-linear loads [8]. The assessment of harmonic distortion in any system requires the identification of the major harmonic producing devices in that system, the accurate determination of both the magnitudes and phase angles of the injected harmonic currents and the analysis of the harmonic propagation in the system [9, 10].

Most harmonic analysis are performed using steady state, linear circuit solution techniques. The harmonic current produced by non-linear components are normally derived on the assumption of a strong (or perfect) sinusoidal voltage supply [11]. These nominal harmonic currents are then injected (injection sources) into an AC linear network to determine the level of voltage distortion. This procedure implies that the interaction between voltage and current harmonics (attenuation effect) is neglected. Unfortunately, this is not a valid assumption in most distribution systems. When the amount of harmonic currents injected into the system is high and the AC system harmonic impedances are large, the load voltage waveform will not be perfectly sinusoidal. Therefore, the derivation of the injected harmonic currents requires an iterative algorithm.

Adding filters for harmonic distortion reduction is a common way to cut harmonic-related losses, protect the system and enhance the performance of the distribution system. However, the filter type, the installation location and the load and source characteristics are all critical to the achievement of the desired performance [12]. Although several passive and active filters have been proposed in the literature for the purpose of improving distribution system performance [13–15], the reactance one-port compensator has attracted much attention for its effectiveness and low cost [16]. To date, however, this

compensation technique has only been applied to linear circuits fed from a periodical non sinusoidal voltage supply.

This thesis is divided into two main parts: determining the accurate voltage and current waveforms in distribution systems with differing types of non-linear loads, while taking into account the attenuation effect, constitute the first part of this thesis; the second part deals with the utilization of the obtained voltage and current waveforms to design a reactance one-port compensator capable of reducing the harmonic distortion levels of both voltage and current in non-linear distribution systems.

1.1 Thesis layout

Chapter 2 presents an extensive survey on harmonics, its sources, effects and methods of analysis. In Chapter 3 the different techniques utilized in defining the powers under non sinusoidal conditions are reviewed. Moreover, a survey of different methods that mitigate harmonic distortion are presented. Chapter 4 describes the technique that is utilized in acquiring the voltage and current waveforms while considering the attenuation effect. Simulation and experimental verification are also presented here. The parameters that affect the harmonic performance of distribution system loads are examined in Chapter 5 while in Chapter 6 the neutral current generation and control in balanced and unbalanced three-phase four-wire distribution systems is investigated. Chapter 7 presents the design algorithm for the reactance one-port compensator along with experimental results aimed to support the simulation outcome. Finally, Chapter 8 offers the main conclusions of this work and suggests subjects for future research.

Chapter 2

Background

In this chapter, the theoretical aspects of distribution system harmonic generation and its effects are discussed. Different system components and load models are presented and various techniques for analyzing harmonics on distribution system are reviewed. Some basic concepts are introduced in Section 2.1 while Section 2.2 presents the basics of Fourier analysis. Section 2.3 highlights the different harmonic indices used to reflect the harmonic distortion levels. The main sources of harmonic distortion in distribution systems are surveyed in Section 2.4. The effect of harmonics are listed in Section 2.5 and Section 2.6 describes the recommended procedure for the analysis of distribution system harmonics along with the typical models of system components and the different methodologies for harmonic analysis. Finally, this chapter is summarized in Section 2.7.

2.1 Basic concepts

2.1.1 Periodic functions

A function $x(t)$ is called periodic if it is defined for all real t and if there is some positive number T such that

$$x(t+T) = x(t), \qquad \forall \ t, \tag{2.1}$$

where T is called the period of the function.

2.1.2 Orthogonal functions

Two non-zero functions $x_1(t)$ and $x_2(t)$ are considered orthogonal over an interval $T_1 \rightarrow T_2$ if

$$\int_{T_1}^{T_2} x_1(t)x_2(t)dt \ = \ 0. \tag{2.2}$$

Furthermore, a set of r functions $\{x_1(t), x_2(t), ..., x_r(t)\}$ form an orthogonal set over the interval $T_1 \rightarrow T_2$ if

$$\int_{T_1}^{T_2} x_i(t)x_j(t)dt \ = \ 0, \ \text{ for } \ i = 1 \text{ to } r, \ \ j = 1 \text{ to } r, \ \ i \neq j. \tag{2.3}$$

2.2 Fourier series

The Fourier expansion of a signal generates the best fit to that signal in terms of the selected fundamental frequency (lowest frequency of the expansion) and integer multiples (harmonics) of that frequency. Under steady state conditions, periodically distorted waveforms can be expressed in the form of Fourier series. The Fourier series of a periodic function $x(t)$, with fundamental frequency ω and periodic time $T = \frac{2\pi}{\omega}$, has the

expression:

$$x(t) = a_o + \sum_{n=1}^{\infty}(a_n \cos(n\omega t) + b_n \sin(n\omega t)). \tag{2.4}$$

In this expression, a_o is the average value of the function $x(t)$,where,

$$a_o = \frac{1}{T}\int_{-\frac{T}{2}}^{\frac{T}{2}} x(t)\, dt. \tag{2.5}$$

The series coefficients, a_n and b_n are the rectangular components of the nth harmonic. The corresponding n^{th} harmonic vector is:

$$\acute{A}_n \angle\phi_n = a_n + jb_n, \tag{2.6}$$

with a magnitude of

$$A_n = \sqrt{(a_n^2 + b_n^2)}. \tag{2.7}$$

and a phase angle ϕ_n, where,

$$\phi_n = \tan^{-1}(\frac{b_n}{a_n}). \tag{2.8}$$

The RMS value of the function $x(t)$ is defined as:

$$RMS = \sqrt{a_o + \sum_{n=1}^{\infty}\frac{1}{2}A_n^2}. \tag{2.9}$$

In distribution systems, devices that produce distortion exhibit a non-linear relationship between voltage and current. Such non-linear relationship may lead to the following forms of distortion [17]:

1. A periodic steady state exists while the distorted waveform can be expressed as a Fourier series with a fundamental frequency equal to the power frequency. This is the common case in distribution system harmonic studies. There are several advantages gained by decomposing the distorted waveform in terms of its harmonic contents. The frequency domain can be used to study the propagation of each harmonic independently. Consequences, such as losses, can be related to the harmonic components and measures of waveform quality can be developed in terms of the harmonic amplitudes.

2. A periodic steady state exists and the distorted waveforms can be expressed as Fourier series with a fundamental frequency that is sub-multiples or sub-harmonics (of the base frequency) as long as they are less than the base frequency. In case they are above the base frequency, the fundamental frequency will be fractional multiples or inter-harmonics. Some types of pulsed or modulated loads and integral cycle controllers can create waveforms that correspond to this category.

3. The waveform is non-periodic or is not related to the power system frequency.

2.3 Harmonic distortion indices

There are several measures available for indicating the harmonic contents of a waveform with a single number. The most common measure of deviation of a periodic waveform from a sinusoidal wave is called Total Harmonic Distortion (THD). It can be calculated for either voltage or current. The THD is given as:

$$THD = 100 \frac{\sqrt{\sum_{n=2}^{N} M_n^2}}{M_1}. \tag{2.10}$$

where M_n is the RMS value of harmonic components n of the quantity M, and M_1 is the RMS value of the fundamental component. The THD is a measure of the effective value of the harmonic components of a distorted waveform, that is, the potential heating value of the harmonic relative to the fundamental. IEEE standard 519 [3] specifies limits on voltage and current THD for low, medium and high voltage.

Several other distortion indices are defined in [3], each intended to capture a specific impact of harmonics. The Telephone Influence Factor (TIF), the C-message weighted indices, the $V.T$ product and the $I.T$ product are used to measure telephone interference. The K-factor index is used to describe the impact of harmonics on losses and is useful in derating equipment such as transformers [18].

2.4 Harmonic sources

There are two main sources of harmonics in a conventional distribution system. The first source include devices that exhibit a non-linear relationship between voltage and current; and the second source includes those devices which involve electronic switching.

2.4.1 Devices with non-linear voltage and current relationship

Iron-core reactors are typical example of such devices. The most common sources in this category are transformers (due to their non-linear magnetization characteristics and overexcitation), fluorescent and other gas discharge (Neon, Mercury, Sodium,..,etc.) lighting and arc-furnaces. In all cases, there exists a non-linear relationship between voltage and current. In devices such as core and coil ballasted fluorescent lights, the voltage-current relationship can be relatively constant over some range of excitation. On the other hand, in the case of transformers, this relationship is demonstrated to be much more complex once the hysteresis characteristics of the magnetic material are considered.

The harmonic currents generated by these devices are greatly affected by the waveform and the peak value of supply voltages. It is, therefore, desirable to represent these devices with their actual non-linear V-I characteristics in harmonic studies, instead of voltage independent harmonic current sources [19].

2.4.2 Devices involving electronic switching

Static power converters are typical examples of such devices. They synchronize their switching to zero-crossing of the AC voltage or its fundamental component. Generally, a periodic steady state exists. Under ideal conditions, devices switch in an identical manner in the positive and negative half cycles and thus, only odd-harmonic components exist. Compared to the non-linear V-I devices, harmonic currents generated from converters are less sensitive to supply voltage distortion. However, the phase angles of the generated currents are functions of the supply voltage phase angle. Typical devices utilizing line-commutated solid state converters include static VAR compensator, adjustable speed drives and DC drives.

Single-phase static power converter

Direct current power for modern electronic and microprocessor-based equipment is commonly derived from a single-phase full-wave diode bridge rectifier which is shown in Figure 2.1. The input AC current to the power supply comes in very short pulses as the capacitor, C, regains its charge on each half cycle. The spectrum consists of all odd-harmonics with magnitudes depending on the shape of the pulse [20, 21]. These devices exist in large numbers in typical distribution systems and therefore, the collective effect of such devices is of great interest [22, 23].

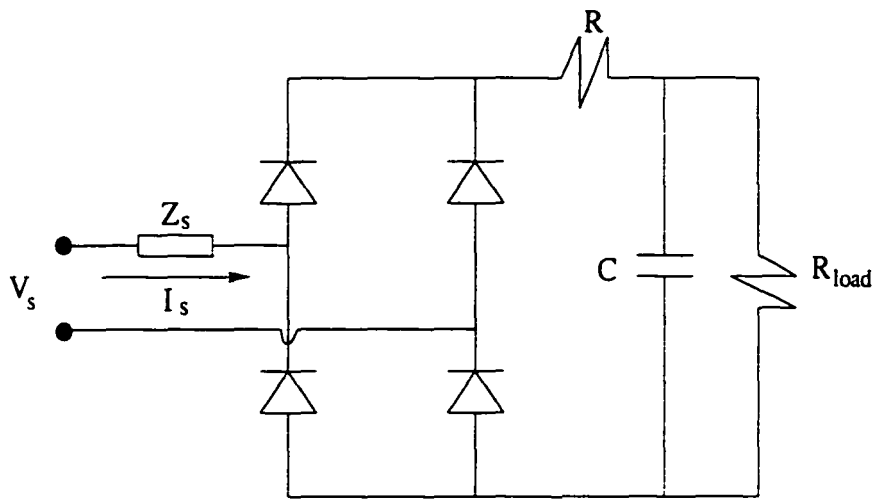

Figure 2.1: Single-phase power converter equivalent circuit

Three-phase static power converter

The most common form of three-phase static power converters is the six-pulse bridge rectifier. It is widely used in adjustable speed drives and DC drives. The nature of the bridge connection precludes the generation of zero sequence harmonics (triplen harmonics) from the converter, even when the supply voltage is unbalanced or distorted. Although the DC drives and the adjustable speed drives are equipped with a similar bridge converter front-end, the harmonic currents generated by these devices differ significantly due to the variation of the DC link designs [24]. In the case of DC drives, the DC motor inductance is used for current smoothing [25]. While, most adjustable speed drives have a large capacitor in the DC link [26]. This capacitor amplifies the DC link current ripples resulting in a higher harmonic levels. The circuit diagram for this converter is given in Figure 2.2.

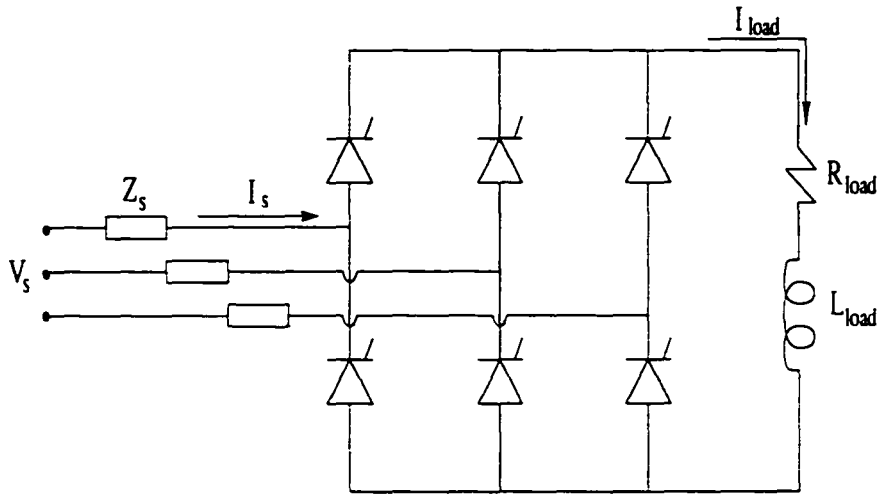

Figure 2.2: Three-phase power converter equivalent circuit

2.5 Harmonic effects

Harmonic distortion has several detrimental effects [27–32], including:

1. Overheating of conductors due to skin and proximity effects;
2. Prolonged circuit breaker interruption that leads to delayed fault current dissipation and causes re-ignition after fast re-closure;
3. Capacitor bank failure due to dielectric breakdown or reactive power overload;
4. Excessive heating and mechanical insulation stresses in transformers due to the frequency dependent core;
5. Overheating, pulsating torque and noise in electrical machines;
6. Unpredictable behavior of relays and other protection devices;
7. Over-voltages and excessive currents on the system from resonance to harmonic voltages or currents on the network;

8. Errors in meter readings;
9. Dielectric breakdown in insulated cables resulting from harmonic over-voltages;
10. Abnormally high currents on the neutral conductor of three-phase four-wire systems feeding single-phase non-linear loads;
11. Elevating the neutral to earth voltage and the electro-magnetic forces;
12. Interference with large motor controllers and power plant excitation system;
13. Unstable operation of firing circuits based on zero crossing detecting;
14. Interference with ripple control and power-line carrier system, and
15. Inductive interference with communication systems.

2.6 Harmonic distortion evaluation

Harmonic studies have become an important component of power system analysis and design. They are used to quantify the distortion in voltage and current waveforms at various points in a power system and to determine whether dangerous resonant conditions exist and how they might be mitigated. The current emphasis on power quality [2] has reinforced the need for harmonic studies as a standard component of power system analysis.

A general harmonic analysis procedure should be adopted whenever large harmonic sources exist in a system or when future harmonic pollution is expected out of further system expansion. The harmonic analysis procedure is becoming an increasingly important part of the general design process due to the growing level of harmonic generation associated with normal system loads.

The following is a proposal for a comprehensive procedure for performing a power system harmonic study.

I. Determination of harmonic analysis goals: This is important to keep the investigation on track. Some possible objectives:

1. Characterizing existing harmonic levels;
2. Identifying and evaluating the case of an existing problem that might be related to harmonic distortion;
3. Evaluating the impact of new harmonic producing loads, devices or dispersed generators on the system, and
4. Designing harmonic mitigation equipment.

II. Developing loads and system models: Modelling power system components in a fashion suitable for handling waveform characteristics of switched loads, impulses, notches and other high frequency phenomenon is the key for any successful power system harmonic study. The main tradeoff is computational complexity versus details and accuracy.

The models should be developed in either the time-domain or the frequency-domain in order to study the harmonic effects on these components or to include these components as harmonic sources in harmonic studies.

III. Performing pre-measurement simulations: Measurements are expensive in terms of time, equipment and possible disruption of plant operations. It is economically useful to have a good idea about what to look for and where to look for it before entering the facility. Simulations can be developed based on the best information available.

IV. Performing harmonic measurements: Often measurements will be needed for one of the following reasons:

1. To characterize sources of harmonics and system bus distortion; or
2. To validate simulation models.

V. Performing detailed simulation: Detailed simulations should utilize any measurement results for model validation and then should expand beyond the specific system conditions associated with the field test. All possible system configurations and load conditions can thus be studied and evaluated. The simulations should expand on the measurements in several ways:

1. Analyzing different system conditions;
2. Determining the effect of new harmonic sources on the system; and
3. Simulating equipment parameters and operating procedures for harmonic control.

VI. Developing solutions to harmonic problems: Simulations are used to develop solutions for any potential harmonic problems and to investigate possible adverse system interactions. The sensitivity of the results to important variables are also checked.

VII. Verification of system performance: After the installation of the proposed solution, monitoring can be carried out to verify the correct operation of the system.

Admittedly, it is not always possible to perform each of these steps to the ideal extent. The most frequently omitted steps are measurement steps due to the high cost involved. Since modelling different system components is the core of any harmonic study, more light will be shed on this phase in the next subsection.

2.6.1 Models for network components

In performing distribution system harmonic analysis, models must be developed for all pertinent system components, including overhead lines, underground cables, distribution transformers and load devices. Over the last three decades, much research has been focusing on the subject of system components modelling [33–48]. This subsection will summarize the typical representations of common network components for harmonic analysis.

Load model

There are two basic approaches to obtaining data on composite load characteristics. The first is to directly measure the voltage and frequency sensitivity of the load P and Q at representative substations and feeders [41]. The second is to build up a composite load model from the mix of load classes served by a substation, the composition of each class and the typical characteristics of each load component [48]. Ideally, since these techniques are complementary, both should be used in order to better understand and predict the load characteristics under varying conditions.

1. **Measurement-based data**

   Data for modelling can be obtained by installing measurement and data acquisition devices at the points where the bus load is to be represented. These devices must measure voltage, frequency variations and the corresponding variation in active and reactive power. The advantage of this approach is that it allows the researcher to obtain data directly from the actual system. Unfortunately, the data gathered at one location might not be applicable to other locations therefore, assigning the characteristics over a wide range of voltages and frequencies may be impractical.

2. **Component-based data**

   In this approach, the load model is developed by aggregating models of the individual components forming the load. This method has the advantages of not requiring field measurements and of being adaptive to different systems and conditions. Its main drawback, though, is the need to gather load class mix and perhaps load composition data, neither of which are always readily available. A general model for passive loads is given in Figure 2.3.

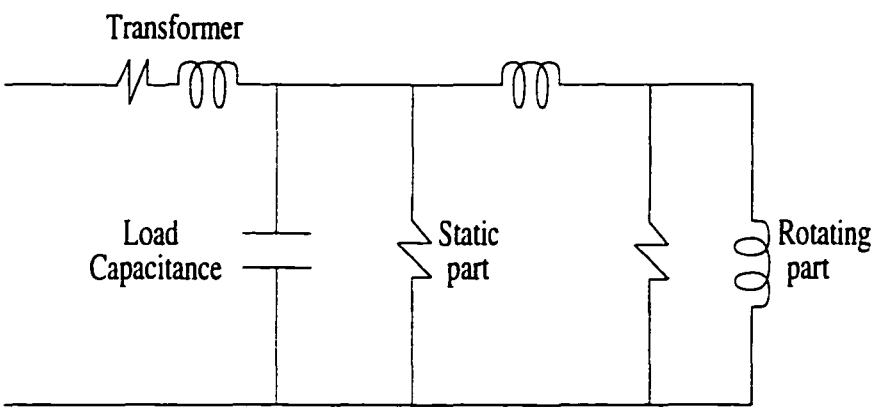

Figure 2.3: General passive load mode!

Rotating machines model

In synchronous and induction machines, the rotating magnetic field, created by stator harmonics, has a speed significantly higher than the rotor magnetic field which rotates with the synchronous speed. Therefore, at harmonic frequencies, the stator impedance approaches the negative sequence impedance. In the case of synchronous machines, the inductance is usually taken to be either the negative sequence impedance or the average of the direct and quadrature subtransient impedances. For induction machines, the inductance is taken to be the locked-rotor inductance. In each case the significance of the

frequency dependency of the resistance is due to the skin effect and the eddy current. An accurate machine model has been proposed in [43].

Transformer model

A general model for a transformer that is adequate for harmonic analysis is shown in Figure 2.4. R_m is a constant resistance that accounts for the core losses. R_i and L_i represent the winding resistance and leakage reactance, respectively. Resistance R_{pi} is used to represent the frequency dependent characteristics of short circuit resistance and inductance. The current source is used to represent the harmonic generating effects of the magnetizing branch and its value is determined from the flux–current curve and the supply voltage.

Short circuit impedance, magnetizing characteristics and winding connections are some characteristics of transformers that affect harmonic flows. Although both the resistance and inductance of the transformer short circuit impedance are frequency dependent, modelling them as constant R and L is generally acceptable for a typical harmonic study. This is acceptable because the frequency-dependent effects are insignificant for the harmonic frequencies of common interest and including the saturation characteristics is important only when the harmonics generated by the transformer is of primary concern.

Since transformers can give a ± 30 degree phase shift to harmonic voltages and currents, modelling phase-shifting effects is essential especially if there is more than one harmonic source in the system. Three-phase representation automatically includes phase-shifting effects. but, for single-phase, a phase-shifter model should be used to represent this effect.

Other factors such as the non-linear resistance characteristics of the magnetization branch and the winding stray capacitance may also affect the harmonic performance of a transformer. Though for most transformers the effects of stray capacitance become

noticeable only for frequencies higher than $4kHz$.

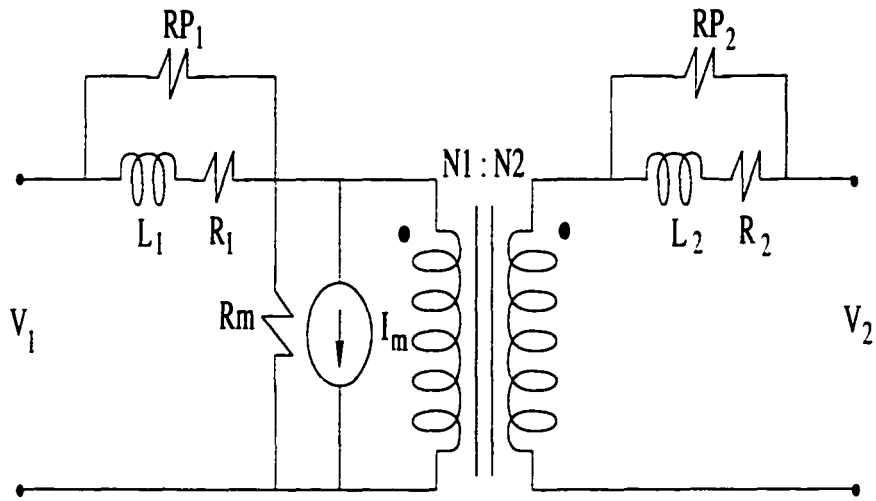

Figure 2.4: General transformer model for harmonic studies

Overhead lines and underground cables model

The modelling of transmission lines over a wide range of frequencies is relatively well documented [34]. Typical overhead lines can be modeled by a multi-phase coupled equivalent pi-circuit, as shown in Figure 2.5. For balanced harmonic analysis, the model can be further simplified into a single-phase pi-circuit determined from the positive-sequence impedance data of the line. The main concerns for modelling overhead lines are:

1. The frequency-dependency of the unit-length series impedance; and
2. The distributed-parameter nature (long-line effect) of the unit-length series impedance and shunt capacitance.

The first step in constructing the model is to compute the unit-length series impedance and shunt admittance parameters. After obtaining these parameters, matrices $[Z]$ and

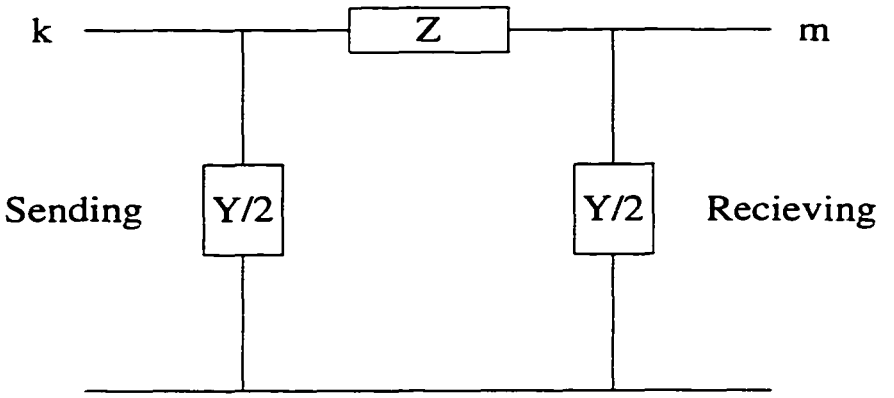

Figure 2.5: Overhead and underground lines model

$[Y]$ can be calculated by including (or not including) the long-line effects. If these effects are ignored, which is only applicable to short lines or low order harmonics, the $[Z]$ and $[Y]$ matrices are the unit-length parameters multiplied by the line length. Underground cable models are very similar to overhead line models. The difficulty for cable modelling is how to determine the unit-length parameters for a cable. Detailed description of the calculation of cable parameters is provided in [44].

2.6.2 Techniques for harmonic analysis

Harmonic analysis is used to quantify the distortion in voltage and current waveforms at various points in a distribution system and to determine whether dangerous resonance conditions exist and how they might be mitigated. These methods can be grouped in two general categories:

1. Frequency-domain methods; or
2. Time-domain methods.

This subsection reviews the techniques currently used for distribution system harmonic analysis. These techniques vary in terms of their data requirement, complexity,

problem formulation and solution algorithms.

1- Frequency-domain methods

The frequency-domain analysis methods are divided into two groups. The first group deals with linear methods. These include the frequency scan and the current injection methods. The second group, that is, the non-linear methods, include the harmonic iteration and the harmonic power flow methods.

Frequency scan method

This method calculates the frequency response of a network as seen at a particular bus or node. The input data requirements are minimized. Typically, a one-per-unit sinusoidal current (or voltage) is injected into the bus of interest and the voltage (or current) response is calculated. This calculation is repeated using discrete frequency steps throughout the frequency range of interest. Mathematically, the process is to solve the following equation:

$$[Y_n][V_n] = [I_n], \tag{2.11}$$

where $[I_n]$ is the known current vector (from current injection), $[V_n]$ is the nodal voltage to be solved and $[Y_n]$ is the system admittance matrix. The results are the positive or zero sequence driving-point impedance of the network. Frequency scan analysis is the most effective tool to detect harmonic resonance in a system.

Current injection method

This method is an expansion of the frequency scan method. Here, if more data are available on harmonic source characteristics, the one per unit injection current can be

replaced by a specific harmonic current. The current has a magnitude determined from the typical harmonic spectrum and rated load current of the harmonic-producing device under study.

Equation 2.11 is then solved only at harmonic frequencies of interest. The results are the harmonic voltages created by the harmonic producing equipment. This approach has been extended to cases with multiple harmonic sources, however, the results are approximate because the phase angles of the injection currents are set arbitrarily. Depending on the phase angles used, the effect of two harmonic sources seen at a particular bus can either add or cancel.

Due to its computational efficiency, this method can accommodate large power systems, unfortunately, modelling non-linear loads as constant harmonic current sources (under the assumption that the harmonic currents generated are independent of the voltage waveform and the system impedance) introduces inaccuracies that might be substantial.

Harmonic iteration method

In order to overcome the current injection method limitations, the harmonic-producing device is modeled as a supply voltage dependent current source. This method couples the non-linear load model with a linear model of the power system. The solution of the system is found using the coordinate method (Gauss method) [24, 49].

Harmonic voltage values are assumed at the interface bus between the power system and the load. Given these voltages and considering the load control variables, non-linear algebraic equations involving the load currents are formulated. The solution of these equations provides the electric current waveforms in an analytical form which are, then subjected to Fourier transform to drive the harmonic current phasors. Then these harmonic currents are multiplied with the power system harmonic impedances to obtain new harmonic voltages at the interface bus which are, in turn, considered for the next

iteration. The procedure is repeated until a pre-specified convergence criterion is satisfied. The poor convergence characteristics of this method, though, is a definite shortcoming.

Harmonic power flow method

Another method that takes into account the voltage-dependent nature of non-linear devices is to solve the system (Equation 2.11) and the device equation simultaneously using Newton-type algorithms [50–52]. This method generally requires the availability of the device model in a closed form or in a form in which derivatives can be efficiently computed. In theory, the convergence of this method is better than that of the harmonic iteration scheme if the iteration starting point is close to the solution point.

2- Time-domain method

Aside from the frequency-domain methods described above, some techniques have also been developed for harmonic analysis in the time-domain [53]. In the time-domain methods, the system model takes the form of differential equations. A solution is obtained by assuming a set of initial conditions and integrating the system equations over time. After the system has reached a steady state, the voltage and current waveforms of interest are subjected to Fourier analysis in order to derive the harmonic spectrum. This method is capable of simulating harmonic instability, voltage dependency and power system non-linearities. However, it is computationally demanding and practically limited to the study of small systems. Moreover, among the main disadvantages of the time-domain based approaches is the lack of load-flow constraints (such as the constant power specification at load buses) at the fundamental frequency. Electro-Magnetic Transient Program *EMTP* [54] has been used as such a tool. Complex techniques, such as the shooting method [55], have been proposed to accelerate the convergence to a steady state.

2.7 Summary

In this chapter, the basic mechanisms for generating periodic distorted waveforms from the major distribution system harmonic sources were surveyed and the different measures and indices for harmonic distortion evaluation were reviewed. Also, the detrimental effects of power system harmonics on equipment and loads were discussed and a general harmonic analysis procedure to evaluate the harmonic distortion in distribution systems was suggested. This procedure highlights the importance of accurate load modelling, harmonic measurement and detailed computer simulations in detecting the propagation of harmonics in distribution systems. Different system components and loads were presented and the various techniques currently used for power system harmonic analysis were reviewed.

Along with the customary power factor correction, voltage and current distortion compensation has become highly desirable by most utilities and customers. Therefore, the electrical quantities relevant to compensation should be clearly defined in order to make accurate measurements and manage both power quality and compensation in actual distribution networks under non-sinusoidal conditions. In the next chapter, the practical definitions for different power quantities in systems with non-sinusoidal waveforms are covered. The different techniques utilized to mitigate the distribution system harmonics and improve the power quality will also be presented.

Chapter 3

Power Definitions and Harmonic Mitigation

In this chapter, the different power definitions under non-sinusoidal conditions are discussed and the advantages and drawbacks of each are pointed out. Furthermore, the different techniques that are utilized to mitigate the harmonic distortion and improve the system power factor are reviewed.

3.1 Preamble

The real, reactive and apparent powers are the notations that are particularly well known to electrical engineers involved in the generation, transmission, distribution and utilization of electrical energy. Power properties and definitions in electrical circuits and power systems are generally settled down in situations where both voltage and current waveforms are pure sinusoidal [56]. As these waveforms differ from sinusoidal conditions, these notations become more and more blurred. Therefore, before discussing power properties in non-sinusoidal situations, it may be profitable to compile the essential properties of

the apparent, real and reactive powers for a sinusoidal waveform.

3.2 Powers in sinusoidal situations

When sinusoidal conditions prevail, the instantaneous values of both voltage and current in a single-phase circuit containing a linear RL load can be written as

$$v(t) = \sqrt{2}V\cos\omega_1 t, \ \textit{and} \quad i(t) = \sqrt{2}I\cos(\omega_1 t - \phi). \tag{3.1}$$

where, V and I are the rms values of both voltage and current, respectively, ω_1 is the frequency and ϕ is the angle between voltage and current waveforms.

The quantity defined, according to the physical definition of power, as the rate of change of energy flow $W(t)$, which flows from the source to the load, is known as the instantaneous power and is given by

$$\frac{\partial}{dt}W(t) \ = \ p(t) \ = \ v(t)i(t). \tag{3.2}$$

However, this power, being a function of time, is not a convenient measure for the description of energy flow. The decomposition of the current into real (in-phase) and reactive (quadrature) components will lead to distinctive instantaneous power components as given in (Appendix A).

The apparent power S is defined as the product of the rms voltage and the rms current at the circuit terminals. Its maximum value specifies the supply rating. The apparent power is given by

$$S \ = \ VI. \tag{3.3}$$

From Equations $A.5$ and $A.7$,

$$S^2 = P^2 + Q^2. \tag{3.4}$$

If a linear circuit consists of k parallel paths and fed from a sinusoidal supply, the total real and reactive powers (P and Q) will be given by

$$P = \sum_{k}^{n=1} P_n \,, \qquad Q = \sum_{k}^{n=1} Q_n. \tag{3.5}$$

Combining Equation 3.4 and Equation 3.5 gives:

$$S^2 = [\sum_{k}^{n=1} P_n]^2 + [\sum_{k}^{n=1} Q_n]^2. \tag{3.6}$$

It is important to note that in general,

$$S^2 \neq \sum_{k}^{n=1} S_n^2, and \tag{3.7}$$

$$S^2 \neq [\sum_{K}^{n=1} S_n]^2. \tag{3.8}$$

It should be noted, however, that the apparent power does not have any physical meaning and it can not be measured by direct instrumentation. The most common way to measure the apparent power is through the measurement of both real and reactive powers.

3.3 Powers under non-sinusoidal conditions

Power properties of electrical circuits are generally clear in situations when both voltage and current waveforms are sinusoidal. As they lose their sinusoidal shape, these notations become more ambiguous [57–62].

Although, voltage and current waveforms may differ from the sinusoidal shape for several different reasons [63, 64], the most common is the supply of different types of non-linear loads. Since these loads, and their resultant harmonics, form an increasing segment of the electric power load base, the operation under non-sinusoidal voltage and current conditions becomes a real practice.

There are many detrimental effects to injecting harmonics into the distribution system. In order to minimize these effects on the system, some form of distortion compensation is necessary where non-linear loads are coupled to the network. The control philosophy of this compensating system is still a major unsolved problem. A proper control philosophy can only be achieved if the definitions of all the components of electric power, under these non-sinusoidal conditions, prove to be accurate and have interpretation in terms of the connected load.

Electrical engineers involved in research on non-sinusoidal systems differ substantially in their approaches to defining the power quantities [65–76]. Expressing them as function of time (in the time-domain) or as function of frequency (in the frequency-domain) is the most remarkable difference. In the coming subsections, some of the most common power definitions are reviewed.

3.3.1 Frequency-domain approach

The frequency-domain approach has been widely utilized in defining the power properties in non-sinusoidal situations [65–72]. The main outline of some concepts that are used for this purpose are presented below.

Budeanu's concept

The power equation as suggested by Budeanu [65] in 1927 is the most widely recognized decomposition of apparent power. Budeanu generalized the power equation of source

in the linear circuit with sinusoidal voltage and current such that it can be applied to circuits with periodical non-sinusoidal waveform. His power equation has the form:

$$S^2 = P^2 + Q_B^2 + D_B^2, \tag{3.9}$$

with a reactive power defined as:

$$Q_B = \sum_{n=1}^{\infty} V_n I_n \sin \phi_n, \tag{3.10}$$

and distortion power defined as

$$D_B = \sqrt{S^2 - P^2 - Q_B^2}. \tag{3.11}$$

While the reactive power Q_B is interpreted as the source useless loading due to the reciprocating flow of energy, the distortion power D_B is interpreted as the loading due to the waveform distortion. However, the reciprocating flow of energy may exist in the circuit even if Budeanu's reactive power is equal to zero [77]. Moreover, it is found [77] that the distortion power is equal to zero if the waveform is sinusoidal (which is acceptable) but is also equal to zero if both voltage and current are distorted with identical waveforms. This means that the distortion power may be considered to be a measure of the current waveform distortion with respect to the voltage, but not a measure of the distortion of the waveform itself.

In summary, the Budeanu reactive and distortion powers do not possess the attributes that could be related to the power definitions in circuits with non-sinusoidal conditions. Their values do not provide the necessary information for compensator design required to improve the system supply quality.

Shephared & Zakikhani's concept

The power equation suggested by Shephared and Zakikhani [66] is based on the source current decomposition into a current i_a which is in-phase with the supply voltage and a current i_r which is shifted by $\frac{\pi}{2}$, as follows:

$$i_a = \sqrt{2}\sum_{n=1}^{\infty} I_n \cos\phi_n \cos(n\omega_1 t + \alpha_n), and \tag{3.12}$$

$$i_r = \sqrt{2}\sum_{n=1}^{\infty} I_n \sin\phi_n \sin(n\omega_1 t + \alpha_n). \tag{3.13}$$

Since these currents are mutually orthogonal, then, multiplying by the square of the voltage will result in the power equation that can be written as:

$$S^2 = S_a^2 + Q_r^2. \tag{3.14}$$

This power equation was strongly criticized because it did not contain the real power P. However, it did enable one to solve, for the first time, the problem of the source apparent power minimization by means of reactive compensator. The power S_a is not affected by such a compensator, so that any reduction of Q_r reduces the apparent power S. This is true only, however, at an ideal voltage source. But when the source has an internal inductive impedance, a series resonance may occur.

Czarnecki's concept

I. Linear circuits

Czarnecki stated that in linear circuits, the current may be nonsinusoidal only if the applied voltage is nonsinusoidal. The supply current is, hence, decomposed into three components namely real, reactive and scattered [67–70]. These currents are given as

$$i_a = \sqrt{2}Re\sum_{n=1}^{\infty} G_e V_n e^{jn\omega_1 t}, \tag{3.15}$$

$$i_r = \sqrt{2}Re\sum_{n=1}^{\infty} jB_n V_n e^{jn\omega_1 t}, and \tag{3.16}$$

$$i_s = \sqrt{2}Re\sum_{n=1}^{\infty} (G_n - G_e)V_n e^{jn\omega_1 t}. \tag{3.17}$$

where G_n is the non-linear load conductance, B_n is the non-linear load susceptance and G_e is the conductance of a fictitious resistive load that when supplied from the same supply, it absorbs the same real power as the actual load.

These three current components are mutually orthogonal, and multiplying them by the square of the voltage *rms* value will result in Czarnecki's power equation, that is:

$$S^2 = P^2 + Q_r^2 + D_s^2. \tag{3.18}$$

From the above power equation, it can be concluded [67,68] that the only two reasons for the source current *rms* value to increase above the value of the active current (which is necessary for the real power transmission) in circuits with non-sinusoidal waveforms are:

1. The reciprocating flow of energy for individual harmonics. The *rms* value of the current i_r is the only measure of this increase; and

2. The variance with frequency of the load conductance G_n around the equivalent conductance G_e, which is represented with the scattered current i_s.

II. Non-linear circuits

In non-linear circuits, the waveforms will be distorted under the influence of two sets of harmonics, one from the supply-voltage harmonics and the other is generated due to the non-linearity of the load. When this occurs, the source current will be decomposed into four components. While the first three components i_a, i_r and i_s preserve their meaning (as in linear circuits), the fourth component i_g can be interpreted as the current resulting from the presence of different harmonics in both current and voltage due to the load non-linearity.

If N_v and N_i denote the harmonic contents in both voltage and current, respectively, and M denotes the difference of the sets N_v and N_i, then:

$$i_g = \sqrt{2}Re \sum_{n \in M} I_n e^{jn\omega_1 t}. \tag{3.19}$$

The power equation can be written as:

$$S^2 = P^2 + Q_r^2 + D_s^2 + D_g^2. \tag{3.20}$$

3.3.2 Time-domain approach

The second approach used in defining the power properties in non-sinusoidal situations is the time-domain approach [73–76]. Below is a brief review of some concepts that utilize the time-domain approach.

Fryze's concept

The power equation as suggested by Fryze [73], early in 1931, was based on the supply current decomposition into two orthogonal components in the time-domain. The two current components are defined as an active current i_a that has the same waveform as

the voltage while the other component is the remaining part of the total current, that represents the useless current loading of the supply. The power equation obtained by Fryze is in the form:

$$S^2 = P^2 + Q_F^2. \tag{3.21}$$

Although Fryze defined the power quantities without using harmonic components, which is very advantageous for the purpose of instrumentation, his definition does not relate the reactive power to the load properties. Fryze's reactive power does not provide any information or data for the purpose of reactive power compensator design.

Kuster & Moore's concept

Kuster and Moore [74] used the time-domain approach to decompose the supply current into three components namely, active, inductive or capacitive reactive, and residual reactive component. The active current component i_a has the same waveform and phase as the supply voltage. On the other hand, the inductive or capacitive reactive component (i_{ql}, i_{qc}) has the same waveform and phase as that of the current in an inductor or capacitor with the same voltage across it. The residual reactive current (i_{qlr}, i_{qcr}), either inductive or capacitive, is what remains from the total current after the active and respective reactive current are subtracted. For inductive loads, capacitive improvement is possible and the power equation will be based on the current decomposition given as follows:

$$i = i_a + i_{qc} + i_{qcr}. \tag{3.22}$$

The power equation is given by:

$$S^2 = P^2 + Q_c^2 + Q_{cr}^2. \tag{3.23}$$

The residual reactive component of the current is always positive and can not be compensated by means of passive components. On the other hand, the capacitive reactive component of the current is negative, and can be completely compensated by a shunt capacitor. However, it is shown in [78] that the capacitive reactive power Q_c is equal to the maximum value of the reactive power that is reducible by a shunt capacitor, only if the source impedance is equal to zero, otherwise it may only approximate this maximum power value. If the source has an inductive impedance, the use of this quantity to improve the system power factor may lead to wrong decisions concerning optimal capacitance level.

3.3.3 Discussion

In Section 3.3, the several concepts used in defining the power quantities under non-sinusoidal conditions were reviewed. The advantages and drawbacks of each were also discussed . Two of these methods have found international recognition, namely, Budeanu's concept [65] and Kuster & Moore's [74], however, it was later found [77, 78] that even these definitions have some essential flaws.

There are two main approaches in defining the power quantities. The first is the frequency-domain approach that is based on the Fourier analysis and provides deep insight into the power properties of the non-sinusoidal power systems. It also fits very well the methods of reactance compensator and harmonic filter design.

The second approach is the time-domain which is simpler and more convenient for measurements. However, the possibility that the parameters of a shunt reactance compensator can be determined in the time-domain approach is not evident.

Among the different techniques utilizing the frequency-domain approach, Czarnecki's

concept proved to be the most suitable for defining the power components and it also provides enough information for reactance compensator design [16,79]. Thus, this concept will be adopted through out the rest of this work.

Since improving the system power quality through voltage and current harmonic compensation is one of the main goals of this study, it will be beneficial to review the common methods utilized in harmonic suppression. This will be the subject of the next section.

3.4 Harmonic mitigation

In an ideal AC power system, the voltage and frequency at the supply terminals should be constant and free from harmonics. However, due to the ever-increasing harmonic pollution in electrical power systems, this situation varies and the power transmitted with distorted waveforms reaches hundred of megawatts. Voltage and current distortion compensation is now required not only to increase the power transmission efficiency, but also to improve the power system quality [80,81].

Power quality refers to the measure, analysis and improvement of the bus voltage, usually a load bus voltage, to maintain that voltage to be sinusoidal at rated voltage and frequency. Load compensation is the management of reactive power to improve the quality of the supply in AC systems. In load compensation, the main objectives are:

1. Power factor correction; and

2. Improvement of voltage regulation.

Power factor correction is achieved by generating reactive power as close as possible to the load that requires it, rather than supplying it from the source. Most industrial loads have lagging power factor, or in other words, they absorb reactive power. The load current therefore, tends to be larger than is required to supply the real power alone. Since

the real power is the only useful power for energy conversion, then the excess load current represents a waste and minimizing it is therefore a necessity.

Compensation of the inactive power and minimization of the supply current while improving both supply power factor and system power quality can be broadly classified according to their nature in one of the two categories to be discussed in the following subsections:

3.4.1 Power electronic solutions

The most common devices in this category are active filters [82], adaptive VAR compensator [83], electronic voltage regulators and frequency discriminators. In addition to these devices, methods such as phase multiplication [84] have been used to achieve the same ends. In all cases, a switching operation of a controlled semiconductor device exists.

Active filters

Active filters are relatively new types of devices for eliminating harmonics. They are based on sophisticated power electronics devices and are much more expensive than passive filters though they can address more than one harmonic at a time. They are based on the basic idea of replacing the portion of the sinusoidal wave that is missing in the current of a non-linear load. Figure 3.1 illustrates the active filter operation concept. An electronic control monitors the line voltage and/or current, switching the power electronics very precisely to track the load current or voltage and force it to be sinusoidal.

Phase multiplication

Half-wave rectification produces even-harmonics that have a DC component that saturates transformers. While, full-wave rectifiers produce only odd-harmonics. The most

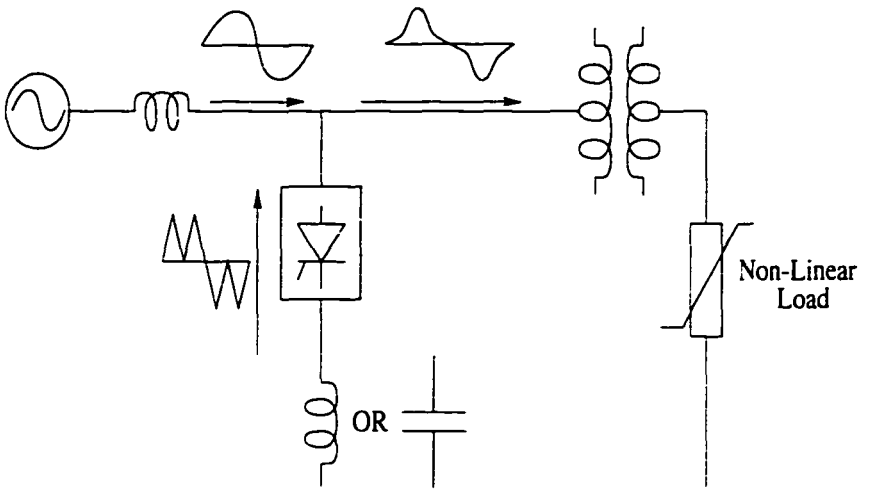

Figure 3.1: Application of an active filter at a non-linear load

common full-wave rectifiers are six-pulse converters. Harmonics can be reduced by converter phase multiplication if m six-pulse rectifier sections:

1. Have the same transformer ratio;
2. Have transformers with identical impedances;
3. Phase shifted exactly $\frac{60}{m}$ degrees from each other;
4. Are controlled at exactly the same delay angle; and
5. Share the DC load current equally.

The only harmonics present will be of the order of, $6mk \pm 1$, the characteristics harmonics. For a 12-pulse converter unit, the only harmonics present will be $11, 13, 23, 25, ...etc.$ Further pulse multiplication will reduce other harmonic currents.

3.4.2 Passive solutions

Passive filters are made of inductive, capacitive and resistive elements. They are relatively inexpensive compared to other means for eliminating harmonic distortion. They are

employed either to shunt the harmonic currents off the line or to block their flow between parts of the system. Different techniques utilizing passive solutions to improve the system power factor and reduce the harmonic levels have been suggested in the literature [12,16, 53,79,85–87]. These methods range from the simple shunt capacitor to the rigorous one-port reactance network. Descriptions of the most commonly used methods are described below.

Shunt capacitors

Compensating the reactive power in the case of linear systems is very simple and effective using shunt capacitors. The situation becomes more complicated, however, in the presence of harmonic distortion. If the supply is non-sinusoidal, but ideal (having no internal impedance), then the minimization of the source current *rms* value is usually realized by a capacitor connected in parallel to the load [74,88] and having the optimal value given by:

$$C_{opt} = -\frac{\sum_{n=1}^{\infty} nB_n V_n^2}{\omega_1 \sum_{n=1}^{\infty} n^2 V_n^2}, \tag{3.24}$$

where B_n and V_n are the load susceptance and voltage at harmonic frequencies n, respectively. However, this equation holds true only if the load current and voltage do not depend on the connected capacitance, *i.e.*, if the source impedance is equal to zero. Otherwise, Equation 3.24 does not determine the capacitance that results in the maximum value of the source power factor. When the supply has an internal inductive impedance, as in most distribution systems, resonance may occur between the source inductance and the compensating capacitance resulting in a capacitor value that differs substationally from the one calculated by Equation 3.24.

Tuned passive filter

If significant harmonic currents are generated locally by a non-linear load, tuned filters may be installed to prevent these currents from being injected into the system. Figure 3.2 illustrates the most common tuned filter arrangements.

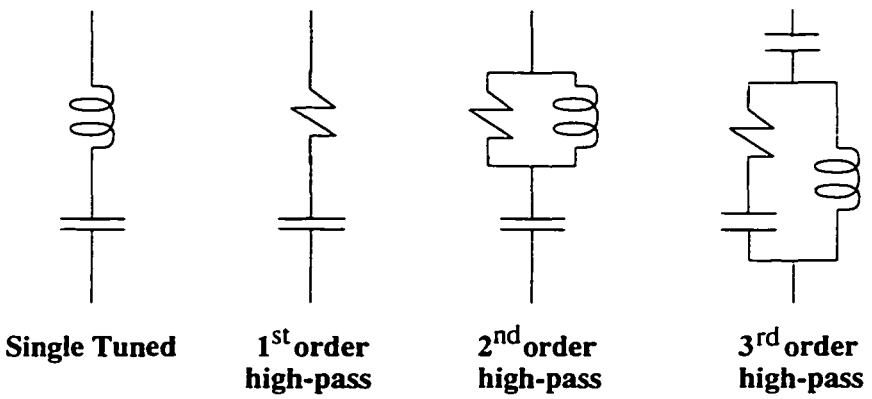

Figure 3.2: Common tuned passive filter configurations

The most common type of tuned passive filters is the single-tuned "notch" filter [53]. The notch filter is series-tuned to prevent a low impedance path to a particular harmonic current. It is connected in shunt with the power system, thus, harmonic currents are diverted from their normal flow path on the line into the filter. Notch filters can also provide power factor correction along with harmonic suppression. One important side effect of adding such a filter is that it creates a sharp parallel resonance point at frequency below the notch frequency. The resonant frequency must be safely far away from any significant harmonic frequency.

Two-element series LC compensator (TESLC)

When the harmonics are mainly caused by source distortion, they can be reduced by using a Two Element Series *LC* compensator. Such a compensator may actually have a lower total volt-ampere rating than that of a pure capacitive compensator to achieve the

same power factor [87]. The design procedure of such a compensator is widely available in the literature [79, 89]. Despite a higher power factor value, the source current harmonics in a circuit with $TESLC$ compensator are higher than they are in the non-compensated circuit. Only the fundamental current is reduced, and this comes at the expense of increasing the remaining harmonic currents. Even the fundamental reactive current will not be totally compensated.

Reactance one-port compensator

Current harmonics have a minimum value and the reactive power is totally compensated [67] if, for each harmonic n,

$$B_{xn} = - B_n. \tag{3.25}$$

where B_{xn} denotes the compensator susceptance for different harmonic frequencies n and B_n represents the load susceptances at those frequencies. This condition can not be fulfilled by a $TESLC$ compensator but require a more complex reactance one-port circuit. According to [90], the compensating one-port for M harmonics has a complexity $N = M(2M-1)$, however, it has been shown in [79], that the required complexity is much lower, not higher than $M \leq N \leq 2M - 1$. Different forms of compensator susceptances as well as structure, parameters calculation and compensator circuit design are found in [91–93].

3.4.3 Discussion

Minimization of the supply current while improving the supply quality and power factor for linear loads fed from non-sinusoidal supply can be achieved through different techniques. In this section the different methods used in improving the supply power quality

by means of either passive solutions or power electronic based solutions are reviewed.

Power electronic based equipment is composed of elements that deal with the control and restriction of electrical energy using power semiconductor devices. Thus, this equipment can either cause power quality problems or help solve them, if applied correctly. Power electronics can cause problems due to the inherent non-linearity associated with the semiconductor elements and the switching operations involved in their use. Power electronics can also provide solutions for power quality since they can be configured and controlled very precisely to mitigate voltage and current harmonics.

For passive solutions, it was shown that the shunt capacitor on its own can not perform well in the presence of distorted waveforms because of problems with resonance. The $TESLC$ compensator improves the power factor greatly, but only at the expense of increasing the current distortion even more than the un-compensated case.

Finally, the reactance one-port compensator succeeded in improving both the power factor and the current distortion level, but it was only applied to linear circuits fed from distorted supply. Furthermore, its use as a compensator may be discouraged or limited because of its complexity.

3.5 Assessment

The recent development and increasing use of power semiconductor switching devices have increased the harmonic pollution in electric distribution systems. As a result, the voltage and current waveforms have become distorted to the point where the apparent power is larger than the real power. The definition of the inactive powers under non-sinusoidal situations was discussed in this chapter using two different approaches, namely, time-domain and frequency-domain. The different techniques that are utilized to compensate the reactive power and improve the system quality under the same conditions ware also

reviewed.

The assumption of ideality with respect to the supply (that is, neglecting the source internal impedance) has lead to the faulty design of harmonic suppression devices. While it may be justifiable to overlook the variations in the fundamental bus' voltage, the failure to take note of the variations in the harmonic voltages, especially in highly distorted systems, will result in inaccuracies and a distorted view of the situation. Therefore, the variation of bus voltages and the corresponding variations in supply current harmonics should be taken into account when designing any harmonic mitigation device.

One of the salient effects of introducing the supply internal inductive impedance is the change in the shape of both load voltage and current waveforms due to the interactions between voltage and current harmonics. Thus, the thorough study of these interactions is important before it is possible to achieve any reliable compensator design. An investigation into the important parameters involved in the distribution system harmonic analysis commences in the next chapter and is continued in the subsequent chapters.

Chapter 4

Attenuation Phenomenon

This chapter discusses the proposed methodology to solve the problem at hand. An iterative technique has been developed to account for the interaction between the voltage and current harmonic. Section 4.1 will introduce the chapter. Section 4.2 describes the motivation behind the work done while Section 4.3 illustrates the proposed methodology. The working strategy employed to achieve the required results will be discussed in Section 4.4. Section 4.5 sheds some light on the non-linear load models to be utilized in this study. Section 4.6 describes the method of analysis used in this study and the simulation results are described in Section 4.7. The experimental work done to support the simulations is summarized in Section 4.8. Finally, the chapter's conclusions and summary are presented in Section 4.9.

4.1 Introduction

Both electric power utilities and end users are becoming increasingly concerned with the quality of electric power. A power quality problem, is any power problem manifested in voltage, current or frequency deviations that results in the failure or the misoperation

of customer equipment. Among the different factors that control the quality of electric power are voltage flickers, surges, transients, impulses, sags and most importantly, harmonic distortion. The assessment of the harmonic distortion in any distribution system requires the identification of the major harmonic producing loads, the determination of the magnitudes and phase angles of the injected current harmonics and the analysis of the harmonic propagation into the system. Serious concerns have been raised over the suitability and the accuracy of the available harmonic analysis methods for studying the generation and propagation of harmonic currents generated by different non-linear loads.

4.2 Motivation

Many distribution-system harmonic studies have focused on large non-linear loads, such as variable-frequency motor speed controllers, induction furnaces, railway traction and electro-platers, as the main contributors to distribution system harmonics. Recently, the proliferation of small non-linear loads within the distribution system has placed more emphasis on the effects of these loads. These small non-linear loads share some common characteristics, the most important of which are the dependency of their harmonic currents on the supply voltage waveform and the sensitivity of their generated harmonics to the distribution system configuration.

Harmonic currents generated by loads such as light dimmers, compact fluorescent lamps, computers, television sets, video recorders, battery chargers and adjustable speed drives are, individually, too small to cause any appreciable distortion in distribution feeders. As the number of these loads increase, however, the cumulative harmonics will be capable of boosting the distribution system distortion levels.

Distributed single-phase non-linear loads are usually treated as fixed harmonic-current injectors in distribution system studies [94–96]. These studies are based on the assumption

that current harmonics are a function of the fundamental current in both magnitude and phase angle, and are therefore independent of the voltage waveform and system harmonic impedance. This assumption, though, only works when the supply voltage waveform is reasonably sinusoidal. Therefore, this method will be inappropriate for non-linear loads where the harmonic currents are a strong function of harmonic voltages, since it would lead to the overestimation of the resultant harmonic distortion due to the fact that it neglects the phase angle dispersion of the individual current harmonics and fails to account for the cross-coupling between harmonics.

In an effort to overcome the limitations of the current-injection method, non-linear frequency-domain methods have been introduced. Two methods in particular have been suggested. The first couples the non-linear load model with the admittance matrix of the system to find an iterative solution. This may be referred to as the extended current-injection method or harmonic iterative method [97, 98]. The second method is the harmonic power flow technique [50, 51, 99, 100], which combines the non-linear load model with the power and volt-ampere equations of the system to find the harmonic performance in terms of specified power flows.

Although both techniques appear to be capable of incorporating general non-linear load models and take into account the effect of harmonic voltages on the generated current waveform, they each suffer from a major drawback in that they deal with each harmonic frequency independently. Consequently, the network solution is performed sequentially, for one harmonic at a time, which implies that the cross-coupling between harmonics is neglected. This results in a significant savings in computational effort, but at the expense of solution accuracy.

The dramatic increase of non-linear and electronically-switched loads has made harmonic studies more complicated. These non-linearities cause a coupling between the fundamental and harmonics so that, generally, the superposition principle can not be

applied. Therefore, using the recognized harmonic analysis methods such as the current-injection or the harmonic-iterative method, will not be general enough to accurately capture all the non-linear load characteristics. It is evident that there is a great need for a rigorous harmonic analysis method that can accurately account for both system non-linearity and voltage dependency while also addressing the cross-coupling between different harmonics. Also the analysis method should scrupulously address the variation of the parameters involved in the computation of the distribution system harmonics generated by large numbers of small non-linear loads. The development of such a method constitutes one of the major contributions of this research.

4.3 Proposed methodology

For the analysis of the system, the methodology chosen is based on the non-linear time-domain analysis. This methodology will avoid many of the approximations of the frequency-domain methods, since it will exhibit cross-coupling between harmonics. In ordinary time-domain analysis, the system and load models are written in ordinary differential equation form. The solution will be obtained by specifying a set of initial conditions for the states of the system then integrating the system equations over time. The results will include the full transient performance of the system from the initial point to the steady state. A major advantage of this is that the waveshapes and, hence an understanding of the distortion, are automatically calculated for all parts of the system.

The aforementioned algorithm, however, does not account for the interaction between the distribution system and the non-linear loads. The non-linear load, by virtue of its demand of current waveform, injects current harmonics into the distribution system. Thus, given the knowledge of the current harmonics of a non-linear load, simply solving the system equations should yield the harmonic voltage profile of the system. A flaw

in this argument, however, is that the amplitude of the current harmonics generated by non-linear loads are influenced by the AC terminal voltage. In other words, there is a strong interaction between the non-linear loads and the distribution system voltage profile. While in an ordinary time-domain method the boundary conditions are specified once and then the solution is obtained, our method proposes that an update for these boundary conditions be implemented. A one-step calculation may give approximate results, but a repetitive implementation of the algorithm, for which the interaction between the distribution system and the harmonic injecting sources is accounted for, would yield a more precise result.

The next subsection illustrates the procedure for applying the proposed iterative technique.

4.3.1 Approach

In practical distribution systems, the load voltage is not a pure sinusoid, but rather is distorted. This is due to the fact that the source inductive impedance can not be neglected. Therefore, the harmonic currents injected by different non-linear loads will create a harmonic voltage drop which will distort the load voltage. In order to account for the interactions between the continuously changing current harmonics injected by different non-linear loads and the resulting variations in the load voltage, an iterative approach is employed. This approach differs from the regular iterative approaches [97,100] in the sense that it accounts for the cross-coupling between harmonics by solving for all harmonics simultaneously. This approach is outlined in the flowchart given in Figure 4.2 and can be described by the following steps and referring to the circuit given in Figure 4.1.

Step #1 Assume an initial estimate for the load voltage at bus #2. Usually this initial assumption is set equal to the supply voltage at bus #1.

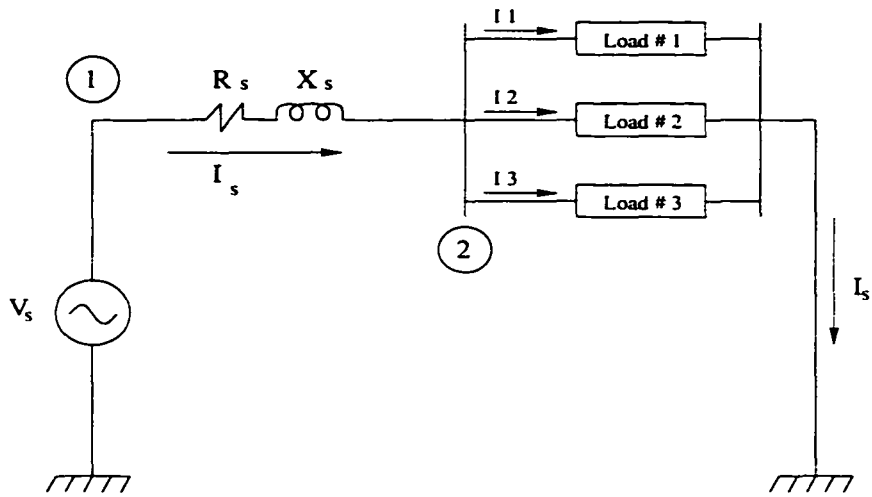

Figure 4.1: Different linear and non-linear loads sharing the same supply impedance

Step #2 Calculate the individual loads currents as well as the total supply current using the models (differential equations) built in the EMTP. The supply current will be the result of the vector summation of all the harmonic currents produced by the individual loads.

$$\vec{I}_{Sn} = \sum_{n=1}^{n} \sum_{L=1}^{k} \vec{I}_{Ln} \tag{4.1}$$

$$k = Total\ number\ of\ loads$$

$$n = Harmonic\ order$$

$$\vec{I}_{sn} = Supply\ current$$

$$\vec{I}_{Ln} = Load\ current$$

Step #3 Draw the initial load voltage and supply current waveforms. These waveforms represent the case without the voltage and current interactions.

Step #4 Using the Fast Fourier Transform FFT, calculate the harmonic contents (both magnitude and phase) of the total supply current (I_s) flowing through the source impedance ($\vec{I}_{sn}$, $n = 1, 2, 3, .., n$).

Step #5 Calculate the harmonic voltage drop on the supply inductive impedance.

$$\sum_{n=1}^{n} \vec{V}_{dn} = \sum_{n=1}^{n} \vec{I}_n \, Z_{sn} \tag{4.2}$$

Step #6 Calculate the new load voltage by subtracting the harmonic voltage drop on the supply impedance from the original supply voltage.

$$\sum_{n=1}^{n} \vec{V}_{load_n}^{new} = \sum_{n=1}^{n} \vec{V}_{supply_n} - \sum_{n=1}^{n} \vec{V}_{dn} \tag{4.3}$$

Step #7 Obtain a new estimate of the supply current waveform from the new bus voltage, including the harmonic voltages. Also calculate the FFT of the new supply current.

Step #8 Check the convergence of the iterative approach. The above cycle is repeated until convergence in the magnitude of the harmonic voltages on all nodes in the distribution system is obtained. The convergence criterion is based on the change in harmonic bus voltages with each step of calculation.

Step #9 Draw the resultant waveforms of both load voltage and supply current and obtain the harmonics contents of each waveform utilizing the Fast Fourier Transform.

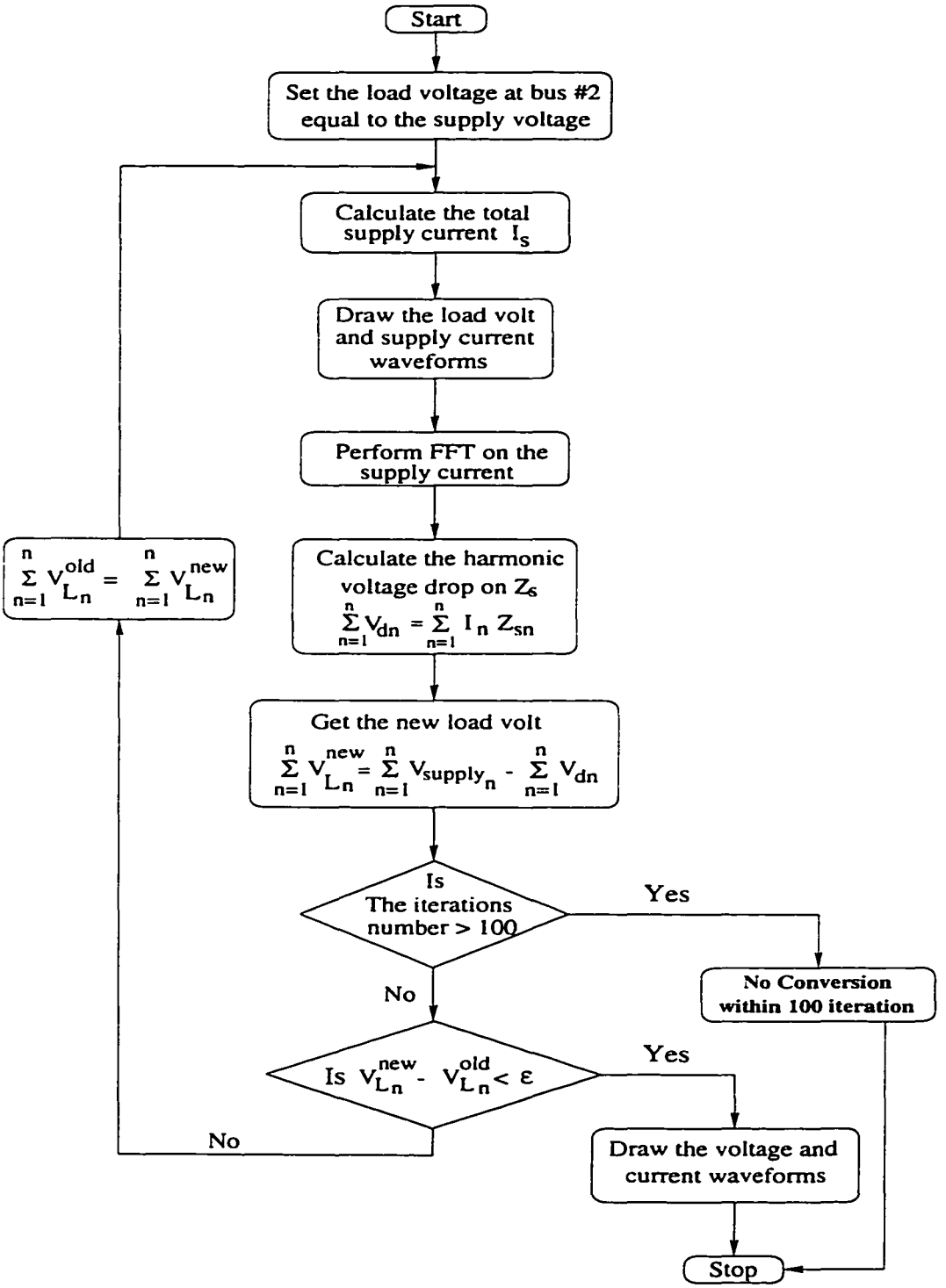

Figure 4.2: Iterative approach flow chart

4.4 Work strategy

In order to achieve the first goal of this research (obtaining the accurate waveforms of both load voltage and supply current while taking into account the harmonic interactions), the following working strategy, consisting of three phases, will be adopted.

Phase I

The first phase deals with the identification and modelling of different non-linear loads that are needed for this study. The participating non-linear loads are chosen based on the following criteria:

1. The load type exists in large numbers in the electric power distribution system and, due to its growing popularity, is expected to proliferate through out the system; and

2. The load has been witnessed to inject a considerable amount of harmonic currents into the distribution system due to either its non-linear characteristics or its switching operation behavior.

After identifying the non-linear loads that have the most significant share in polluting the electrical distribution system, detailed models for these loads will be developed in the time-domain utilizing the electro-magnetic transient program.

Phase II

In order to apply any of the harmonic suppression techniques effectively, the load voltage and current waveforms should be accurately determined, therefore, the effect of the attenuation (the interaction of voltage and current harmonics) should be taken into account. The developed iterative approach was used to solve the load models under different modes

of operation. The load current was analyzed to determine the harmonic contents and to examine the effect of attenuation on the waveform distortion of both load voltage and supply current. Additionally, the effect of this phenomenon, on the distribution system distortion level, was investigated.

Phase III

In order to validate the simulation results, physical experiments were conducted on some of the study cases. A comparison between the simulation and the laboratory results were offered to reflect the agreement.

4.5 Harmonic sources models

In order to examine the effects of the interaction between the voltage and current harmonics on the harmonic performance of an electrical distribution system, detailed models for the harmonic producing loads under study were developed in the time-domain. Using the time-domain offers the advantage of considering the system non-linearity and voltage dependency. The Electro-Magnetic Transient Program $EMTP$ [54] will be utilized in developing these models as well as the overall system model. The chosen non-linear loads were placed into three groups based on the common features in the waveforms of their current. It should be also maintained that the studied loads represent samples of the loads commonly utilized in distribution systems.

4.5.1 Group #1 load model

The loads of this group are mainly the iron-core reactors. A typical example of this group is the magnetic ballast compact fluorescent lamps (CFL) and other gas discharge lighting. With their significant energy saving over incandescent lighting, CFLs are being promoted

as part of the energy conservation programs by many electric utilities. As a result, more and more of these lamps are expected to be installed over time. The magnetic ballast CFL used in this study consumes $40W$ when energized from a $120v$ (RMS) power supply. For this study, the CFL load voltage and current characteristics (result of experiment) that is given in Figure 4.3, were utilized to construct a tentative model for the lamp. The CFL load model is formed from two parallel switched non-linear resistors. Each resistor has a V-I characteristics of one half of the CFL load characteristics. The CFL load model is shown in Figure 4.4. The current waveform and its harmonic contents are given in Figures 4.5 and 4.6, respectively.

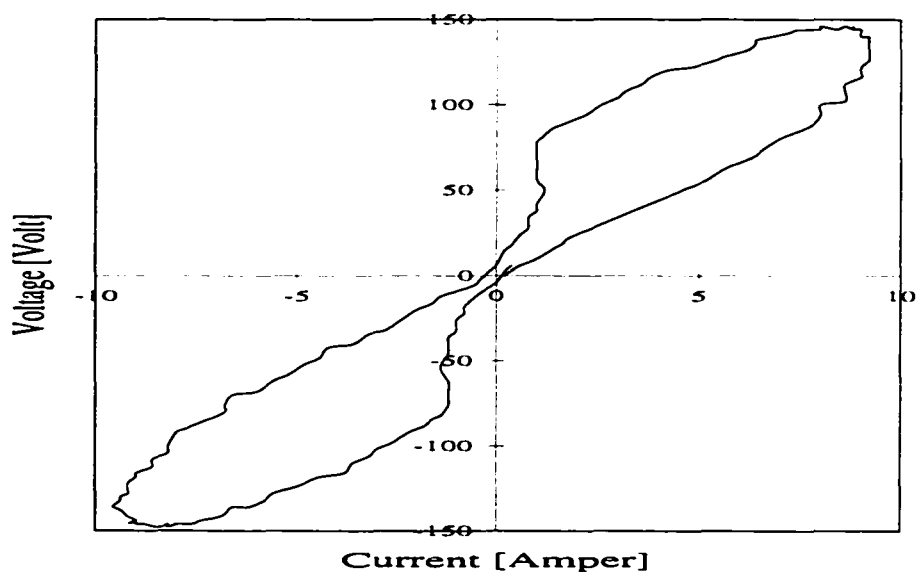

Figure 4.3: Voltage-Current characteristics for CFL load

4.5.2 Group #2 load model

This group contains those loads that employ different versions of the single-phase capacitively filtered diode bridge rectifiers (DBR). These single-phase rectifiers are the most popular choice in low-power applications due to the fact that they are economical in design

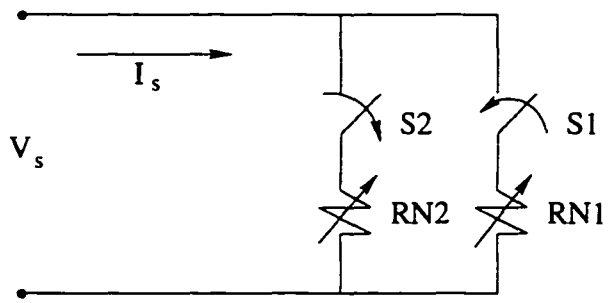

Figure 4.4: Single-phase, magnetic ballast CFL load model

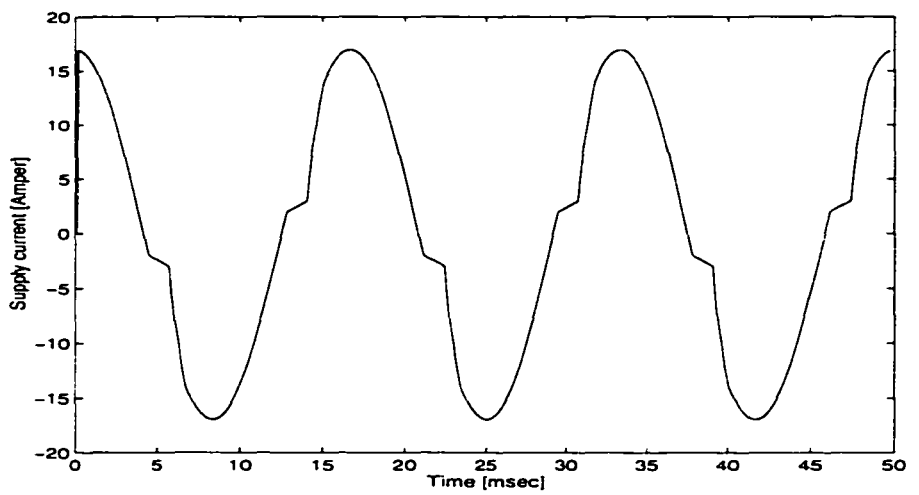

Figure 4.5: The current waveform for CFL load

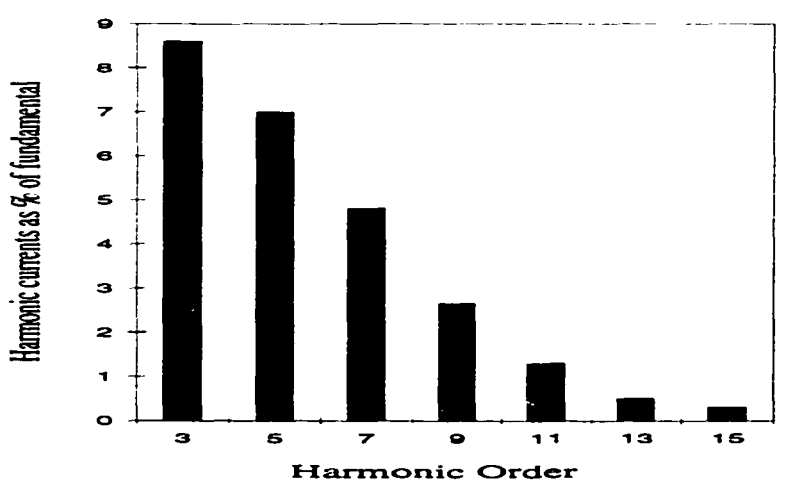

Figure 4.6: The harmonic contents for CFL load

and are not affected by minor variations in the supply voltage. Computers and color television sets head the list of loads utilizing the DBR, which also includes electronic ballasts for gas discharge lamps, battery chargers and small adjustable speed drives (ASD) for heat pumps. Their input current waveform is discontinuous since the current is drawn only when the capacitor is charging. The pulsed current waveform generated by this group of loads is rich in harmonics and the current total harmonic distortion (THDI) is normally near 100%.

The circuit diagram of the DBR load is illustrated in Figure 4.7. In this study we choose a DBR unit that has a resistance equal to 20Ω on its DC side to represent full load condition. The unit absorbs $0.9kW$ when supplied from a $120v$ (RMS) voltage power supply that has a fundamental frequency equal to $60Hz$. The snubber circuit mounted in parallel with each diode consists of a series RC circuit, where $R = 1\Omega$ and $C = 33\mu F$. The smoothing capacitor connected in parallel with the load is equal to $1000\mu F$. The pulsed current waveform generated by this load when energized from a sinusoidal voltage supply and the harmonic spectrum associated with this waveform are shown in Figures 4.8 and 4.9, respectively.

4.5.3 Group #3 load model

The single-phase; phase-angle voltage controllers (PAVC) represent the main element of this group. This device controls the input AC voltage and power to the load utilizing the phase control of thyristors. The major loads in this group are heaters, light dimmers and single-phase induction motor control circuits. These controllers produce waveforms with substantial harmonic contents. For the simulation purpose we choose a unit which is rated at $0.9kW$ and $120v$ (RMS). The PAVC unit consists of two back-to-back thyristors with a snubber circuit has $R = 1\Omega$ and $C = 20\mu F$. The equivalent circuit of this load is shown in Figure 4.10. The load current as well as the harmonic content of the current

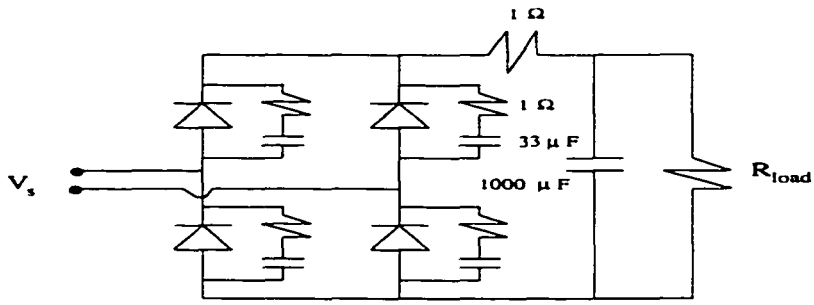

Figure 4.7: Single-phase DBR load model

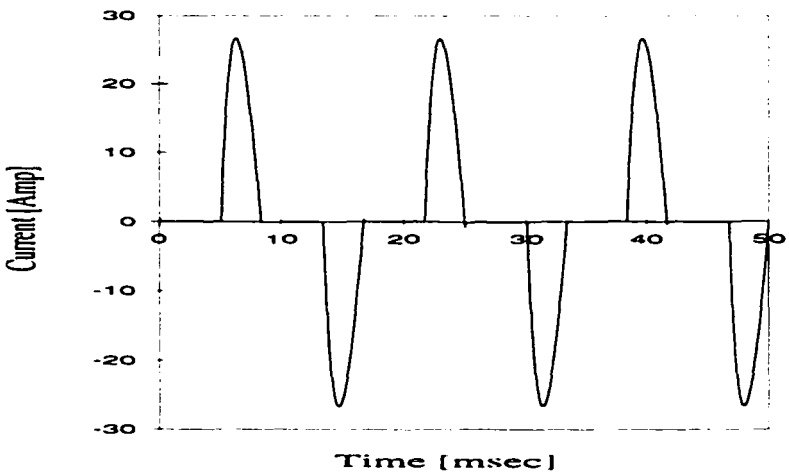

Figure 4.8: The current waveform for DBR load

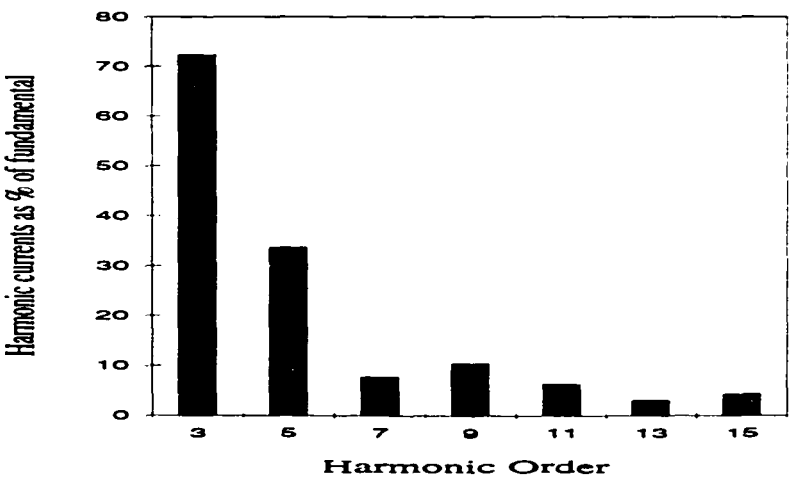

Figure 4.9: The harmonic contents for DBR load

waveform are given in Figures 4.11 and 4.12, respectively.

4.6 Method of analysis

The objective of this study is to investigate the effect of voltage and current harmonic interactions and how this phenomenon can affect the harmonic distortion level of electrical distribution systems [101]. Additionally, the determination of an accurate voltage and current waveforms that are used in the design of the suppression equipment will be studied.

To achieve the goals of this study, an analysis of the distorted waveforms of the currents drawn by the loads under study was performed. The main assumption made through out this analysis was that the loads are supplied from a practical voltage source (having internal inductive impedance). The study of the harmonic performance of different non-linear loads was carried out according to the following steps:

Step #1 Detailed models for the harmonic producing loads under study were developed in the time-domain utilizing the EMTP program. The circuit diagrams used for these models are given in Figures 4.4, 4.7 and 4.10, respectively. For the analysis, a long simulation time was employed to ensure that all the voltage and current transients had died away and the steady state had been reached. Also, the integration time step chosen was small enough to increase the solution accuracy since the solution involved repeated switching.

Step #2 To observe attenuation due to the load voltage and current harmonics interaction, a source inductive impedance was introduced. The simulation ran twice for each harmonic producing load. The first time was to consider the source impedance to allow for the interaction and the other time neglecting the source impedance. The

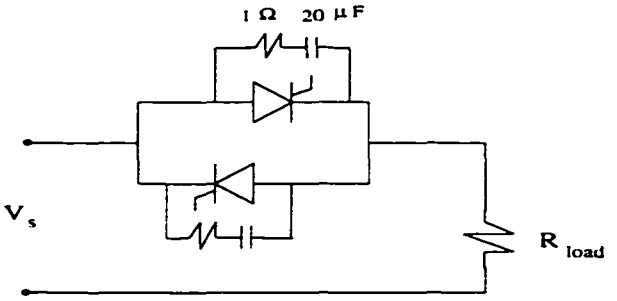

Figure 4.10: Single-phase PAVC load model

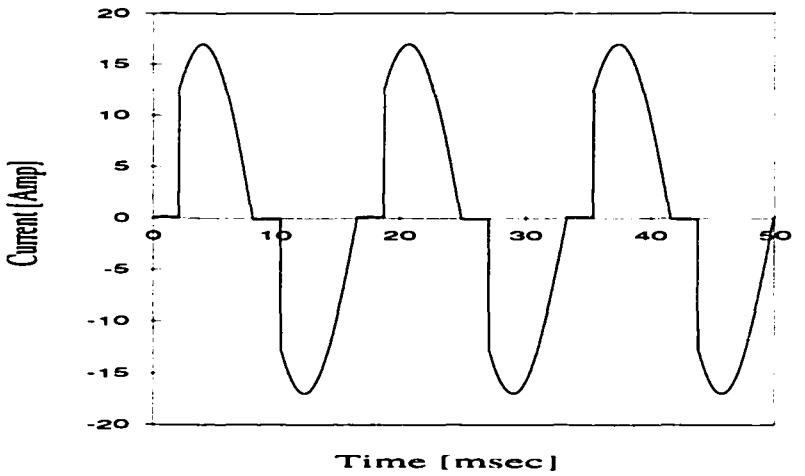

Figure 4.11: The current waveform for PAVC load

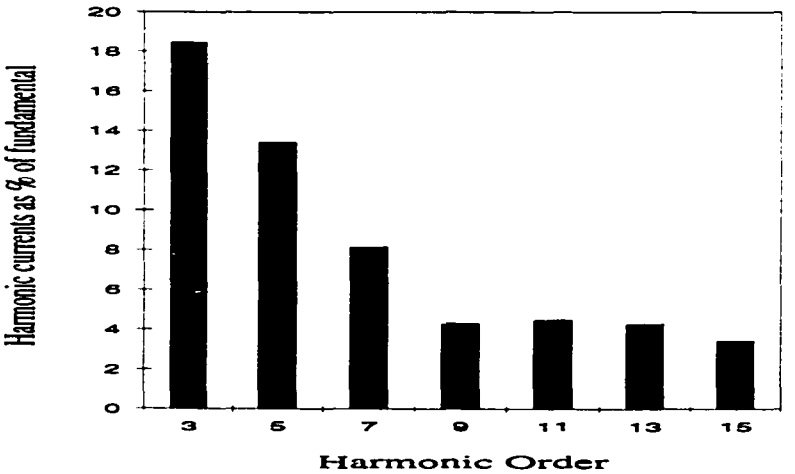

Figure 4.12: The harmonic contents for PAVC load

developed iterative technique was utilized for this study. The variation of the load voltage and supply current waveforms due to the interactions between the voltage and current harmonics was the main contribution of this step and will be discussed in the next section. The system used for this study is outlined in Figure 4.1.

4.7 Simulation results

In this section, the results for the outlined two-step analysis method are presented. In order to visualize the attenuation phenomenon and to illustrate its dramatic effect on the distribution system distortion levels, the variation of the different harmonic current components as produced by different types of non-linear loads, were calculated as a percentage of the fundamental current. The variation of the waveshape of both load voltage and supply current as affected by this phenomenon was also demonstrated. Further, the supply current total harmonic distortion (THDI) for each load type was calculated with and without the attenuation effect. The results are presented in the following sequence:

Figures 4.13 and 4.14 show the voltage and current waveforms with and without the attenuation effect for the CFL load. Figure 4.15 gives the variation of the percentage harmonic currents of this load type. Figures 4.16, 4.17 and 4.18 illustrate the same results for the DBR load and in similar fashion, Figures 4.19, 4.20 and 4.21 are for the PAVC load. The THDI for these loads before and after considering the interaction effect are listed in Table 4.1.

It is evident, from the results presented in Figures 4.13 through 4.21, and given in Table 4.1, that the interaction between the voltage and current harmonics led to a reduction in the distribution system harmonic levels. These interactions tended to bring the supply current more towards the sinusoidal form while increasing the load voltage distortion.

NOTE TO USERS

Page(s) not included in the original manuscript are unavailable from the author or university. The manuscript was microfilmed as received.

59-80

UMI

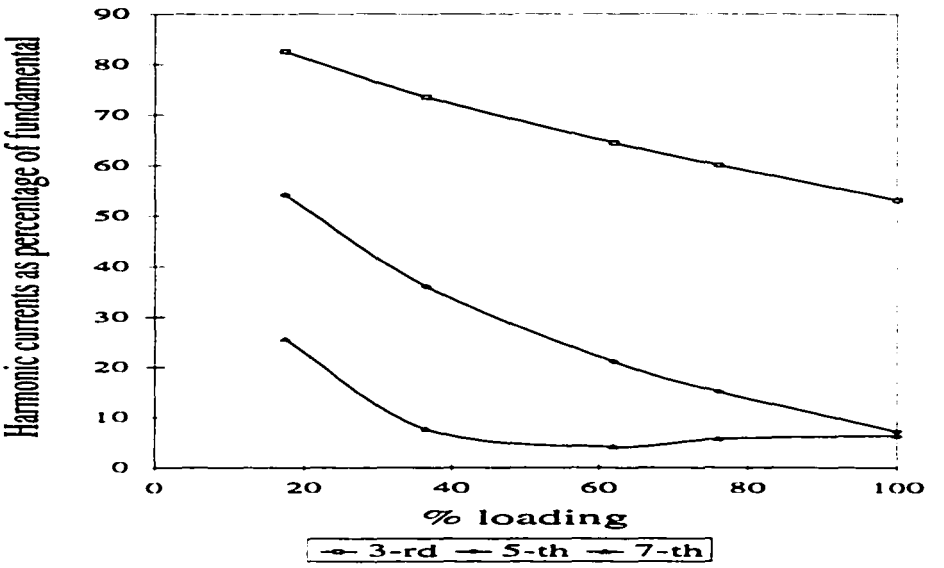

Figure 5.10: 3rd, 5th, $and 7^{th}$ harmonic currents for different loading levels of single DBR unit

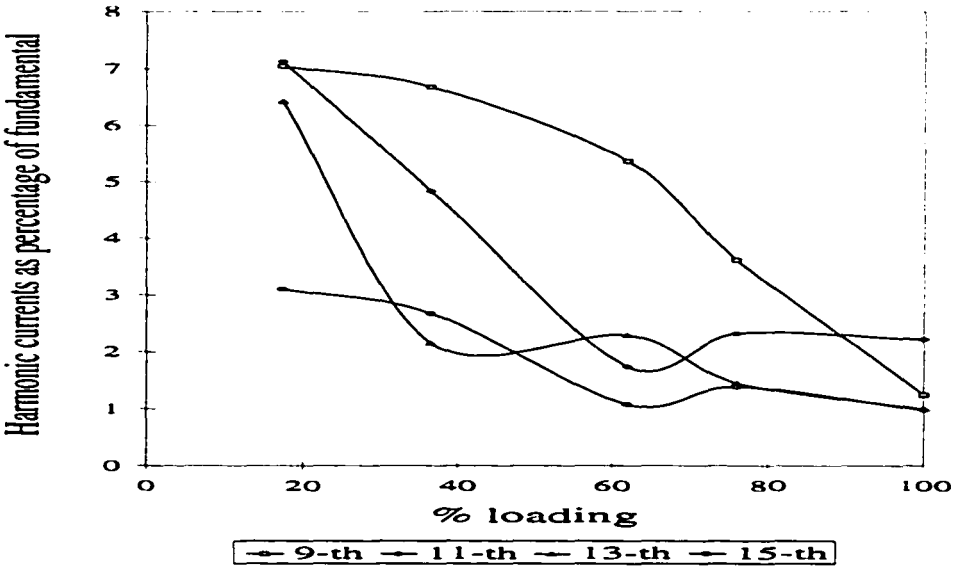

Figure 5.11: 9th, 11th, 13th, and 15th harmonic currents for different loading levels of single DBR unit

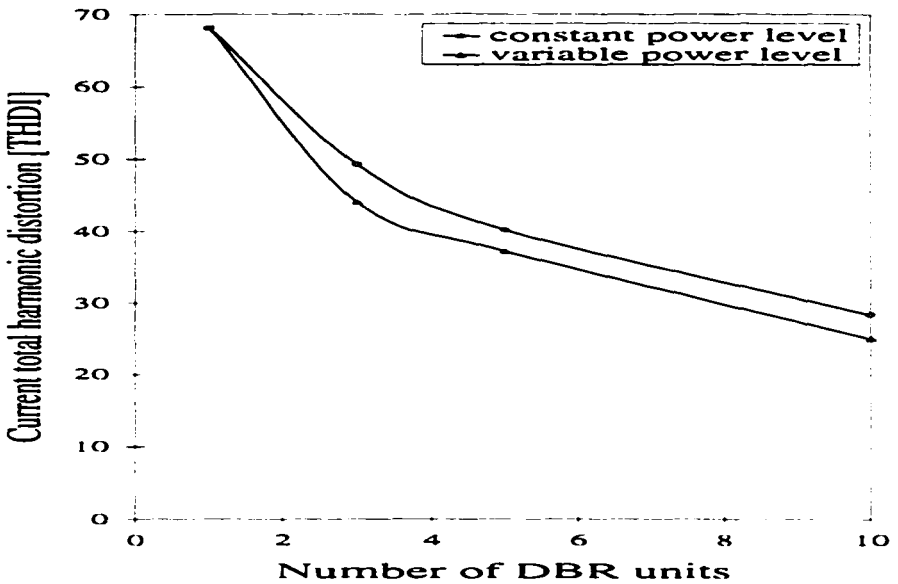

Figure 5.12: Variation of current THD as affected by increasing the number of DBR load units

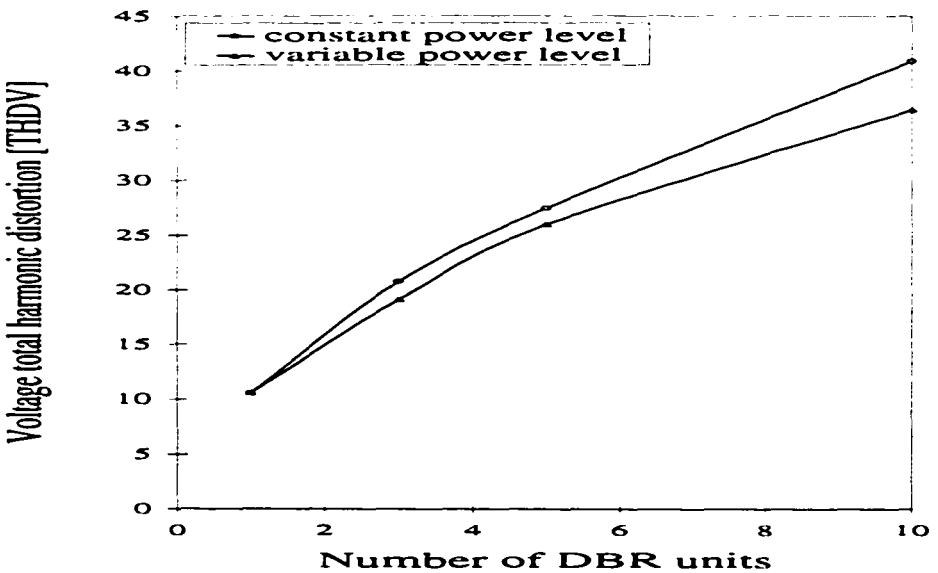

Figure 5.13: Variation of voltage THD as affected by increasing the number of DBR load units

Table 5.4: Current harmonics variation as affected by constant loading level DBR units

# *ofunits*	Percentage of fundamental current							THDI	THDV
	I3	I5	I7	I9	I11	I13	I15		
1	64.36	21.06	4.2	5.36	1.74	2.29	1.08	68.16	10.55
3	48.23	5.96	6.29	2.6	1.95	1.7	1.01	49.18	20.76
5	39.18	6.3	3.84	3.01	1.76	1.2	1.18	40.01	27.46
10	26.27	7.96	3.04	1.8	1.53	1.57	1.45	28.31	40.91

1. The source impedance X/R ratio will remain constant at 3.65;
2. The percentage sharing of each load type in the total demand will remain unchanged; and
3. The position of the individual loads will remain unchanged.

The results of this study are given in Table 5.6, where the supply current harmonic contents are given in percentage of the fundamental component.

The results presented in Figures 5.12 and 5.13 and listed in Tables 5.4 through 5.6 reveal the following conclusions:

1. All the harmonics under study demonstrated a tendency to decrease with the increase of the number of loads supplied from the same source;
2. For the case of increasing the number of DBR units that have the same loading level, the main source of harmonic reduction was the attenuation effect. This is attributable to the fact that the loads were energized from the same supply and

Table 5.5: Current harmonics variation as affected by variable loading level DBR units

# *ofunits*	Percentage of fundamental current							THDI	THDV
	I3	I5	I7	I9	I11	I13	I15		
1	64.36	21.06	4.2	5.36	1.74	2.29	1.08	68.16	10.55
3	42.98	6.32	5.09	3.23	1.42	1.6	1.1	43.95	19.09
5	36.02	7.47	3.2	2.71	2.0	1.18	1.0	37.15	25.94
10	23.32	7.48	3.27	1.94	1.45	1.38	1.24	24.97	36.45

had the same parameters, thus all loads generated identical harmonic currents in both magnitude and phase angles. Therefore, the diversity phenomenon was not effective in this case;

3. When the energized loads have different loading levels, the generated harmonic currents differed in both magnitudes and phase angles. Therefore, harmonic cancellation due both to the dispersion in the generated harmonic current phase angles and to attenuation due to voltage and current harmonics interactions were experienced; and

4. In the case of the secondary distribution feeder loaded with different non-linear load types, the harmonic cancellation were attributed to both diversity and attenuation. Phase angle dispersion in this case was not only a result of varying the power level, but was also due to utilizing different non-linear load types that have varying characteristics.

Table 5.6: Current harmonics variation as affected by constant loading level DBR units

Load %	Percentage of fundamental current							THDI
	I3	I5	I7	I9	I11	I13	I15	
100	21.62	4.2	1.55	1.51	0.88	0.34	0.03	22.18
83	23.76	5.29	1.79	1.98	0.68	0.75	0.61	24.53
59	26.92	7.68	2.6	2.6	0.25	1.25	0.3	28.28
44	29.36	10.32	3.75	2.7	1.23	1.13	0.7	31.54
29	31.44	13.55	6.01	1.92	2.53	0.13	1.4	34.97

5.4.4 Effect of load combination

Combining different non-linear loads may result in improving the system total harmonic distortion, while the variation of the load sharing percentage among a specific combination may lead to either increasing or decreasing these harmonic distortions. In order to investigate this effect, some DBR and CFL loads were combined together and the load sharing among this combination were varied. The supply current and the source impedance X/R ratio remained constant during this study. The results of this study are shown in Table 5.7, where the harmonic currents as a percentage of the fundamental component are given. Also, Figure 5.14 illustrates the variation in the current THD due to the different sharing percentages.

These results clearly demonstrate that some sort of harmonic reduction can be achieved by combining different non-linear loads. This is rationalized since the harmonic current phase angles were scattered because of the different load characteristics. Moreover, the attenuation effect contributed to the harmonic reduction in this case due to the presence

Table 5.7: Current harmonics variation as affected by variable loading level DBR units

Load type	% *sharing*	Percentage of fundamental current							THDI	THDV
		I3	I5	I7	I9	I11	I13	I15		
DBR only	DBR=100%	45.24	6.12	5.65	3.17	1.8	1.71	1.31	46.24	23.68
DBR&CFL	DBR=65.%	32.18	4.84	4.67	1.62	1.23	0.87	0.23	32.94	16.87
DBR&CFL	DBR=33.5%	19.82	4.51	3.14	0.86	0.95	0.6	0.36	20.63	10.94
DBR&CFL	DBR=10.%	13.97	3.77	2.46	1.13	0.77	0.1	0.12	14.75	8.63

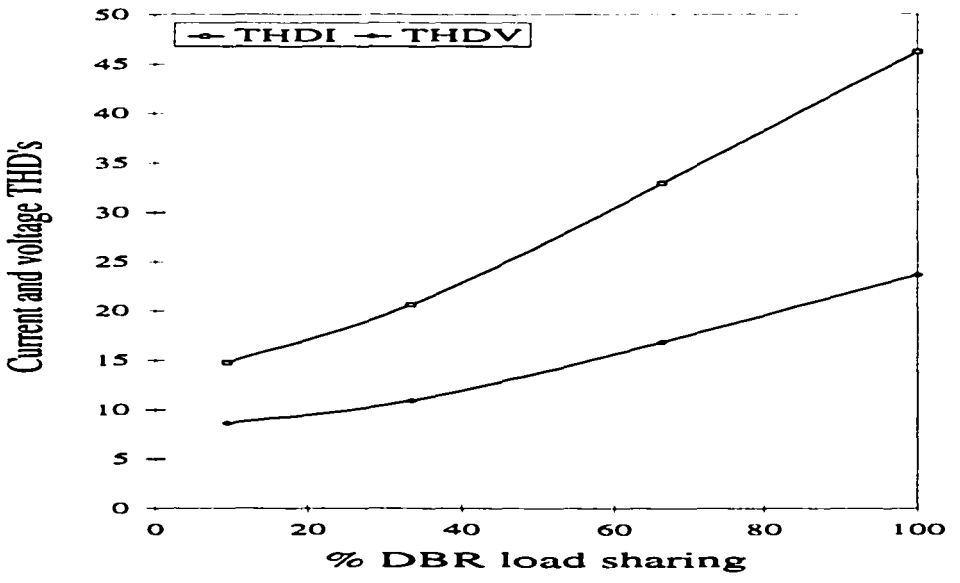

Figure 5.14: Current and voltage total harmonic distortion factors as affected by combining different loads

of the source internal impedance which allowed for the interactions between the voltage and current harmonics to take place.

5.4.5 Effect of changing the load position

The intention of this study is to show the effect of interchanging the non-linear load position on the system distortion level. The distribution feeder described in Figure 5.1 was adopted for this study. The position of the loads were interchanged according to Table 5.8 and with reference to Figure 5.1. The loads remained at their full capacity and the load sharing percentage were unchanged at; $DBR = 40\%, PAVC = 20\%, CFL = 20\%$ and the remaining 20% were linear loads. The supply impedance X/R ratio was constant at 3.65. The results are presented in Table 5.9 .

Table 5.8: Different system configuration for load position interchanging study

Conf-	Connected loads			
ig. #	Bus #1	Bus #2	Bus #3	Bus #4
1	DBR_1	$R_1, CFL_1, PAVC_1$	$R_2, CFL_2, PAVC_2$	R_3, DBR_2, DBR_3
2	R_3	R_1, R_2, CFL_1	DBR_1, DBR_2, CFL_2	$PAVC_1, PAVC_2, DBR_3$
3	R_3	R_1, R_2, CFL_1	$PAVC_1, CFL_2, DBR_2$	$DBR_1, DBR_3, PAVC_2$
4	R_3	R_1, R_2, CFL_1	$PAVC_1, CFL_2, PAVC_2$	DBR_1, DBR_2, DBR_3

Table 5.9: Effect of interchanging load position on the distribution system distortion level

Configuration #	Percentage of fundamental current							THDI
	I3	I5	I7	I9	I11	I13	I15	
1	21.2	4.2	1.55	1.51	0.88	0.34	0.59	22.18
2	20.0	3.65	1.48	1.45	0.87	0.30	0.58	20.51
3	19.8	3.5	1.43	1.42	0.85	0.29	0.57	20.25
4	19.5	3.31	1.42	1.39	0.85	0.27	0.57	19.89

The results demonstrate that the level of each harmonic component changes with the interchange of the position of harmonic producing devices along the feeder. It is important to note that the feeder loading level and the supplied load types remained the same, the only difference being that their positions had been changed. The clear conclusion of the presented results is that the interaction between voltage and current harmonics can take the form of either harmonic cancellation or addition, depending on the magnitudes and phase differences of each harmonic component. Since the phase angles of the generated harmonic currents from each load depended mainly on the applied voltage magnitude and phase angle, then changing the load position might lead to the change in the voltages phase angles which in return will affect the amount of cancellation experienced due to the diversity effect.

5.5 Physical experiment

In order to support the computer simulation findings presented in section 5.4, some laboratory experiments were conducted for some of the case studies. These tests were

performed on two types of loads namely, CFL and DBR. The experimental work was conducted according to the following scenarios:

1. Verifying the simulation results obtained for the case of multi units having the same loading level as described in subsection 5.4.3. The effect of changing the load power was also be examined for the CFL load. This was achieved by varying the CFL load from 320W to 640W; and

2. Investigating the effect of combining two different loads on the system distortion level. How changing the percentage of the load sharing among certain combination can affect the system distortion will also be illustrated.

5.5.1 Loading level effect

Increasing the number of energized DBR units was done experimentally and it was found that the simulation outputs are in agreement with the laboratory results. A comparison between the two sets of results, simulation and experimental, is found in Table 5.10. The same conclusion holds true for the CFL load, where the load was energized once at full load and another time at half load. The load voltage and current waveforms for both loading conditions are given in Figures 5.15 and 5.16. The net current harmonics flowing through the supply impedance for both CFL load percentages is shown in Figure 5.17.

5.5.2 Combination effect

To illustrate the effect of combining different load types on reducing the overall current harmonics, combination $\#A$, which consists of a 624W CFL load and a DBR unit having a load resistance equal to 68Ω on its DC side was compared with a single DBR unit having load resistance equal to 20Ω on its DC side. These two loads forced the same RMS current to flow through the supply impedance. The results show that the THDI is decreased from

Table 5.10: Simulation and experimental net harmonic currents generated by DBR loads

# of units	Percentage of fundamental current (simulation/experimental)							THDI
	I3	I5	I7	I9	I11	I13	I15	
1	64.4/66.2	21.1/22.1	4.2/3.8	5.4/5.1	1.7/1.8	2.3/2.7	1.1/1.2	68.1/70.2
3	48.2/50.8	5.9/6.5	6.3/6.9	2.6/2.8	1.9/2.7	1.7/2.1	1.0/1.5	49.2/51.9
5	39.2/41.3	6.3/6.7	3.8/4.1	3.0/3.4	1.8/2.0	1.2/1.4	1.2/1.5	40.1/42.23

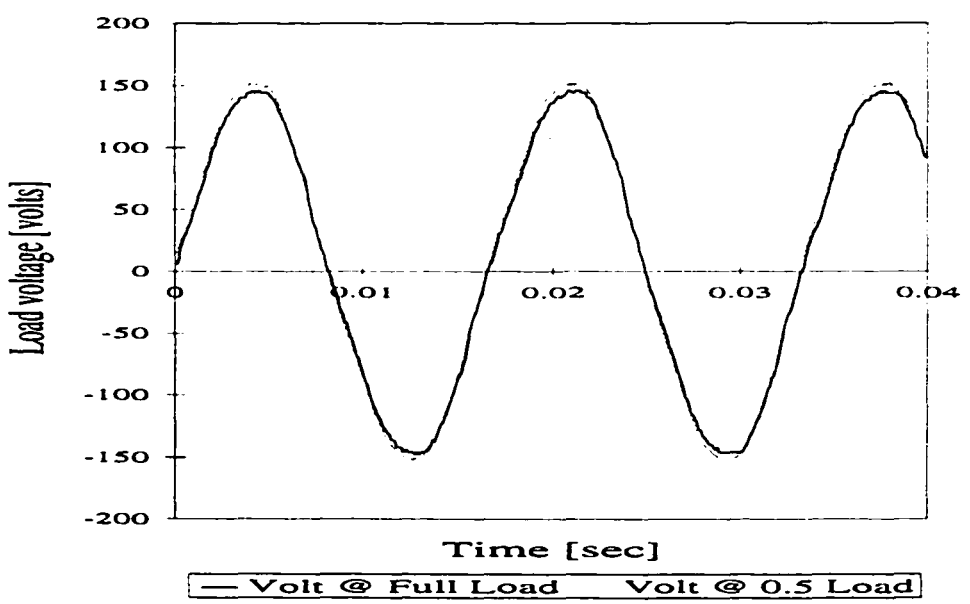

Figure 5.15: Voltage waveform for different CFL load percentage obtained experimentally

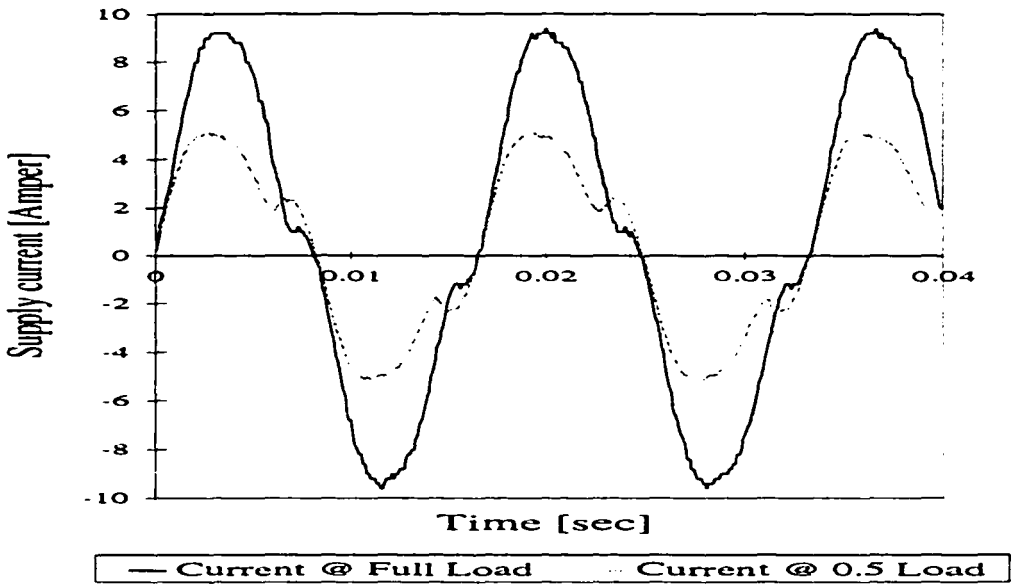

Figure 5.16: Current waveform for different CFL load percentage obtained experimentally

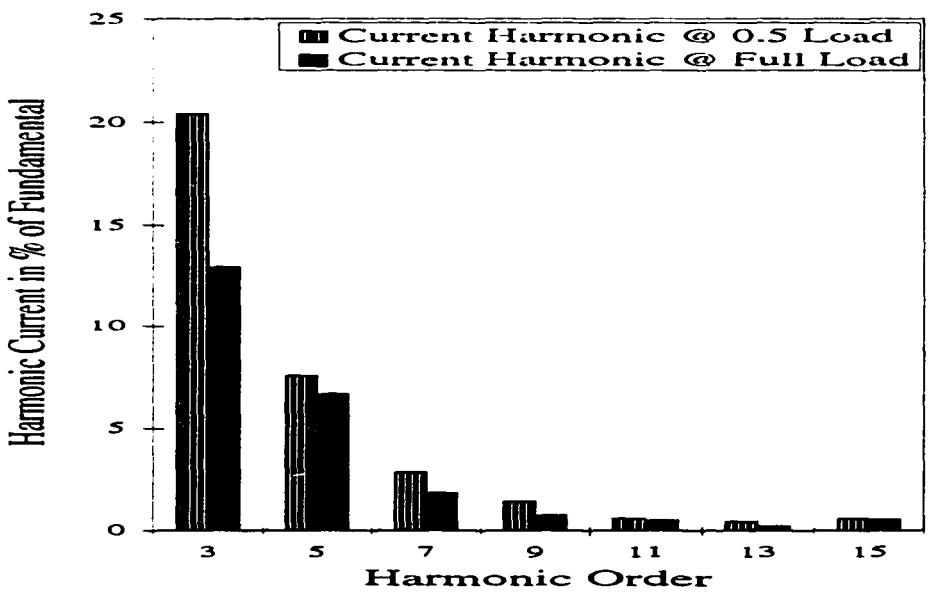

Figure 5.17: Reduction in current harmonics due to varying the loading level of CFL load; experimental results

53% (DBR unit alone) to 24.8% (combination $\#A$). The current harmonics for the two cases are given in Figure 5.18.

This test demonstrate that lower current distortion can be obtained by combining two or more different non-linear loads. The reduction is attributed to both the attenuation and diversity effects. Furthermore, the experimental results showed that varying the respective percentage sharing of the loads in a certain combination may lead to either more reduction or increase in the system distortion. This result can be visualized utilizing Figure 5.19 in which the harmonic current of the previous combination (combination $\#A$) is compared with another combination (combination $\#B$). The latter combination consists of a DBR unit having resistance equal to 32Ω combined in parallel with a 320W CFL load. While combination $\#A$ current total harmonic distortion (THDI) was 24.7%, combination $\#B$ has THDI equal to 36.8%. The working assumption during the test was that both combinations draw the same RMS current from the supply. This test indicates that an optimal combination of loads to reach minimum THDI may exist.

5.6 Assessment

In this chapter, a comprehensive study was performed to evaluate the harmonic performance of different types of non-linear loads and to identify the parameters that affect the generation and propagation of different current harmonics. The loads under study were modeled in the time-domain to allow for a precise representation of the loads' non-linearity and voltage dependency. An iterative approach was employed to permit the interactions between voltage and current harmonics to take place.

To investigate the cumulative harmonic current characteristics of different non-linear and electronically switched loads, the effects of shared source impedance were examined as well as the variations in the source impedance X/R ratio, loading level, load combination

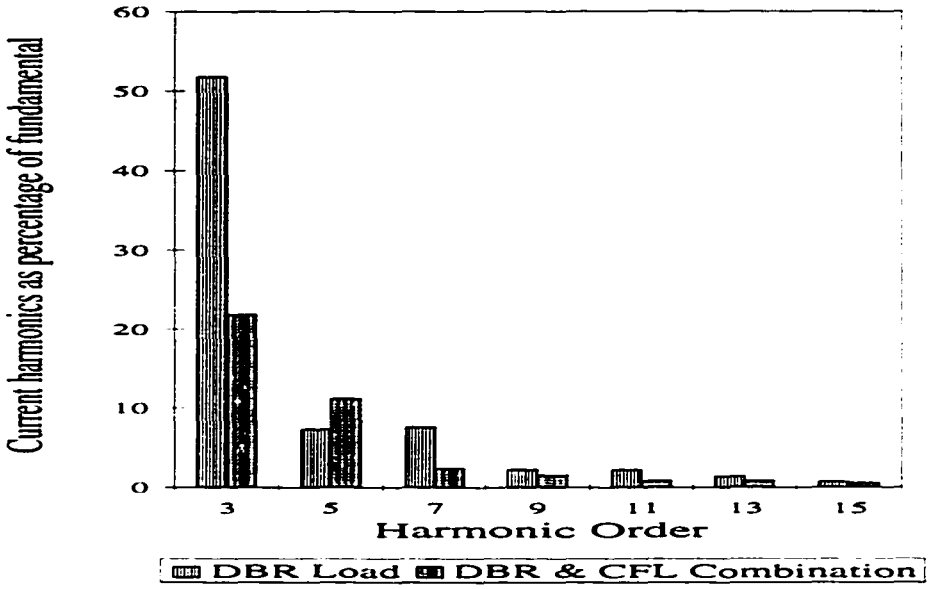

Figure 5.18: Reduction in the system THDI due to combining different loads; experimental result

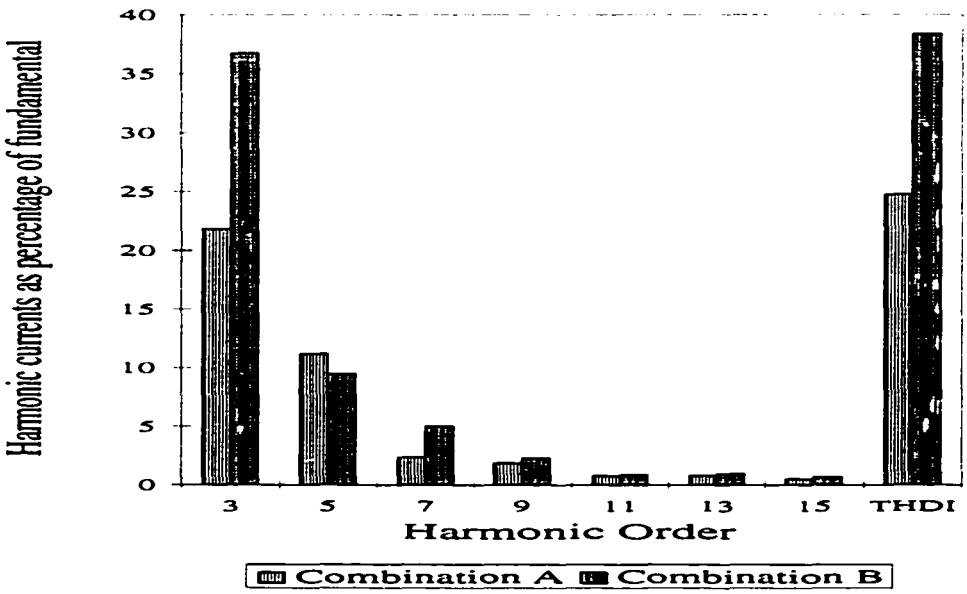

Figure 5.19: Reduction in current harmonics due to changing the percentage sharing among load combination; experimental result

and load position interchanging. The results here are valid for the types of loads under study, however, similar conclusions are likely for other types of loads. The results show that:

1. Harmonic phase cancellation (diversity) can be experienced even if identical loads are operating together. This is due to individual and/or composite variations in power level and source impedance X/R ratio;

2. The harmonic characteristics of the supply current are dependent not only upon the magnitudes of the load voltage harmonics, but also on their phase angles. These phase angles are affected by the source impedance X/R ratio;

3. The reduction in harmonic currents due to phase angle dispersion is relatively independent of the system loading level, whereas reduction due to attenuation increases significantly with the system loading;

4. Combining different non-linear loads can lead to significant harmonic cancellation. This fact is mainly due to the diversity among phase angles of current harmonics produced by different load types; and

5. The level of each harmonic component changes with the interchange of the position of the harmonic producing device along the feeder. This is due to both diversity and attenuation effects.

In general, attenuation and diversity are very important factors in predicting the harmonic behavior of distributed non-linear loads. Thus, ignoring these two phenomena may lead to the overestimation of any harmonic-related problem. This overestimation might be unimportant when dealing with a single small load, however, when dealing with a group of non-linear loads, these effects may be very significant. In order to complete the picture of the harmonic performance of different harmonic producing loads, the effects

of different system parameters on the propagation and generation of neutral currents in three-phase four-wire distribution circuits will be highlighted in the next chapter.

Chapter 6

Neutral Current Harmonics in Three-Phase Four-Wire Distribution System

6.1 Introduction

A typical low voltage electrical distribution system consists of a 208/120 volt three-phase four-wire system. This system is widely utilized to supply electricity to most commercial and residential areas. In three-phase four-wire systems, the neutral current is the vector sum of the three line-to-neutral currents. For balanced, three-phase, linear circuits, this sum at any instant is zero and no neutral current exists. In most three-phase systems supplying single-phase loads, there will be some phase current imbalance and perhaps a small amount of neutral current may exist. However, small neutral currents do not cause significant problems to the distribution system. When the system becomes non-linear, even perfectly balanced single-phase loads can result in significant neutral currents since

the vector sum of balanced, nonsinusoidal, three-phase currents is not equal to zero.

In view of the recent significant increase in the use of advanced power conversion technologies, neutral currents are expected to increase drastically. Typical loads connected to a low voltage three-phase four-wire distribution system include: television sets, personal computers, adjustable speed drives for heat pumps and air conditioning, fluorescent lighting with either magnetic or electronic ballasts, light dimmers and motor controls. All these non-linear loads draw currents that are rich in harmonics of which a significant portion is the third and other triplen harmonic components [21–23, 104, 105].

Triplen harmonics have frequencies that are $3n$ times the fundamental power frequency ($n \in 1, 3, 5, ..etc.$), therefore, these currents are in-phase with each other (zero sequence currents) and add in the neutral instead of cancelling each other. Moreover, the diversity (the partial cancellation due to current harmonic phase angle dispersion) among the third harmonic currents produced by different non-linear loads and all other triplen harmonics ($9^{th}, 15^{th}, ...etc.$), is very small and can be neglected [106]. Therefore, these currents add together in a cumulative manner resulting in excessive neutral currents in three-phase four-wire distribution systems.

Recent trends in computer systems have increased the likelihood of significant neutral currents. Instead of utilizing three-phase power supplies that only generate harmonics of order $(6n \pm 1)$, single-phase power supplies are increasing in number. These single-phase switched-mode power supplies generate a good deal of triplen harmonics and are connected directly to the line-to-neutral voltage. A recent survey conducted by Liebert Customer Service Engineering in 146 computer sites across the United States revealed that 22.6% of the sites had neutral currents in excess of 100% of the phase current [107]. Potential problems directly related to excessive harmonic currents in the neutral conductor include:

1. Neutral wire damage due to improper sizing;
2. Overheating of transformers that may result in insulation failure;
3. Increasing the electro-magnetic force (EMF) levels; and
4. Excessive neutral-to-earth voltage (NEV) due to the voltage drop caused by neutral current.

Electric shock sensation occurs when humans contact two conductive objects at different voltage levels. The current passing through their body causes the shock sensation. This condition is commonly referred to as stray voltage. Since stray voltage can be caused by the voltage on the neutral conductor, the neutral voltage should also stay low, typically less than four volts AC (RMS) [108]. Neutral-to-earth voltage (NEV) is the voltage measured between the system neutral and a remote earth. The voltage depends on the neutral current flowing between the neutral and the earth. It also depends on both neutral and earth impedances. Larger neutral currents generally increase the NEV and this is why the increased neutral currents from triplen harmonics is a concern.

The effects of different system parameters on the net harmonic currents generated by different harmonic producing devices are well investigated in Chapter 5. The previous study, however, was limited to only single-phase loads and loads connected in three-phase three-wire configuration. In this chapter, the investigations will be extended to include the effect of these parameters on both neutral current harmonics and neutral-to-earth voltage in three-phase four-wire systems. Additionally the effect of the phase imbalance will be considered in this study. The detailed description of the studied three-phase system is given in the next section.

6.2 Three-phase four-wire system

In order to investigate the effect of different system parameters on both neutral current and neutral to earth voltage, the simple system shown in Figure 6.1 was employed. This system supplies residential and commercial customers with the non-linear loads previously described in section 4.5. The non-linear loads were of the single-phase type and will be distributed among the three phases. The supply consisted of a three-phase star-connected transformer whose secondary line-to-line voltage was adjusted to 208 volt (RMS). The internal impedance of the supply and the impedance of the line connecting the transformer to the distribution panel was combined together and given by $Z_s = R_s + jX_s$, which was equal to $0.8+j0.943\,\Omega$, with the X/R ratio to be 1.2 to represent a low-voltage transformer. The neutral conductor, which is usually sized the same as the phase conductor, has an impedance equal to $Z_N = R_N + jX_N$, which was equal to $0.05 + j0.19\Omega$.

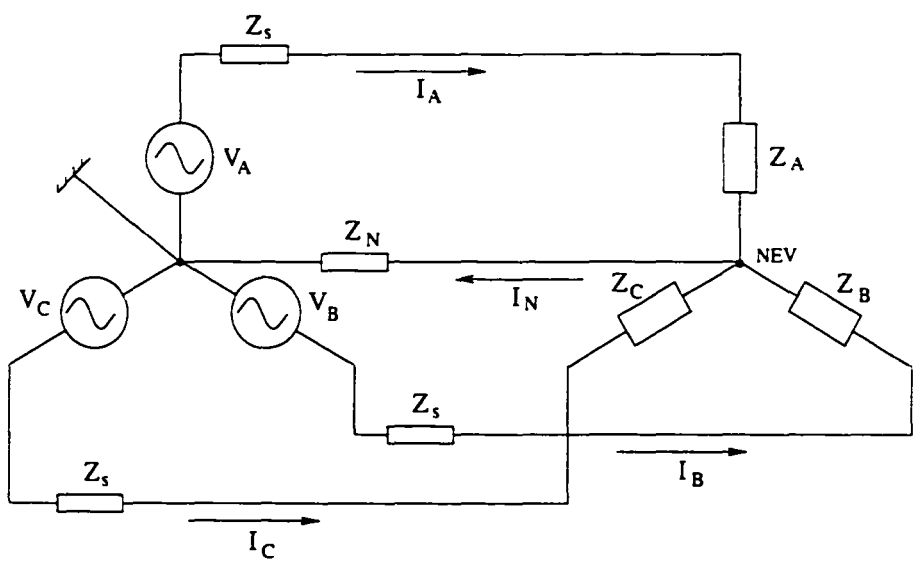

Figure 6.1: Three-phase four-wire balanced system

In grounded distribution systems, the neutral current returns to the source via two paths. Some portion of the neutral current returns on the neutral wire and the remaining

portion flows through the earth. The division of the neutral current depends on load location, neutral impedance, ground impedance and the grid impedance. Since the grounded distribution system is too complex to model, the neutral to earth voltage (NEV) will be deemed to equal the neutral current multiplied by the neutral impedance, that is:

$$NEV = I_N * Z_N \tag{6.1}$$

6.3 Simulation method

This study examines the performance of the proposed three-phase four-wire system with regards to several mission critical operational parameters:

1. Voltage and current harmonic interactions;
2. System loading level;
3. Different load combinations; and
4. System unbalance.

To achieve the goals of this study, the distorted waveforms of the currents drawn by the loads under study for different modes of operation and circuit parameters must be analyzed. Once the effect of both voltage and current harmonic interactions were studied, the rest of the analysis was carried out with the assumption that the attenuation effect has been taken into consideration. To justify this assumption, the iterative technique described in section 4.3 was utilized. The results obtained from this study are presented in section 6.4.

6.4 Simulation results

The first simulation covers the effect of attenuation due to voltage and current harmonic interactions and does not consider any variations in the system parameters. After demonstrating the importance of considering the attenuation effect, the analysis was carried further to include different system parameters and operational modes.

6.4.1 Attenuation effect

In order to demonstrate how the voltage and current harmonic interactions can significantly affect the system distortion and neutral current magnitude, simulations were performed while including the supply internal inductive impedance. This impedance refers to the secondary distribution transformer impedance as well as the impedance of the line connecting the transformer to the distribution panel. For this study, the balanced three-phase four-wire system were loaded with single-phase diode bridge rectifier loads. Each DBR load had a load resistance equal to 10Ω to represent the full load capacity of the unit. The smoothing capacitor connected in parallel with the load was equal to $1000\mu F$. The snubber circuit connected across each diode was composed of series R-C circuit, where $R = 1\Omega$ and $C = 33\mu F$. The neutral conductor impedance was equal to $0.05 + j0.19\Omega$. The simulation was carried out twice, once considering the source impedance and the second time neglecting it. Tables 6.1 and 6.2 contain the harmonic contents of the phase current, neutral current as percentage of phase current and the neutral to earth voltage.

An examination of Tables 6.1 and 6.2 reveals that including the source impedance in the simulation decreases the estimated system current distortion as well as the neutral current and the NEV magnitudes. It might be noted that as the current distortion is reduced, the voltage distortion is increased. The latter is attributed to the harmonic voltage drop created on the supply impedance by the harmonic currents generated by non-linear loads.

Table 6.1: Phase and neutral current harmonics without attenuation effect

	Percentage of fundamental‡							RMS	THD	% of phase
	3rd	5th	7th	9th	11th	13th	15th			current
I_{ph}	59.6	14.68	5	2.35	6.1	3.7	0.7	19.77	62.08	100.0
V_{ph}	14.08	—	—	1.5	—	—	0.7	120	14.2	—
I_N	**$1.4*10^4$**	59	29	**537**	9.5	7.4	**140**	30.0	$1.4*10^4$	151.7
NEV	$1.4*10^4$	59	29	537	9.5	7.4	140	5.89	$1.4*10^4$	—

‡ I_{ph} is based on its own fundamental.

I_N is based on its own fundamental which is very small.

Table 6.2: Phase and neutral current harmonics with attenuation effect

	Percentage of fundamental‡							RMS	THD	% of phase
	3rd	5th	7th	9th	11th	13th	15th			current
I_{ph}	37.8	7.9	4.1	2.4	1.95	1.0	0.7	15.57	39.07	100.0
V_{ph}	22.1	4.5	2.8	3.3	1.7	0.9	1.4	114.07	23.15	—
I_N	**$1.6*10^4$**	72	22	**1021**	35	21	**297**	16.57	$1.6*10^4$	106.4
NEV	$1.6*10^4$	72	22	1021	35	21	297	3.26	$1.6*10^4$	—

‡ I_{ph} is based on its own fundamental.

I_N is based on its own fundamental which is very small.

It is worth noting that the dominant harmonics presented in the neutral current are the triplen harmonics. All other harmonics, including the fundamental, are of negligible value due to the fact that the system is balanced and loaded with similar loads in each phase. Therefore, the summation of any of the positive or negative sequence harmonics will be equal to zero.

The main reason behind the decrease of the neutral current is the attenuation effect. This can be explained based on the fact that the voltage and current harmonics interactions are translated into a decrease in the harmonic contents of the phase currents. Since the phase current harmonics (specially the triplen) are the main contributors to the neutral current, then a decrease in the phase current harmonics will consequently result in a reduction in the neutral current. Figure 6.2 demonstrates the reduction in the system neutral current due to the attenuation effect.

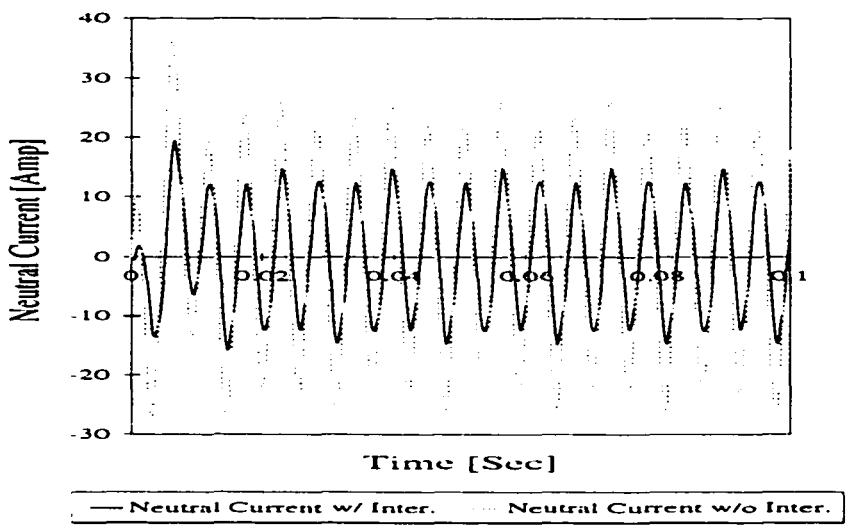

Figure 6.2: Neutral current waveform with and without attenuation effect

6.4.2 Effect of loading level

The loading level of the secondary distribution system is not fixed, but rather, is variable. The variation in the loading level may be due to either a variance in the percentage loading of a certain unit or a variance in the number of units connected to the system by simply switching some loads on or off.

Varying the percentage loading

The three-phase four-wire system was loaded with single-phase DBR units, that were equally distributed on the three phases. The percentage loading of the three phases was gradually increased from 18% till the full load capacity of all units was reached. This scenario had to be done without violating the balancing condition. The results obtained from this test are given in Table 6.3. The variation in the neutral current magnitude as a percentage of the phase current vs. the percentage load change is shown in Figure 6.3.

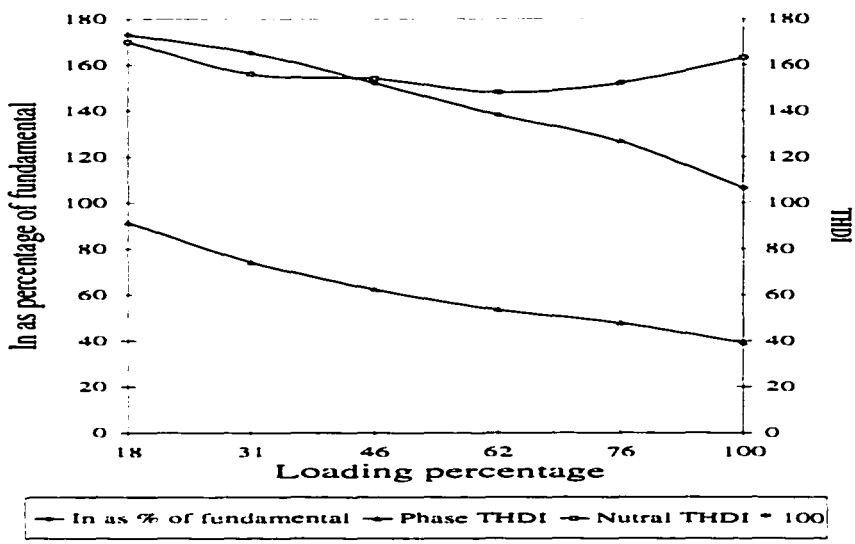

Figure 6.3: Variation of neutral current magnitude with the change in the DBR unit loading level

Effect of changing the number of units

To shed more light on how changing the feeder loading may affect the magnitude and distortion level of both phase and neutral currents, the number of DBR units supplied by each phase was increased by one unit at a time until the maximum number of units per phase

Table 6.3: Effect of changing the loading level of DBR units arranged in three-phase balanced configuration on neutral current

load level%		Percentage of fundamental‡							RMS	THDI	% of I_{ph}
		3rd	5th	7th	9th	11th	13th	15th			
18	I_{ph}	78.06	43.9	13.6	5.9	7.9	3.2	2.3	2.82	91.31	100.0
	I_N	**$1.7*10^4$**	73.8	47	**1230**	4.3	20.9	**514**	4.88	$1.7*10^4$	173.05
31	I_{ph}	68.3	27.2	4.9	6.3	3.2	2.8	1.3	4.86	74.2	100.0
	I_N	**$1.55*10^4$**	79	56	**1413**	14	17	**309**	8.03	$1.56*10^4$	165.23
46	I_{ph}	59.5	15.7	7.3	3.4	3.8	1.6	1.5	7.15	62.27	100.0
	I_N	**$1.54*10^4$**	71	53	**913**	14.5	27	**395**	10.9	$1.54*10^4$	152.03
62	I_{ph}	51.9	9	7.8	2	2.95	1.25	1.0	9.63	53.46	100.0
	I_N	**$1.48*10^4$**	61.2	37.3	**572**	19.7	26.9	**294**	13.3	$1.48*10^4$	138.11
76	I_{ph}	46.4	7	6.85	2.38	1.94	1.7	0.67	11.8	47.6	100.0
	I_N	**$1.51*10^4$**	66	17	**767**	29	7	**214**	14.9	$1.52*10^4$	126.46
100	I_{ph}	37.8	7.9	4.1	2.4	1.95	1.0	0.7	15.6	39.07	100.0
	I_N	**$1.62*10^4$**	72	22	**1021**	35	21	**297**	16.6	$1.63*10^4$	106.4

‡ I_{ph} is based on its own fundamental.

I_N is based on its own fundamental which is very small.

(which were limited by the feeder capacity) was reached. It has to be mentioned that the three-phase system remained balanced during this test. Table 6.4 describes the effect of varying the number of energized units on the neutral current, NEV and the system THDI. Figures 6.4 and 6.5 show the variation of the phase current harmonic contents with varying the number of units. The neutral to earth voltage variation is given in Figure 6.6.

Table 6.4: Effect of varying the number of DBR units on the neutral current, NEV and phase current harmonic contents

# of units	Phase current harmonics as % of fundamental							THDI	NEV	I_N as % of I_{ph}
	3rd	5th	7th	9th	11th	13th	15th			
1	45.2	9.5	7.8	1.9	2.3	1.4	0.5	47	2.06	123.5
2	29.2	9.0	4.8	1.6	2.2	1.33	0.48	32.2	2.36	84.8
3	22.3	8.2	4.1	1.08	2.0	1.25	0.4	26.16	2.44	64.9
5	15.0	7.5	3.8	1.08	1.6	1.18	0.35	19.26	2.4	44.7
10	8.1	6.6	3.6	0.96	1.34	1.04	0.26	13.36	2.03	24.7

Tables 6.3 and 6.4 reveal considerable insight into the effects of changing the loading level on both neutral and phase currents harmonics. It becomes apparent that the third harmonic component represents the most considerable portion of the neutral current. As the load increases whether by increasing the unit loading or the number of units, the third harmonic component in phase currents decreases due to the attenuation effect. This will be translated into a reduction in the neutral current magnitude as a percentage of the phase current. While the phase current THD decreases as the loading level increases, the neutral current THD remains almost constant since it is mainly composed of the third harmonic component.

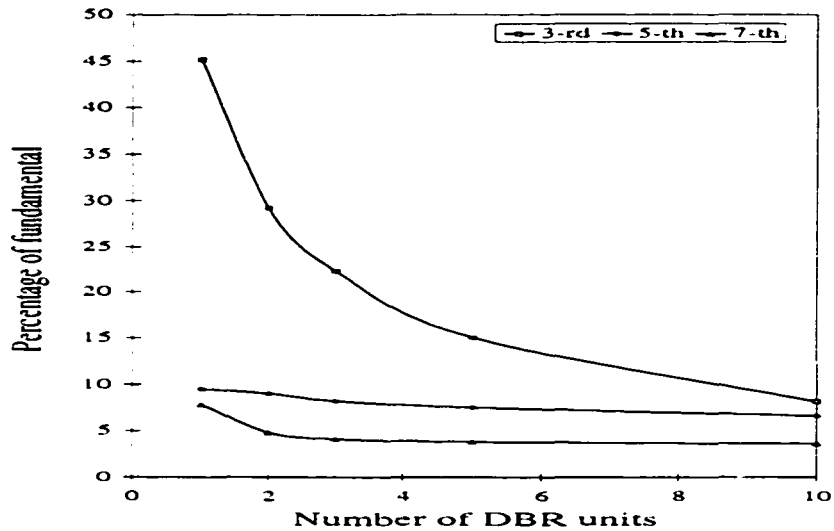

Figure 6.4: The variation of the 3rd, 5th, and 7th harmonic currents with the number of DBR units

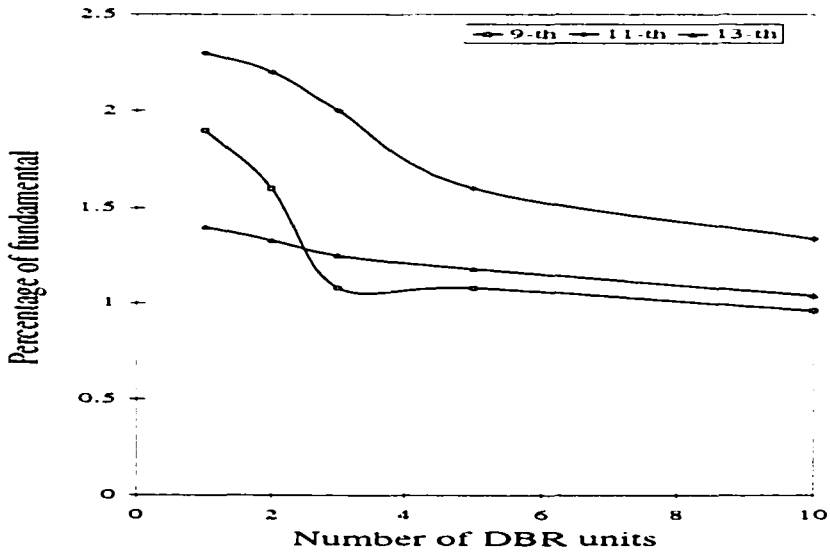

Figure 6.5: The variation of the 9th, 11th *and* 13th harmonic currents with the number of DBR units

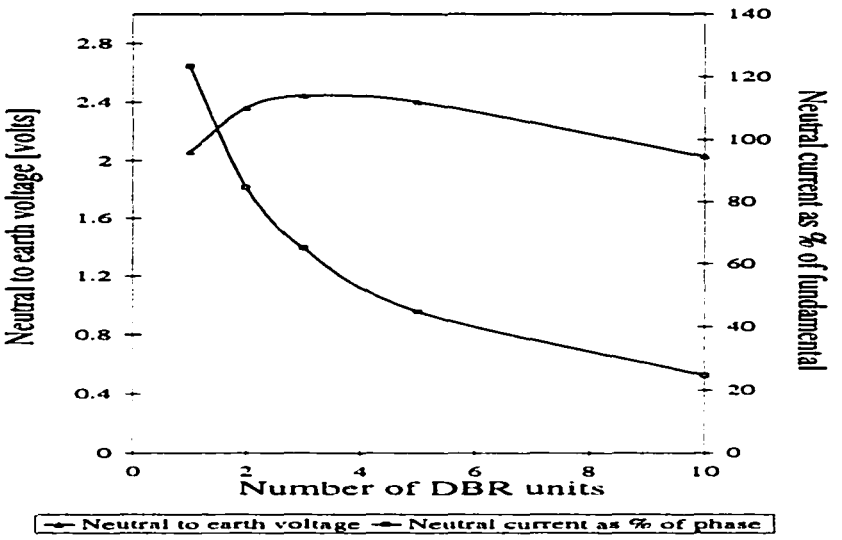

Figure 6.6: Neutral to earth voltage variation with changing the number of DBR units

6.4.3 Effect of load combination

Currents generated from electronic equipment utilizing an input rectifier supplying ripple-smoothing capacitor are very rich in harmonics, especially triplens. These harmonic currents do not upset the end users, but they load neutral conductors. Feeders supplying computer systems alone have experienced high levels of neutral currents that may reach 1.73 times the phase current. However, combining different types of non-linear loads together may result in phase current harmonic cancellation that could end up decreasing the neutral current as well as the system total harmonic distortion.

The variation of the load sharing percentages among a specific load combination may lead to further reductions to neutral currents. In order to study this effect, the three-phase four-wire balanced system described in Figure 6.1 was utilized. The system was loaded with a combination of DBR and magnetic-ballast CFL loads and the load sharing percentage was changed. The system was analyzed under the following constraints:

1. The three-phase system was balanced for all load sharing percentages;

2. The phase currents was constant for all load sharing percentages;

3. The source impedance X/R ratio remained constant; and

4. The load distribution was similar in all phases.

The results are shown in Table 6.5, where the phase current harmonics, neutral current and the system THDI are given for different load sharing percentages. The harmonic contents of the phase current are given in Figures 6.7 and 6.8 respectively.

Table 6.5: Effect of combining different loads on both neutral current and system THD

load sharing %		Percentage of fundamental‡							RMS	THDI	I_N as % of I_{ph}
		3rd	5th	7th	9th	11th	13th	15th			
DBR=100	I_{ph}	61.9	17.7	3.3	2.85	6.3	4.5	0.6	18.34	65.1	—
CFL=0.0	I_N	**$1.4*10^4$**	58	30	**664**	10	7	**100**	28.57	$1.4*10^4$	155.7
DBR=48	I_{ph}	23.8	1.4	2.6	1.1	0.7	0.1	0.5	18.15	24.05	—
CFL=52	I_N	**1090**	34	27	**52**	12	8	**6**	12.39	1093	68.26
DBR=25	I_{ph}	17.35	2.85	2.9	0.9	1.1	0.9	0.4	18.4	17.93	—
CFL=75	I_N	**702**	51	21	**37**	3.5	10.3	**21**	9.9	706	52.8

‡ I_{ph} is based on its own fundamental.

I_N is based on its own fundamental which is very small.

It is apparent from Table 6.5 that, as the percentage sharing of the CFL load increases, the neutral current decreases. This is attributed to the lower triplen harmonic currents generated by this type of load. This result suggests that wherever a high concentration of line-to-neutral power supplies exists, a separate feeder phase is not recommended to supply these loads. Every distribution point might supply one load type, however, the

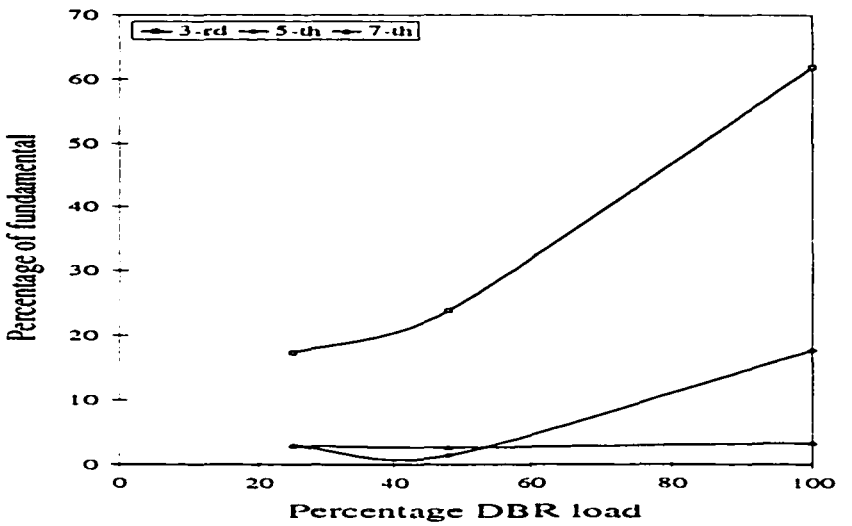

Figure 6.7: 3rd, 5th, and 7th harmonic currents contents due to different combination percentages

phase should supply a mixture of load types. Using more than one feeder to supply a mixture of different load types will help to reduce the system distortion as well as the neutral current magnitude.

6.4.4 Effect of system unbalance

In most three-phase system supplying single-phase loads, there will be some phase imbalance. This will result in some neutral current in addition to the base neutral current that is created by the triplen harmonic generated by different types of non-linear loads. To examine the effect of phase imbalance on the net neutral current generated in three-phase four-wire system, the system described in Figure 6.1 was loaded with fifteen DBR units distributed symmetrically in the three phases to create a balanced system. The neutral current was then calculated and analyzed in order to distinguish its harmonic contents. The next step was to redistribute the same fifteen units in the three phases so as to create some phase imbalance. The neutral current was then recalculated and the effect

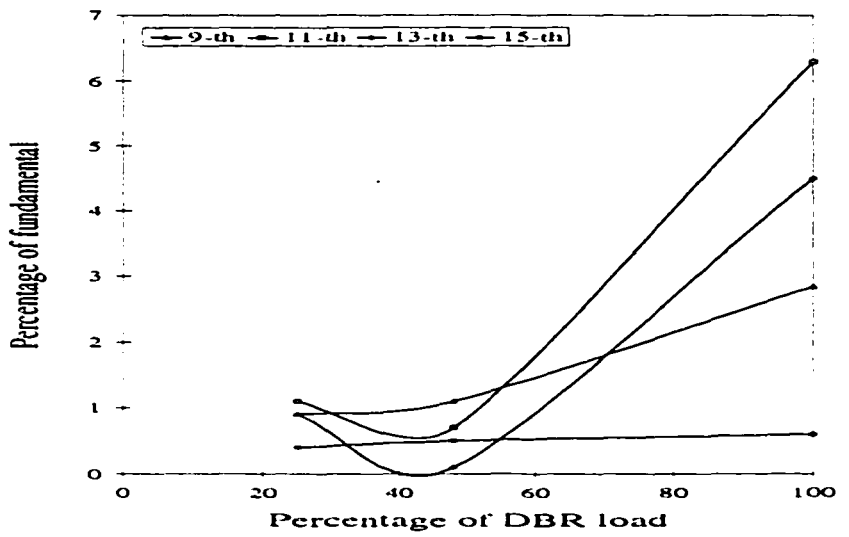

Figure 6.8: 9th, 11th, 13th, and 15th harmonic contents due to different combination percentages

of phase imbalances was studied by calculating the ratio of the neutral triplen harmonic currents to both the total neutral current and the average phase current. These ratios are of interest because they illustrate the extent of the harmonic neutral current loading resulting from simple phase current imbalance. It is worth noting that all the fifteen DBR units were fully loaded and remained at the same loading level throughout the two tests. The results are summarized in Table 6.6.

To evaluate the effect of the phase imbalance on the total neutral current magnitude, the share of both triplen and non-triplen harmonic currents in the neutral current has to be determined. The share of the triplen harmonic currents will be given by:

$$I_{TR} = \frac{\sum_{n=3}^{\infty} I_n^2}{I_N^2} \quad , \ (n \in 3, 9, 15, \ldots etc.) \tag{6.2}$$

Table 6.6: Phase and neutral current harmonics in balanced and unbalanced three-phase four-wire system

Condition		Percentage of fundamental‡							RMS	THDI	I_N as % of I_{ph}
		3rd	5th	7th	9th	11th	13th	15th			
Bal.	I_A	20.72	10.45	4.28	1.36	1.36	1.26	0.6	31.96	23.75	
	I_B	20.80	10.45	4.27	1.36	1.38	1.27	0.6	31.87	24.0	
	I_C	20.70	10.45	4.27	1.36	1.38	1.27	0.6	31.95	23.64	
	I_N	**$4.66*10^4$**	306	179	**2948**	26	36	**1224**	19.48	$4.67*10^4$	61.0
Unbal.	I_A	21.11	9.3	4.7	1.8	0.6	1.2	1.04	31.52	23.73	
	I_B	28.1	11.7	2.66	3.27	1.65	1.47	0.8	22.57	30.9	
	I_C	17.94	8.04	4.2	2.5	0.9	0.9	0.67	39.82	20.34	
	I_N	**126.7**	16.98	5.3	**3.2**	5.96	0.7	**0.3**	23.49	128	74.5

‡ I_{ph} is based on its own fundamental.

I_N is based on its own fundamental which is very small.

and the share of the non-triplen harmonic currents will be given by:

$$I_{NTR} = \frac{\sum_{k=1}^{\infty} I_k^2}{I_N^2} \quad , \ (k \in 1, 5, 7, 11, \ldots etc.) \tag{6.3}$$

where:

I_{TR} = Share of the triplen harmonics in the total neutral current;

I_{NTR} = Share of the non-triplen harmonics in the total neutral current;

I_N = RMS value of the total neutral current;

I_n = RMS value of the triplen harmonic components; and

I_k = RMS value of the non-triplen harmonic components.

Table 6.7 illustrates the share of both triplen and non-triplen harmonic currents in the total neutral current. The ratio of both neutral triplen and non-triplen harmonic currents to the average phase current is also given. The contributions of each harmonic component in the neutral current magnitude in both balanced and unbalanced cases are shown in Figure 6.9.

Table 6.7: Neutral triplen and non-triplen harmonic currents share in the total neutral current in balanced and unbalanced cases

Condition	% share in neutral current		as % of average phase current	
	Triplen	Non-triplen	Triplen	Non-triplen
Balanced	100.0	0.0	61.02	0.0
Unbalanced	60.8	39.2	45.34	29.23

Tables 6.6 and 6.7 show that since neutral current portion which results from phase imbalance will vanish as the loads are better balanced, then the total neutral current will be minimized. The system neutral to earth voltage is also decreased slightly with balancing the system.

6.5 Assessment

In this chapter, a rigorous investigation was carried out to examine the effects of different system parameters on the generation of neutral current in three-phase four-wire distribution circuits. The iterative approach described in Chapter 4 was employed to account for the voltage and current harmonics interactions (attenuation effect).

The neutral current in three-phase distribution system is often thought to be the result

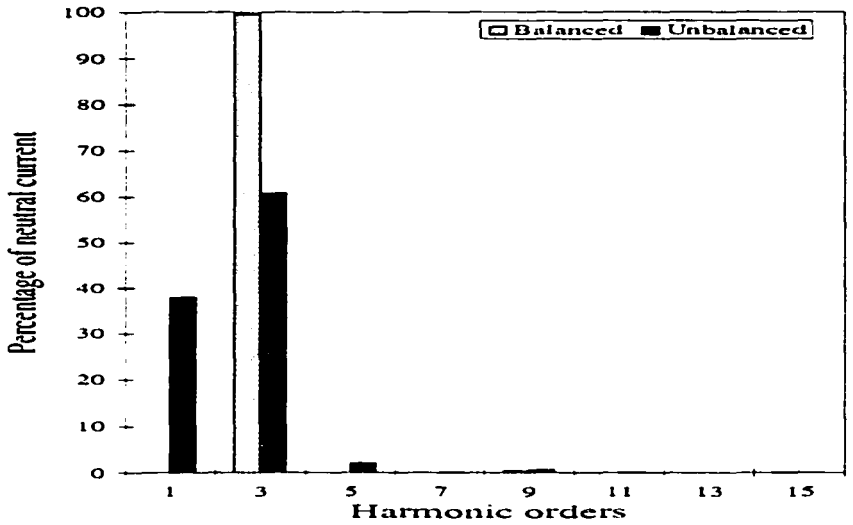

Figure 6.9: Different harmonic currents contribution to the neutral current in both balanced and unbalanced case

of an imbalance in the phase currents. However, with high concentrations of non-linear loads which inject currents that are very rich in triplen harmonics, even perfectly balanced systems will have significant neutral currents. The percentage sharing of different harmonic currents in the neutral current shows that the triplen harmonic currents have the highest share. This is true even in unbalanced systems where the non-triplen harmonics contribute not more than 40% of the total neutral current. It is strongly recommended that the loading on the three phases should be kept as balanced as possible, and in this way, the neutral current in excess of the triplen harmonic current is minimized.

It was found that the loading level of the three-phase system is one of the major factors that affects the neutral current level and, hence, the neutral to earth voltage. Although increasing the system loading level will help reduce the neutral current magnitude as a percentage of the phase current, systems consisting mainly of non-linear loads should not be loaded to their full load capacity since this may cause overheating of transformers and excessive voltage distortion. Combining different types of non-linear loads is important

for enhancing system quality and controlling both neutral current and neutral to earth voltage magnitudes. It is strongly recommended to avoid concentrating load types that utilize the single-phase line-to-neutral electronic power supplies in only one feeder. Mixing these loads with other load types such as magnetic ballast CFL loads will help bring the system distortion, neutral current magnitude and neutral-to-earth voltage to acceptable levels.

Modern distribution systems are drifting towards the use of different non-linear and electronically switched loads. This trend has led to a tremendous increase in the harmonics propagating throughout the systems, resulting in severe power quality problems. Having demonstrated the effects that different system parameters have on the generation and propagation of distribution system harmonics, it becomes apparent that there is a need for a method that can improve system power quality. The following chapter will concentrate on the investigation and analysis of a comprehensive design algorithm of passive filters that are capable of improving the distribution system quality by decreasing system harmonic levels.

Chapter 7

Harmonic Mitigation Using Reactance One-Port Networks

In the previous three chapters, the system harmonic performance as affected by different parameters, was investigated. This chapter will be directed towards designing a reliable and efficient compensator in order to improve the system power quality. The previously investigated parameters, including both attenuation and diversity effects, will be considered in the design of this compensator. Section 7.1 offers a brief introduction to the different methods utilized for harmonic distortion suppression. A detailed description of the algorithm employed in the estimation of the non-linear load susceptance is presented in Section 7.2. Section 7.3 presents the reactance one-port synthesis procedure. The obtained simulation results are presented and discussed in Section 7.4. Section 7.5 offers some experimental results aimed to support the simulation findings. In Section 7.6, the designed compensator sensitivity to both compensator parameter's values and system load variation are examined. Finally, Section 7.7 offers a brief assessment.

7.1 Introduction

Harmonic distortion in power systems has escalated in recent years due to the large amount of electrical energy that is conditioned by power electronic devices as well as other non-linear loads. Devices such as rectifiers, inverters and fluorescent lamps lead to non-linear current waveforms that are fed into the supply system. The effect of harmonics in the supply lines is an increase in the distribution system losses and a general degradation of the quality of the supply. Harmonics have been also shown to have deleterious effects on equipment including transformers, rotating machines, switchgears, capacitor banks, fuses and protective relays [31, 32].

In order to maintain the supply quality at an acceptable level, national standards such as IEC 1000-3-2 (Europe) and IEEE-519 (USA) recommend limits for harmonic levels at various points within the system. IEEE-519 (Appendix C) limits harmonics primarily at the service entrance while IEC 1000-3-2 is applied at the terminals of end-user equipment. Therefore, IEC limits will tend to reduce harmonic related losses in building wiring, while IEEE harmonic limits are designed to prevent interactions between neighbors and power systems. These differences have been described and analyzed in [109]. To comply with these harmonic standards, systems utilizing power electronic and non-linear loads must either add substantial hardware or undergo redesign. The additional hardware is a passive or active line-current shaping circuit which is inserted in parallel between the line and the rest of the equipment (point of common coupling PCC).

The most popular single-phase active line-current shaping circuit is the boost rectifier [110] which can provide an essentially harmonic free line current waveform. Other active electronic devices such as active filters [15, 82, 111, 112], electronic voltage regulators and adaptive VAR compensators can be utilized in the harmonic suppression process. Because power-electronic based equipment is composed of elements that control electrical

energy using power semiconductor devices, these equipment can cause further distortion to the distribution system because of the inherent nonlinearity associated with the semiconductor elements and the switching operations involved in their use. Additional drawbacks are the high cost, reduced reliability and injection of high frequency noise into the line.

In passive solutions, the undesired harmonic currents may be prevented from flowing into the power system by one of the following two methods:

1. Using a high series impedance to block them; or

2. Diverting them by means of a low impedance shunt path.

Series filters must carry full load current and be insulated for full line voltage. In contrast, shunt filters carry only a fraction of the current that a series filter must carry. The series filter also causes high voltage distortion due to the harmonic voltage drop created by the line current and the system series impedances. Given the greater expense of a series filter, and the fact that shunt filters may supply reactive power at fundamental frequency, it becomes apparent that the most practical approach is to install shunt filters.

The shunt passive circuits that are used to reduce the distribution system current and voltage harmonics can be divided into four types. The first is to use shunt capacitors [66, 74, 113, 114] which can effectively reduce the harmonic levels, but sacrifices the 60Hz performance. Moreover, shunt capacitors may generate unexpected harmonic voltages due to the series resonance between the capacitor and the inductive source impedance at some harmonic frequencies. This resonance will provide a low impedance path for the harmonic currents injected by loads at neighboring buses.

The second method is to use a shunt Two Element Series LC compensator TESLC [87, 89]. The main function of the TESLC compensator is to compensate for the harmonic reactive power and thus improve the system power factor and reduce the voltage harmonic.

However, since the susceptance of the load and of the TESLC compensator are increasing functions of frequency, then only one frequency exists for which both susceptances mutually compensate. This frequency should be in the vicinity of the fundamental frequency. Therefore, despite the higher power factor value gained by TESLC compensators, the source current harmonics in the circuit having such a compensator are higher than they are in the non-compensated circuit. Only the fundamental is reduced, but at the expense of increasing the remaining harmonics.

The third method to reduce system harmonics is to employ a single-tuned or notch filter. This filter is one of the most popular shunt filters and is dependent on the provision of a low impedance path to the current at the frequency for which it is tuned [115]. A common method of reducing harmonic currents is to install banks of individually tuned filters at the power supply terminals, one filter per phase for each harmonic to be attenuated. The main drawback of this solution, however, is the cost associated with installing banks of tuned filters. Such expense is only justifiable when it is necessary to compensate large amounts of reactive power. Another disadvantage of the notch filter is the creation of parallel resonance peaks which result from the interaction between the filters and the inductive source impedance. These resonance peaks always occur at frequencies lower than the frequencies for which the filters are tuned.

Another tuned filter is the high-pass filter that has a characteristically low impedance above some corner frequency. This filter can shunt a large percentage of all harmonics at or above the corner frequency. An obvious solution to the harmonic problem is to employ one high-pass filter whose corner frequency is located at the lowest harmonic which is to be eliminated. Unfortunately, two factors may discourage such an application:

1. The minimum impedance of the high-pass filter in its passband never achieves a value comparable to that of the single-tuned filter at its notch frequency; and

2. The shunting of a large percentage of all system harmonics through one filter may require that filter to be vastly overrated from the fundamental frequency point of view.

The fourth method of compensating harmonic reactive power and reducing harmonic distortion is to utilize a reactance one-port network. This method can provide total compensation of harmonic reactive power and minimize both current and voltage distortion for different harmonic frequencies simultaneously. The main drawbacks of this method is its complexity and difficulty in determining the necessary number N of reactance elements. According to [90], the compensating one-port for M harmonics has complexity $N = M(2M-1)$. Though it is hard to expect that at such a high complexity this compensator could have a practical meaning, in [79] it was shown that the required complexity is much lower, not higher than:

$$M \leq N \leq 2M - 1 \tag{7.1}$$

Thus, such a compensation can be taken into account. In [16, 79] a reactance one-port compensator has been employed successfully to reduce the current harmonics generated in circuits having linear loads and feed from a source of periodic nonsinusoidal voltage supply having zero internal impedance. Although this method gave a total compensation of the reactive power and improves the system power factor greatly, it did not address two crucial concerns:

1. The distribution system is heavily loaded with different non-linear loads; and

2. The source inductive impedance can not be neglected in any practical system. The presence of such impedance will allow for the voltage and current harmonic interaction to be accounted for.

The goal of this chapter is to design reactance one-port compensators capable of reducing the voltage and current harmonics generated in circuits having different types of non-linear loads and are being supplied from a voltage source that has internal inductive impedance. In order to accomplish this task, two important issues have to be resolved. The first is the determination of the accurate voltage and current waveforms and the second is the calculation of the non-linear load susceptances that are needed for the compensator design. Both issues have to take into account both the attenuation and diversity phenomena. While the first issue was thoroughly investigated in the previous three chapters, the calculation of the non-linear load susceptances will be the aim of the next section.

7.2 Equivalent load susceptance calculation

One of the important quantities in the design and testing of a harmonic filter is the impedance of the system at the harmonic frequencies as seen at the harmonic filter's bus. This impedance can cause resonance with the harmonic filter. The value of this impedance at a given time depends on the configuration, load level and operating condition of the system at that time. In the case of linear loads, the load impedance at different harmonic frequencies can easily be calculated using the superposition principle, however, in circuits with non-linear loads, the situation is more complicated. In [116, 117] it was assumed that if the bus bar voltage is purely sinusoidal, then the AC network harmonic impedance can be evaluated by the ratio between the harmonic voltage and the harmonic current. However, this method suffers from two major drawbacks. The first is that superposition is not applicable in non-linear circuits, and the second is the assumption that the non-linear loads are represented by constant magnitude harmonic current injection sources. This latter assumption implies that the voltage and current harmonic interactions are

neglected.

In order to account for the attenuation effect while calculating the non-linear load susceptance at different harmonic frequencies, a time-domain approach was utilized. This approach was used to estimate a single-phase as well as balanced three-phase susceptances for the load-side network seen at a bus. The employed procedure can be described as follows:

Step I From the voltage and current waveforms obtained in Chapter 5, observe whether the current leads or lags the voltage. This will give an indication of whether the equivalent load is inductive or capacitive.

Step II Depending on the load impedance type, insert either an inductor or a capacitor in parallel at the point of common coupling. For capacitive loads, an inductor will be inserted.

Step III For a capacitive load, change the inserted parallel inductor value in steps. For each step calculate the supply current by running the EMTP program.

Step IV Perform Fast Fourier Transform FFT on the total supply current in order to obtain its harmonic contents.

Step V Keep changing the inserted coil value and observe the harmonic contents for each variation until a minimum current at a specified harmonic frequency n is reached. In this case the value of the coil susceptance at that frequency n will be equal to the negative of the load susceptance at that frequency.

Step VI Tune the coil again until a minimum current at a different harmonic frequency is reached.

Step VII Repeat for all harmonics of interest.

This procedure is summarized by the flow chart given in Figure 7.1. Having calculated the non-linear load susceptances at the required harmonic frequencies, the subsequent section will focus on the design procedure of a reactance one-port network.

7.3 Reactive power compensation

In order to achieve the minimum voltage and current distortion, the current harmonics should have minimum values and their reactive components should be compensated. To accomplish this task, the proposed filter should have for each harmonic n :

$$B_{Cn} = -B_{Ln}. \tag{7.2}$$

Where,

B_{Cn} = Reactance one-port compensator susceptance at harmonic n.

B_{Ln} = Load susceptance at harmonic n.

This condition cannot be fulfilled, in general, by a TESLC compensator, so a more complex one-port is required. According to [79], for M harmonics, it has been proven that the necessary number of reactance elements N is given by: $M \leq N \leq 2M - 1$. If an inductive behavior of the compensator is desired, an additional reactance element is required. In such a case, the compensator complexity will be:

$$N = 2M. \tag{7.3}$$

The compensator complex admittance $Y_c(S)$ or complex impedance $Z_c(S)$, where S is the complex variable, is determined by the number of parameters equal to its complexity, or, $2M$. However, according to Equation 7.2 there are only M equations. Thus the remaining M parameters may be chosen arbitrarily by assuming the values of the

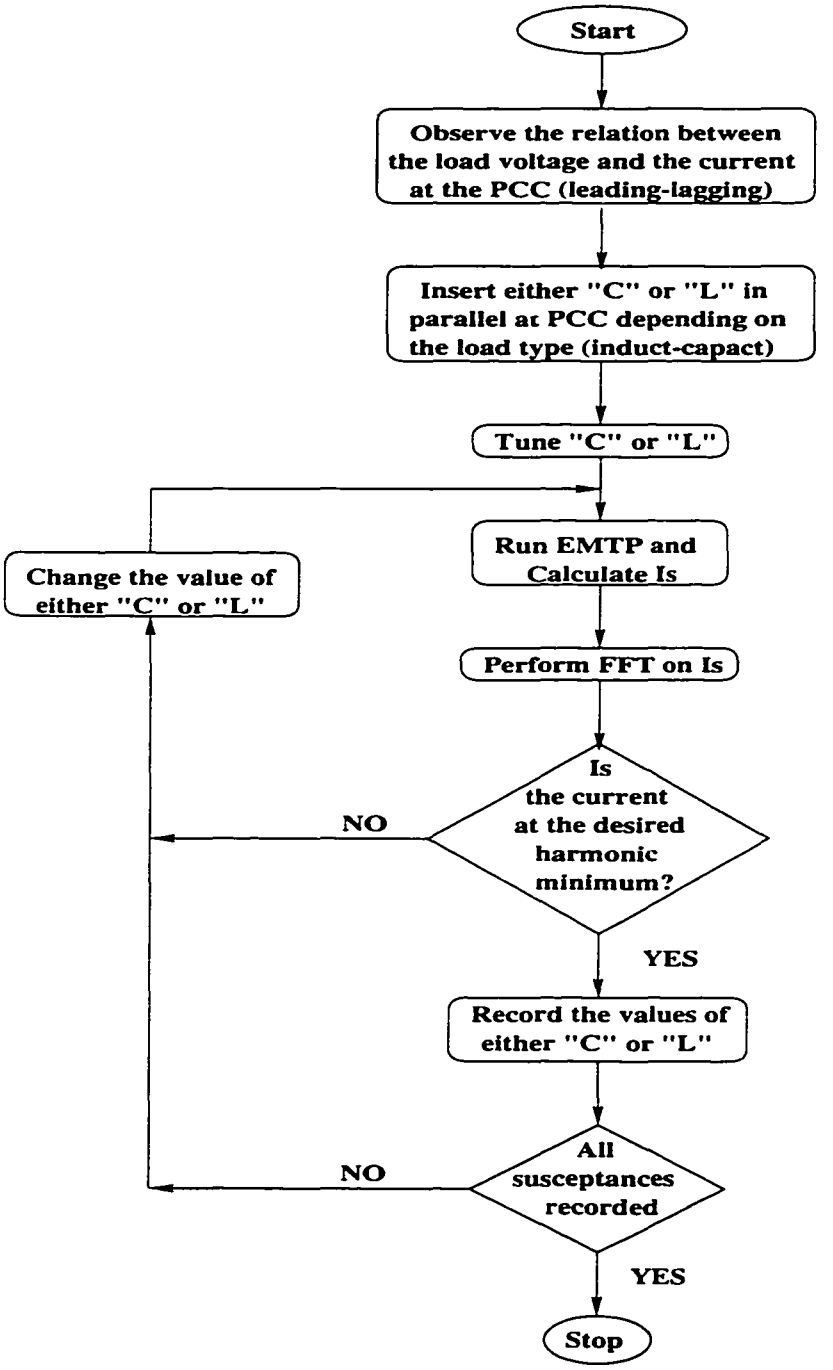

Figure 7.1: Flow chart describing the non-linear load susceptance calculation

compensator poles.

7.3.1 One-port network synthesis

In order to illustrate the reactance one-port compensator synthesis procedure [91], a compensator will be assumed, having a complex admittance in the form:

$$Y_c(s) = As\frac{(s^2+Z_1^2)(s^2+Z_2^2)}{(s^2+P_1^2)(s^2+P_2^2)(s^2+P_3^2)}. \tag{7.4}$$

Where

'A' is the gain, and A$\geq$0.

Z_1 *and* Z_2 are the compensator's zeros and P_1, P_2 *and* P_3 are the compensator's poles.

If the one-port compensator is to be designed to compensate for n harmonics, where $n \in \{1,3,5\}$, the compensator locus will be the line joining the negative of the load susceptances at these frequencies. The compensator susceptance function $B_C(\omega)$ should has the locus given in Figure 7.2 and the compensator poles and zeros should satisfy the following equation:

$$\begin{aligned} 1 \leq P_1 \leq Z_1 \leq 3 \\ 3 \leq P_2 \leq Z_2 \leq 5 \\ 5 \leq P_3 \end{aligned} \tag{7.5}$$

The numerator of Equation 7.4 can be expressed in the form:

$$As(s^2+Z_1^2)(s^2+Z_2^2) = a_5s^5 + a_3s^3 + a_1s. \tag{7.6}$$

The coefficients a_1, a_3 *and* a_5 can be determined using Equation 7.2, and substituting

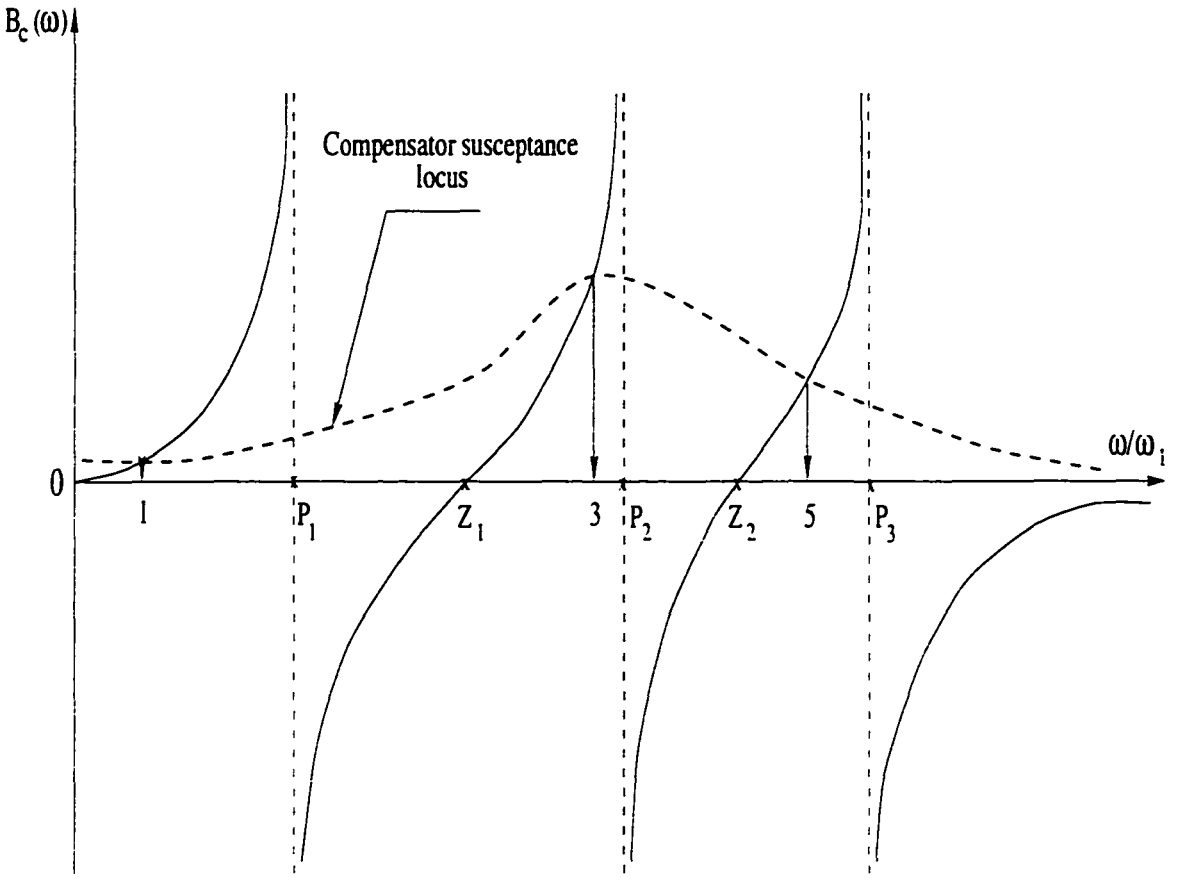

Figure 7.2: Plot of the compensator susceptance locus for 1st, 3rd *and* 5th harmonic reactive power compensation

for $s = jn$, where $n \in \{1, 3, 5\}$. The equation:

$$Im\{Y_c(jn)\} = -B_{Ln}, \tag{7.7}$$

results in

$$a_5 n^5 - a_3 n^3 + a_1 n = -B_{Ln}(P_1^2 - n^2)(P_2^2 - n^2)(P_3^2 - n^2). \tag{7.8}$$

If the load susceptances at different harmonic frequencies are known, Equation 7.8 can

be solved for the values of the coefficients a_1, a_3 *and* a_5 which will reveal the compensator admittance. By using the partial fractions method, the compensator admittance can be simplified to the following form:

$$Y_c(s) = \frac{As}{(s^2 + P_1^2)} + \frac{Bs}{(s^2 + P_2^2)} + \frac{Cs}{(s^2 + P_3^2)}. \tag{7.9}$$

Where A, B and C are known constants. Finally, the compensator will be constructed according to the form illustrated in Figure 7.3, where:

$$\begin{aligned} L &= \frac{1}{A}, and \\ C &= \frac{A}{P^2}. \end{aligned} \tag{7.10}$$

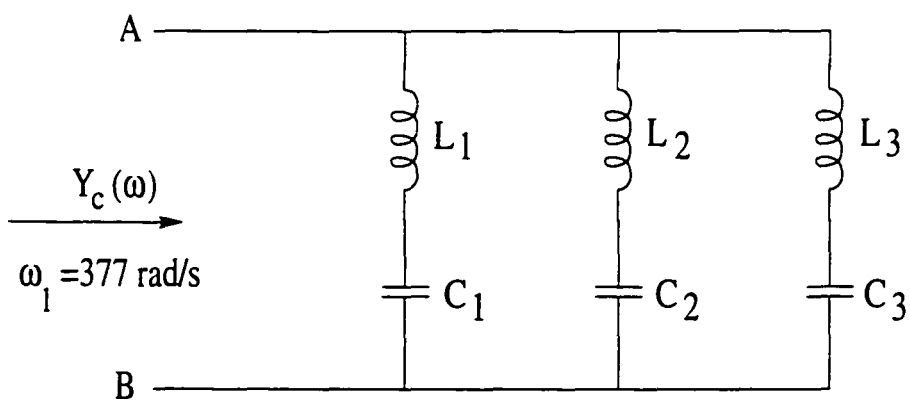

Figure 7.3: One-port compensator for inductive loads harmonic reactive power compensation

The compensator with the configuration given in Figure 7.3 is normally used to reduce the harmonic reactive power in the case of non-linear loads that have inductive behavior. However, in the case of non-linear loads that behave capacitively, the compensator

function should be expressed as an impedance function rather than an admittance function. The same synthesis procedure should be utilized in obtaining such a filter. The impedance function will be in the form:

$$Z_c(s) = As\frac{(s^2+Z_1^2)(s^2+Z_2^2)}{(s^2+P_1^2)(s^2+P_2^2)(s^2+P_3^2)}. \tag{7.11}$$

The equation:

$$Im\{Z_c(jn)\} = -\frac{1}{B_{Ln}}. \tag{7.12}$$

results in

$$a_5n^5 - a_3n^3 + a_1n = -\frac{1}{B_{Ln}}(P_1^2-n^2)(P_2^2-n^2)(P_3^2-n^2). \tag{7.13}$$

The compensator complex impedance will be in the form:

$$Z_c(s) = \frac{As}{(s^2+P_1^2)} + \frac{Bs}{(s^2+P_2^2)} + \frac{Cs}{(s^2+P_3^2)}. \tag{7.14}$$

Finally, the compensator will has the construction given in Figure 7.4, where:

$$\begin{aligned} L &= \frac{A}{P^2}, and \\ C &= \frac{1}{A}. \end{aligned} \tag{7.15}$$

It is important to note that despite the same structure, the compensator considered here is not a 'harmonic filter' in the sense of it being used in distribution systems. Notch harmonic filters are in voltage resonance for some harmonic frequencies. These harmonics are part of the frequencies generated by the non-linear loads, so, the notch filter forms for

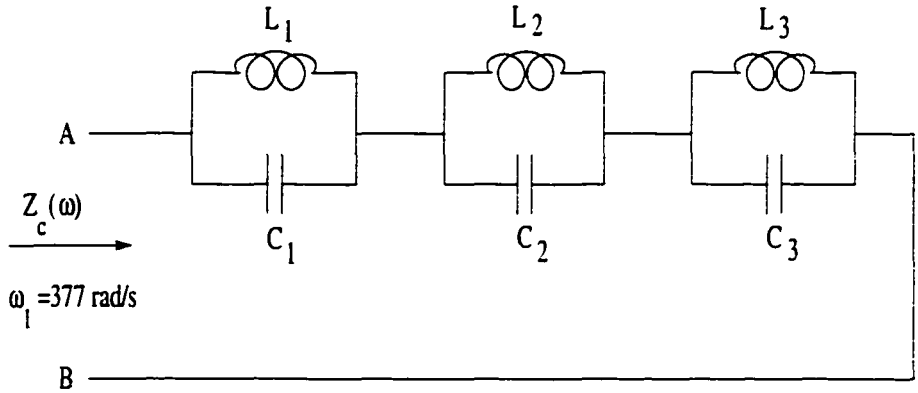

Figure 7.4: One-port compensator for capacitive loads harmonic reactive power compensation

them a low impedance path. In contrast to a normal harmonic filter, the compensator being considered is in current resonance with the load and this resonance appears simultaneously for all harmonics of order from the set M that the compensator is designed for. This will result in a maximum impedance for these harmonics at the point of common coupling. Thus, the source current harmonics will have the minimum rms current and consequently the load voltage distortion will be minimized. Due to its complexity, this compensator is only recommended in cases of strongly distorted voltage with small numbers of harmonics. Moreover, it is also recommended for high demands as to current harmonic reduction.

7.4 Simulation results

Some previous studies of distribution system harmonic performance [118, 119] have investigated the nature of small, widely distributed harmonic sources. In [106, 118], it was shown that these loads will generate smaller currents at higher frequencies. Moreover, the phase angles of these currents are widely distributed, resulting in a high degree of cancellation. At the lower harmonic frequencies, especially the third and the fifth har-

monics, the cancellation will be insignificant so, there will be harmonic excitation at these frequencies.

More recently, measurements of harmonic levels on distribution systems have been performed [120–123]. These measurements show a dominance of the lower order harmonics for a majority of cases including many large industrial sites. Accordingly, the reactance one-port compensators utilized in this study were designed in order to compensate for both the third and the fifth harmonic reactive powers. Although this compensator is only designed to suppress the 3rd and the 5th harmonics, it can be designed to cancel more harmonics. The next subsection will illustrate the compensator design through a numerical example and the subsequent subsections will show the simulation results for the different case studies.

7.4.1 Numerical example

In order to illustrate how the reactance one-port compensator can reduce the harmonic reactive power of a circuit having a non-linear load while, consequently, reducing the current total harmonic distortion THDI, let us consider the following example [124]:
A 0.34 Kw DBR load that is supplied from a 110V (RMS) sinusoidal source is considered. The voltage source has an internal inductive impedance that is equal to $0.8 + j0.94\,\Omega$. The DBR load has a smoothing capacitor of $1000\mu F$ and the DC load resistance is equal to 20Ω. Since this load behaves capacitively due to the presence of the smoothing capacitor, a tuned inductor is to be utilized in order to estimate the equivalent load susceptance at different harmonic frequencies n, where $n \in \{1, 3, 5\}$. The procedure previously described in section 7.2 will be utilized in order to accomplish this task. The non-linear load susceptances were found to be: $B_1 = 0.044S$, $B_3 = 27.8S$ *and* $B_5 = 8.5S$. The plot of the required susceptance function $Y_c(\omega)$ is given in Figure 7.2. The compensator will have such a susceptance if its impedance is in the form given in Equation 7.11. The values of the

compensator poles and zeros should be governed by Equation 7.5. Assuming, for example, the values of the required compensator poles are: $P_1 = 1.2$, $P_2 = 4.0$ *and* $P_3 = 8.0$, substituting in Equation 7.13 and solving these equations will result in the compensator impedance given as:

$$Z_c(s) = \frac{50.9s^5 + 1695.0s^3 + 11050s}{(s^2 + 1.2^2)(s^2 + 4.0^2)(s^2 + 8.0^2)}. \tag{7.16}$$

This equation can be further simplified, resulting in:

$$Z_c(s) = \frac{9.566s}{(s^2 + 1.2^2)} + \frac{4.37s}{(s^2 + 4.0^2)} + \frac{36.96s}{(s^2 + 8.0^2)}. \tag{7.17}$$

Utilizing Equation 7.15, the compensator elements can be determined. The resulting compensator will has the structure shown in Figure 7.5.

Inserting this compensator in parallel with the DBR load will reduce the THDI from 58.9% to 8.6%. Also the load voltage total harmonic distortion THDV will be reduced from 14.57% to 5.09%. The waveforms of the supply current and the load voltage, before and after inserting the compensator, are given in Figures 7.6 and 7.7 respectively. The change in the supply current harmonic contents due to the insertion of the reactance one-port compensator is illustrated in Figure 7.8.

7.4.2 PAVC load

The same design procedure described in subsection 7.4.1 will be followed to design a reactance one-port compensator capable of reducing both current and voltage harmonic distortion in a circuit having a PAVC load [125]. The thyristors were supplied from a 110V (RMS) source that has an internal inductive impedance. The load resistance is taken equal to 10Ω and the thyristors firing angles are adjusted to 45°. For harmonic frequencies n, where $n \in \{1, 3, 5\}$, the non-linear load susceptances were found to be:

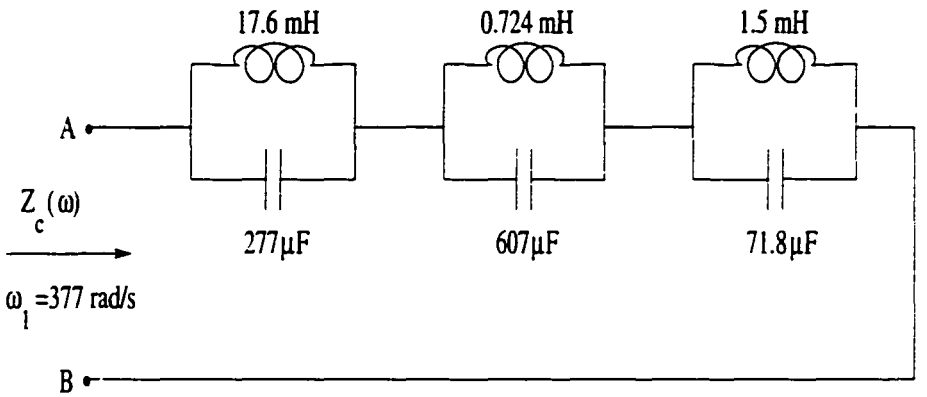

Figure 7.5: One-port compensator for DBR load reactive power compensation

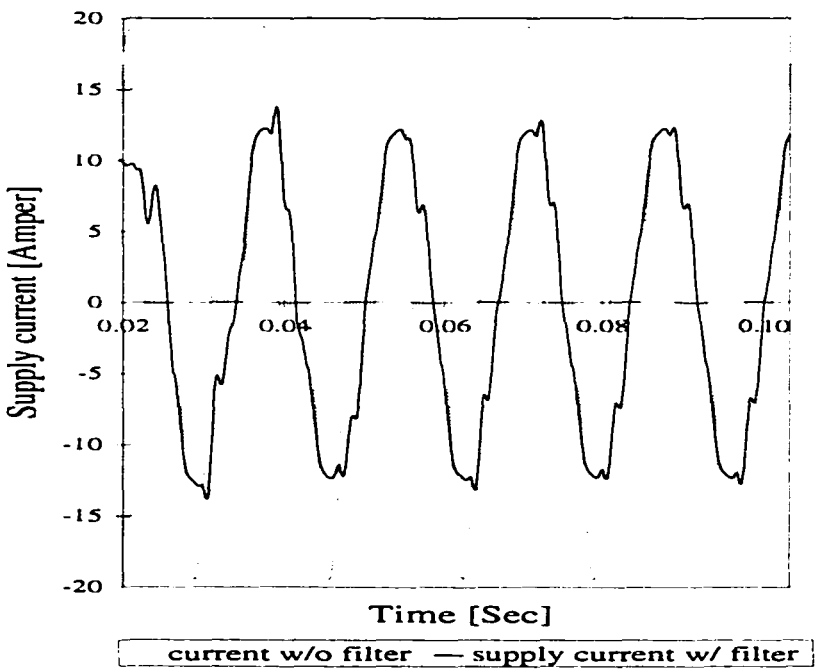

Figure 7.6: Supply current of circuit having DBR load before and after compensation

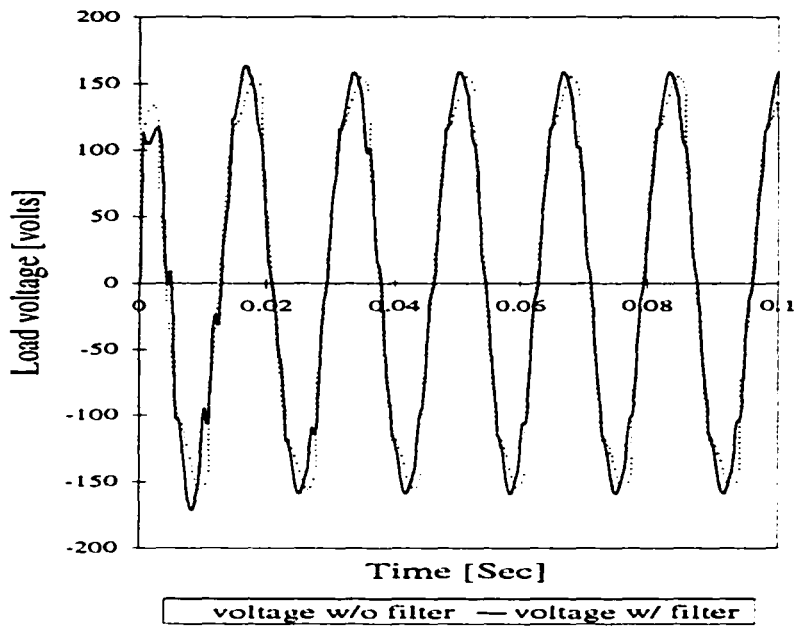

Figure 7.7: Load voltage of circuit having DBR load before and after compensation

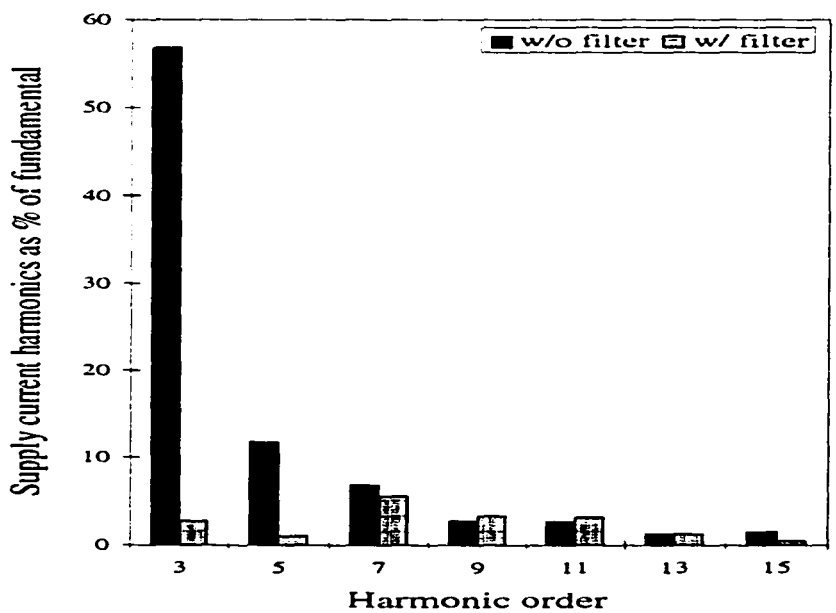

Figure 7.8: Net harmonic currents for DBR load with and without reactance one-port compensator

$B_1 = 0.014S$, $B_3 = 6.31S$ *and* $B_5 = 2.52S$. The compensator will has an impedance function given as:

$$Z_c(s) = \frac{30.3s}{(s^2 + 1.2^2)} + \frac{13.97s}{(s^2 + 4.0^2)} + \frac{113.69s}{(s^2 + 8.0^2)}. \tag{7.18}$$

The designed compensator structure and parameters are shown in Figure 7.9, where the inductive and capacitive elements are obtained according to Equation 7.15. Applying this compensator will result in the improvement of the THDI from 16.63% to 5.32% and the THDV from 26.3% to 11.2%. The waveforms of both supply current and load voltage, with and without the compensator, are presented in Figures 7.10 and 7.11 respectively. Figure 7.12 illustrates the reduction in the supply current harmonic contents due to the insertion of the compensator.

7.4.3 Three-phase four-wire circuit

In order to further demonstrate the capability of the proposed reactance one-port compensator, simulations were performed on a three-phase four-wire system that was loaded with a combination of DBR and CFL loads [126]. The DBR sharing in the phase current was kept at 50%. On four-wire balanced systems loaded with non-linear loads, the neutral current constitutes a major problem and hence, the proposed filter should be capable of reducing the neutral current to the lowest level. A reactance one-port network was designed for this purpose following the previously outlined procedure. Utilizing the non-linear load susceptance calculation algorithm described in section 7.2, the equivalent load susceptances were found to be: $B_1 = 0.033S$, $B_3 = 16.08S$ *and* $B_5 = 5.31S$. The compensator impedance function was found to be given as:

$$Z_c(s) = \frac{12.76s}{(s^2 + 1.2^2)} + \frac{5.86s}{(s^2 + 4.0^2)} + \frac{97.97s}{(s^2 + 8.0^2)}. \tag{7.19}$$

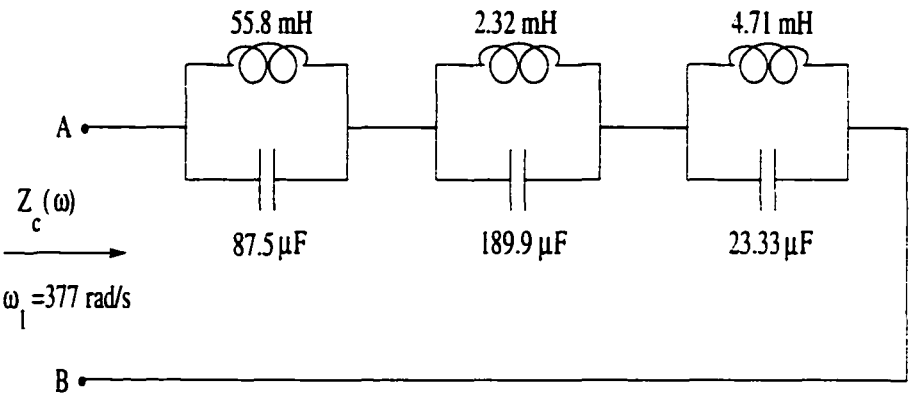

Figure 7.9: One-port compensator for PAVC load reactive power compensation

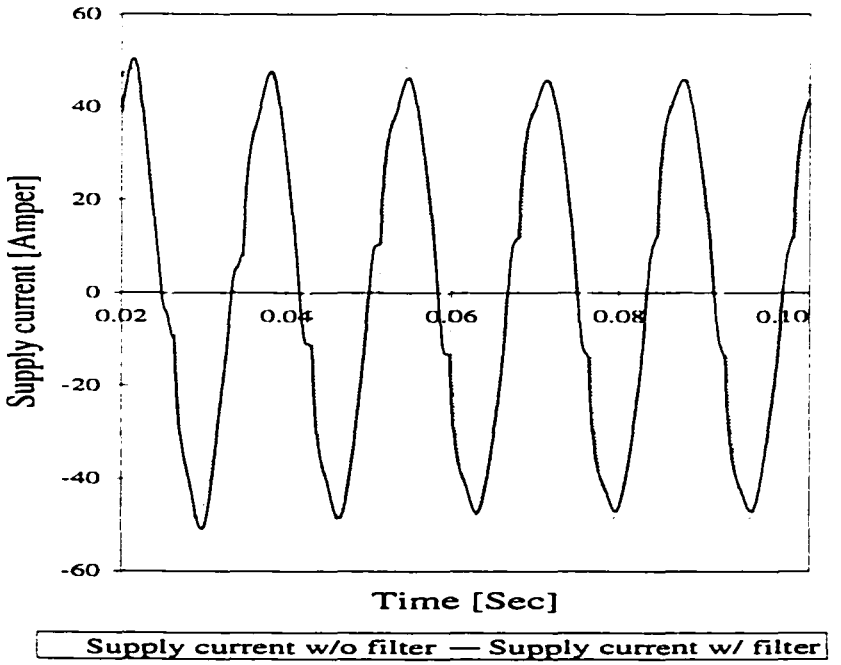

Figure 7.10: Supply current of circuit having PAVC load before and after compensation

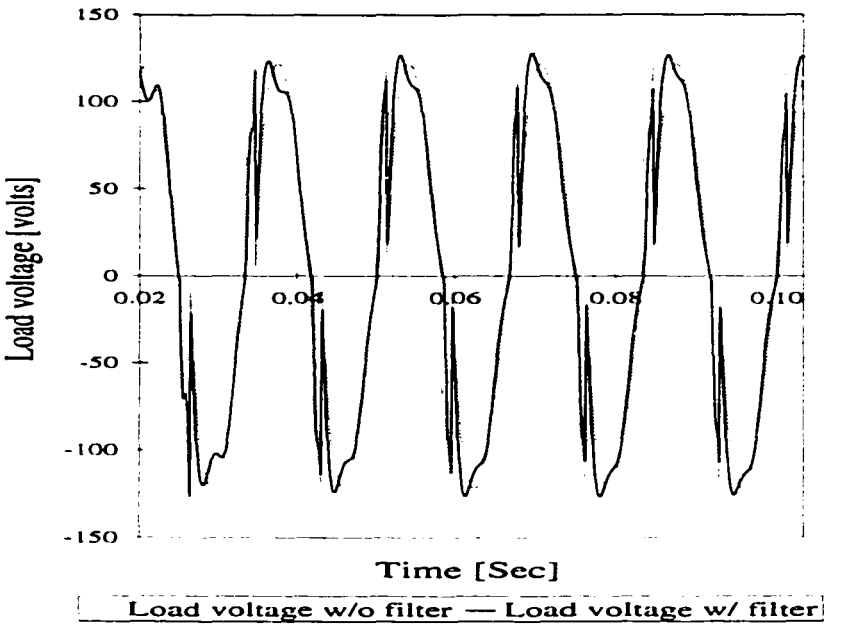

Figure 7.11: Load voltage of circuit having PAVC load before and after compensation

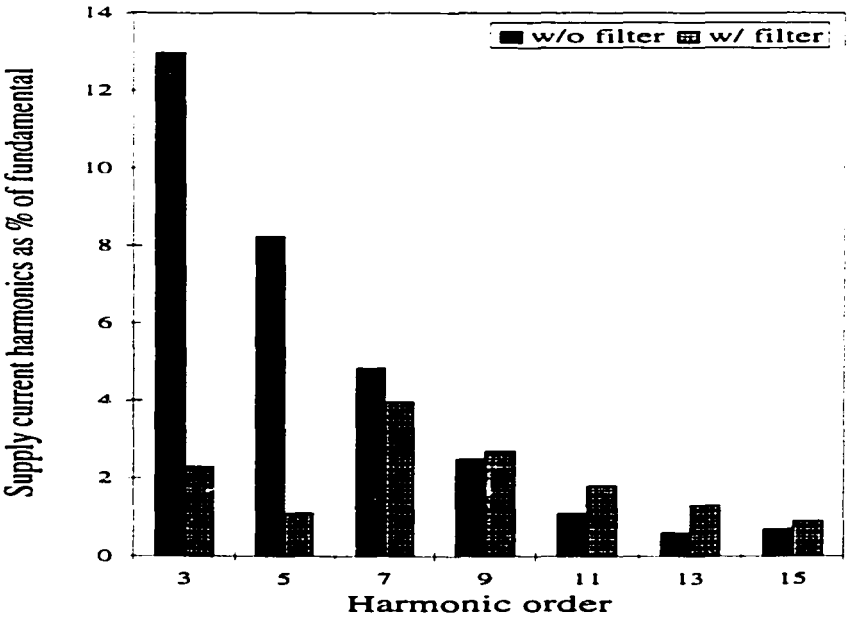

Figure 7.12: Net harmonic currents for PAVC load with and without reactance one-port compensator

The compensator had the structure and parameters shown in Figure 7.13. The application of this filter in parallel with the load in each phase resulted in the reduction of the THDI from 19.62% to 3.51% as well as the reduction of the THDV from 19.42% to 4.18%. The system neutral current magnitude was reduced from 9.08 Amp. to 0.954 Amp. as a result of the filter application. The RMS and THD values for the phase currents, the phase voltages and the neutral current are given in Table 7.1. The waveforms of the supply current, load voltage and neutral current, before and after inserting the filter, are given in Figures 7.14, 7.15 and 7.16 respectively. The harmonic content of the supply current (phase A), before and after the compensation, is presented in Figure 7.17.

7.4.4 Test distribution system

The reactance one-port compensator was further examined utilizing a more complex distribution system [127] that is given in Figure 7.18. The distribution system feeder section data are listed in Table 5.1. The proposed three-phase secondary distribution system supplied a mixture of non-linear and linear loads and the system was loaded until it reaches its rated capacity. The load sharing percentages will be equal to: DBR=40%, PAVC=20%, CFL=20% and the remaining 20% is three-phase, star-connected linear loads that have 90% power factor lagging.

The supply impedance which is equal to the secondary distribution transformer impedance plus the impedance of the line connecting the transformer to the distribution panel, was equal to 0.032+j0.1169Ω, with the X/R ratio equal to 3.65.

For harmonic frequencies n, where $n \in \{1, 3, 5\}$ and utilizing the non-linear susceptance calculation procedure described in section 7.2, it was found that the equivalent load susceptances seen at the point of common coupling PCC were equal to: $B_1 = 0.028S$, $B_3 = 125.01S$ and $B_5 = 75.76S$. The reactance one-port compensator was found to have an impedance equal to:

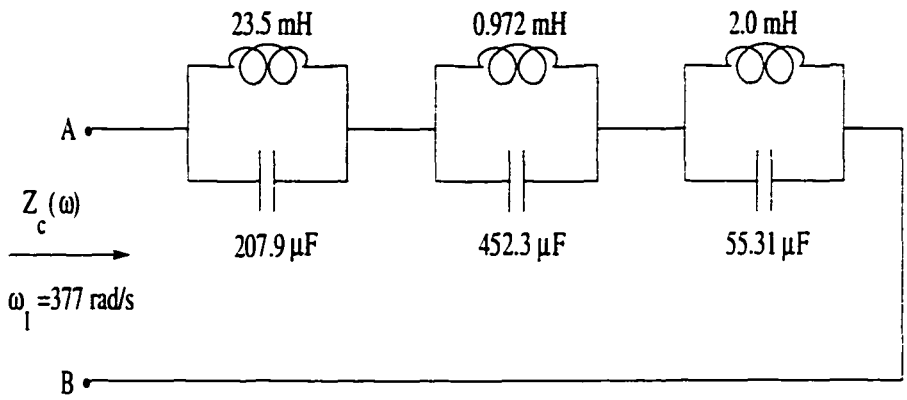

Figure 7.13: One-port compensator for three-phase four-wire system loaded with DBR and CFL load combination reactive power compensation

Table 7.1: RMS and THD values for phase voltage, phase current and neutral current in 3-phase system having DBR and CFL load combination before and after compensation

	Without compensator		With compensator	
	RMS	THD	RMS	THD
V_A	105.06	19.4	101.7	4.18
V_B	105.4	18.8	102.2	6.21
V_C	105.9	19.7	102.9	5.31
I_A	16.63	19.6	17.13	3.51
I_B	17.08	18.4	18.02	3.42
I_C	16.27	20.4	16.7	4.81
I_N	9.073	1168	0.954	360

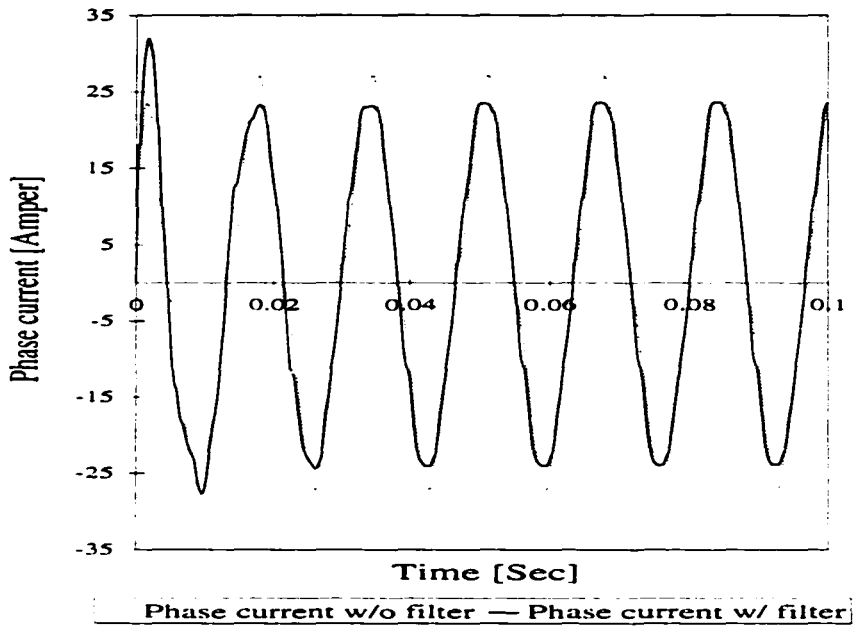

Figure 7.14: Phase current of 3-phase system having DBR and CFL load combination before and after compensation

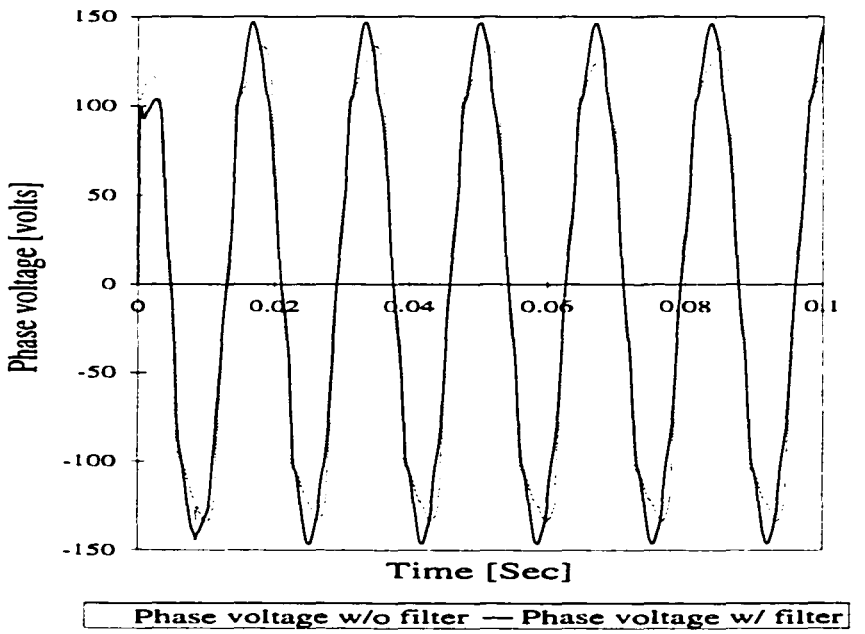

Figure 7.15: Phase voltage of 3-phase system having DBR and CFL load combination before and after compensation

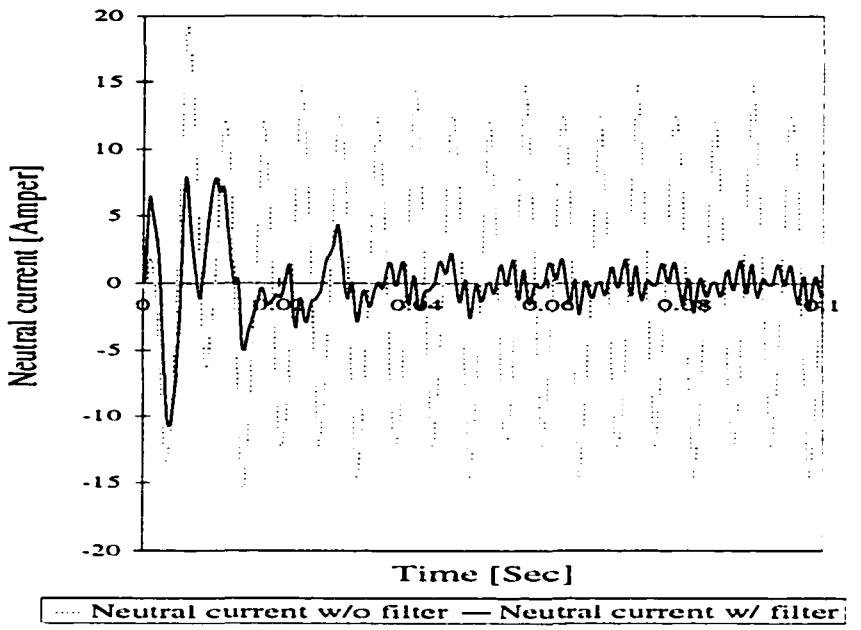

Figure 7.16: Neutral current of 3-phase system having DBR and CFL load combination before and after compensation

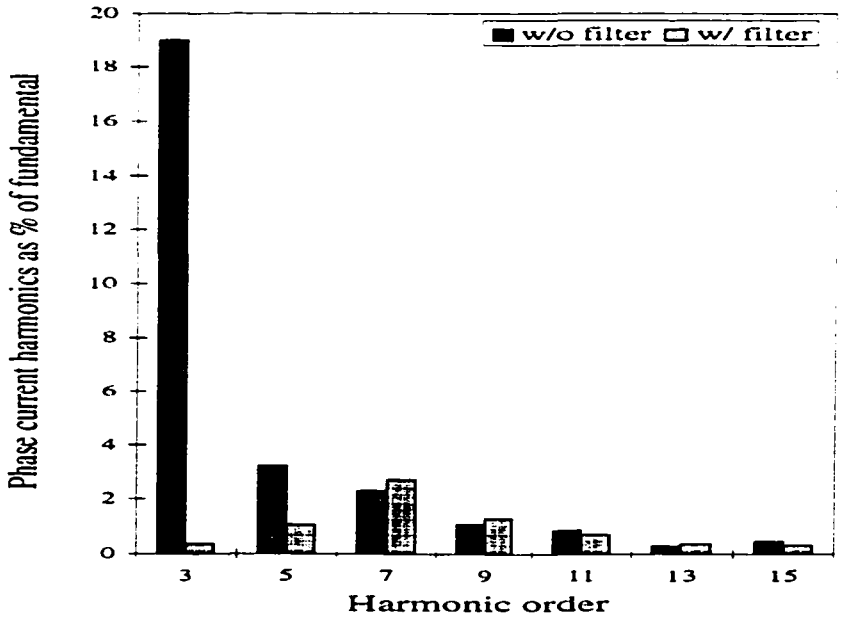

Figure 7.17: Phase current harmonic contents for 3-phase system having DBR and CFL load combination with and without reactance one-port compensator

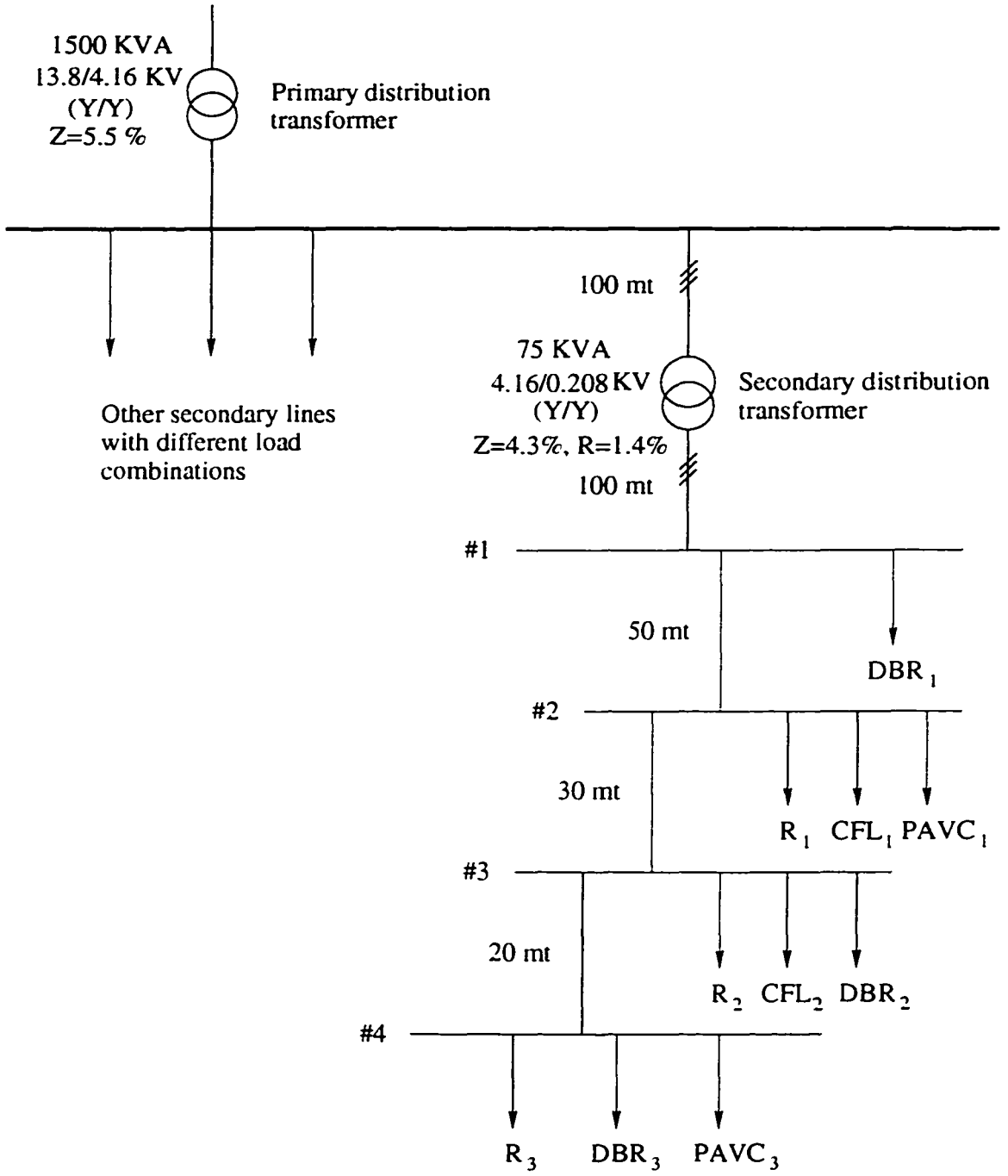

Figure 7.18: Test secondary distribution system to examine the reactance one-port compensator performance

$$Z_{c1}(s) = \frac{14.318s}{(s^2+1.2^2)} + \frac{6.608s}{(s^2+4.0^2)} + \frac{52.423s}{(s^2+8.0^2)}. \tag{7.20}$$

The filter had the structure and parameters given in Figure 7.19. Inserting this filter at the point of common coupling succeeded in reducing the total harmonic distortion of both the supply current and the load voltage. The THDI was reduced from 30.18% to 18.51% and the THDV was reduced from 19.9% to 13.19%. However, these distortion levels violate the recommended values [3], thus another filter stage had to be designed in conjunction with the first stage to further reduce the harmonic distortion levels to acceptable levels. The susceptances of the equivalent load (including the first compensator stage) was recalculated and was found to be equal to: $B_1 = 0.279S$, $B_3 = 88.49S$ and $B_5 = 0.885S$. The impedance function of the second stage filter was obtained following the same design procedure and was found to be:

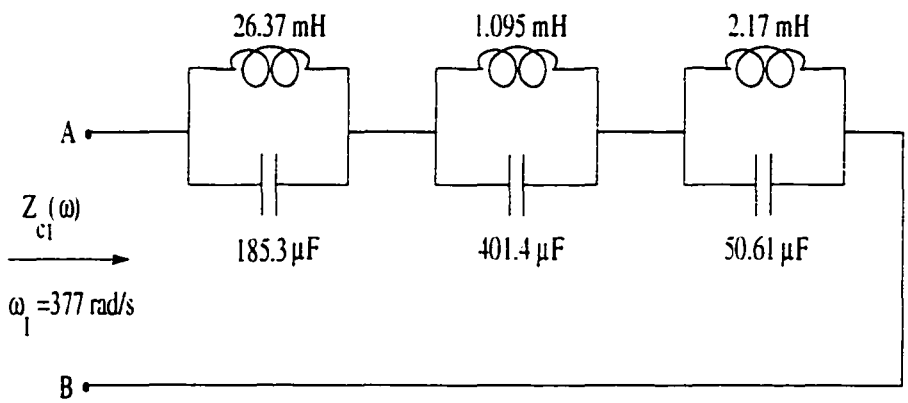

Figure 7.19: 1st stage One-port compensator for test system reactive power compensation

$$Z_{c2}(s) = \frac{1.385s}{(s^2+1.2^2)} + \frac{0.1s}{(s^2+4.0^2)} + \frac{11.215s}{(s^2+8.0^2)}. \tag{7.21}$$

The second filter stage had the structure and parameters shown in Figure 7.20. Applying the second filter stage in parallel with the first stage resulted in a further reduction in

the system harmonic distortion. The THDI was further reduced to 8.66% and the THDV was reduced to 8.01%. These results indicate that the non-linear susceptance calculation was not too accurate, leading to an un-optimum filter design. This can be attributed to the system complexity, since the voltages across different loads connected at different buses are different due to the presence of the feeder section impedance.

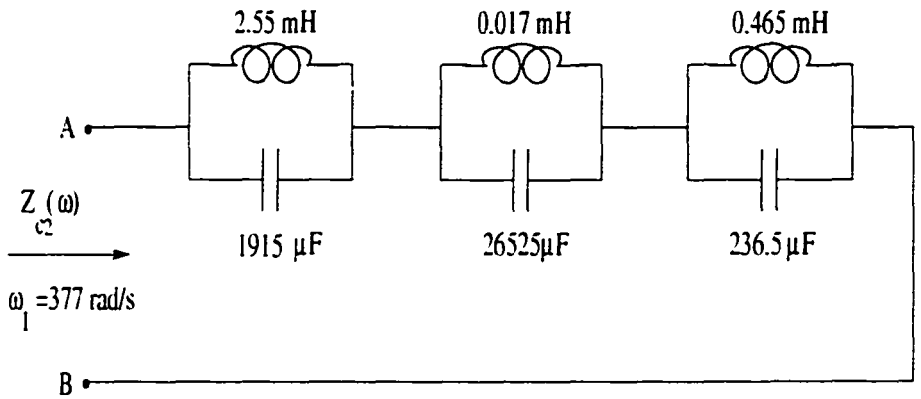

Figure 7.20: 2nd stage One-port compensator for test system reactive power compensation

In order to minimize the filter complexity and cost, the two reactance one-port stages were combined together leading to the combined compensator transfer function given as:

$$Z_{c_{tot}}(s) = \frac{1.283s}{(s^2 + 1.2^2)} + \frac{0.582s}{(s^2 + 4.0^2)} + \frac{4.805s}{(s^2 + 8.0^2)}. \tag{7.22}$$

The parameters and structure of the combined filter is given in Figure 7.21. Examining the performance of this combined filter results in a great reduction in the system distortion levels. The THDI was reduced to 2.35% and the THDV was reduced to 3.87% which comply with the recommended standards. The supply current and the voltage at the point of common coupling after inserting the combined filter are given in Figures 7.22 and 7.23, respectively. The harmonic contents of both current and voltage before and after inserting the filter are presented in Figures 7.24 and 7.25, respectively.

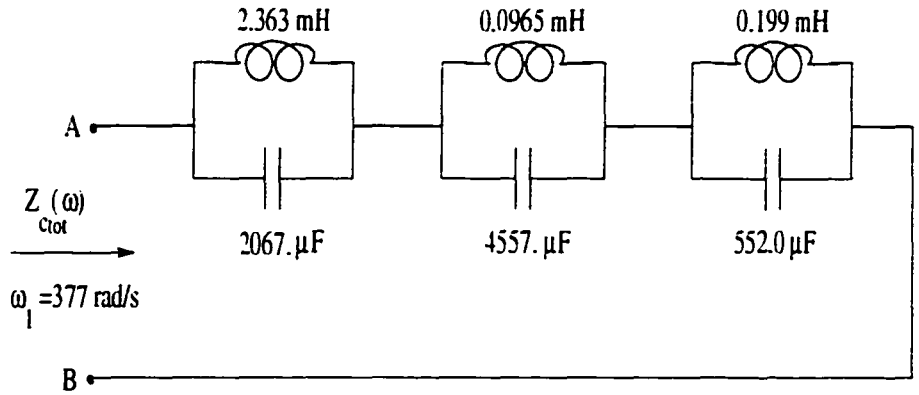

Figure 7.21: Combined reactance one-port compensator for test system reactive power compensation

7.5 Experimental verification

To support the computer simulation results, some laboratory experiments have been conducted. These tests were performed for two load cases: the first was the DBR load; the second was the three-phase four-wire balanced system supplying DBR and CFL load combination. The ratings of the capacitors and the inductors used in building the proposed filters are listed in Appendix D. The equipment utilized in carrying out these experiments and recording both voltage and current magnitudes and waveforms are described in Appendix B. For the DBR load case, the current total harmonic distortion THDI was reduced from 58.9% to 23.5% and the voltage total harmonic distortion THDV was reduced from 14.35% to 5.35%. Figures 7.26 and 7.27 show the experimental current and voltage waveforms before and after inserting the compensator.

For the three-phase four-wire system loaded with a combination of DBR and CFL loads, the supply current THD was reduced from 19.62% to 8.2%, the phase voltage THD was reduced from 19.42% to 6.54%, and the neutral current magnitude was reduced from 9.08 Amp to 1.86 Amp. Figures 7.28, 7.29 and 7.30 show the experimental phase current, the phase voltage and the neutral current before and after the compensator

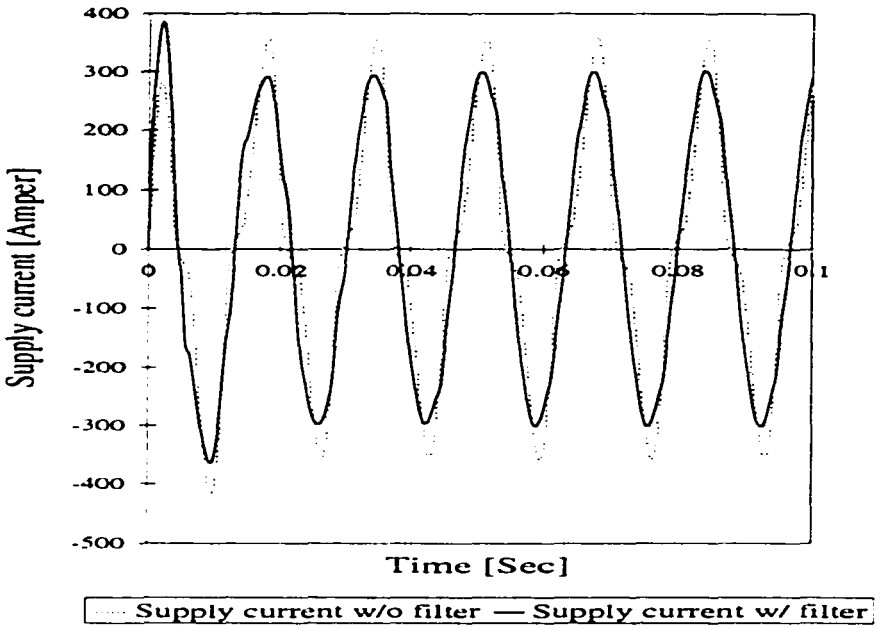

Figure 7.22: Supply current of the test distribution system before and after compensation

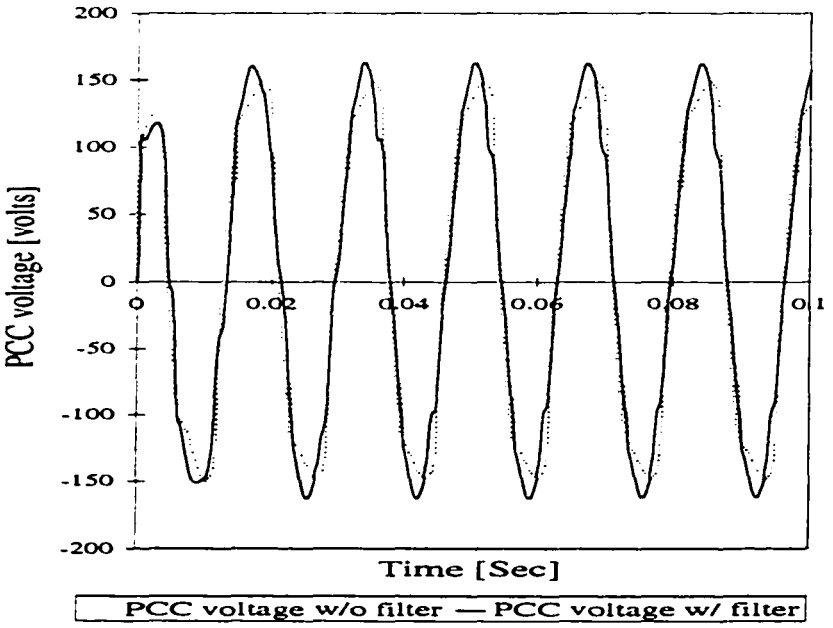

Figure 7.23: Load voltage of the test distribution system before and after compensation

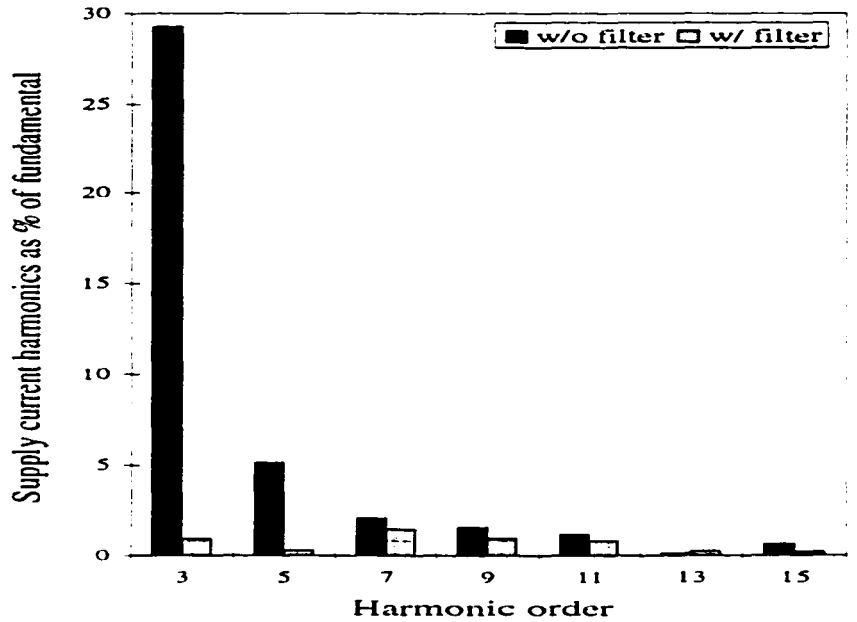

Figure 7.24: Supply current harmonic contents for the test distribution system before and after compensation

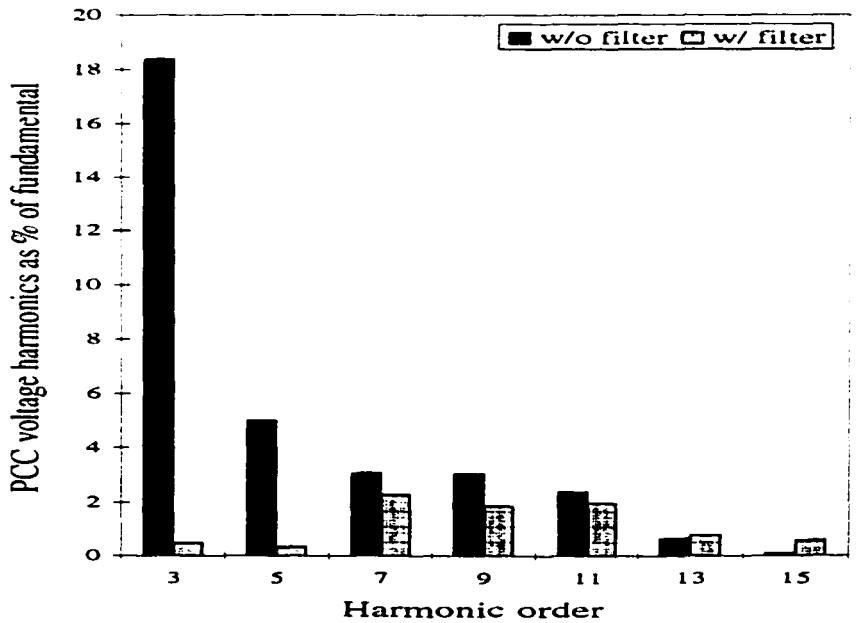

Figure 7.25: Test distribution system point of common coupling voltage harmonic contents before and after compensation

insertion.

These experimental results reveal complete agreement with the simulation output. The main observation to note is that the current and voltage distortion attenuation in both simulation and experimental results differ slightly. It is evident, however, that these differences are only attributable to the fact that the components that were used in the laboratory did not have exactly the same values and characteristics as those designed and used in the simulation. The reason for this is that the available component ratings in the market did not match the values used in the simulator. Also, the manufacturing tolerance may affect the performance of the designed filter. Another important factor that may affect the laboratory results is the different characteristics associated with the semiconductor elements. Since the simulation dealt with the diodes as ideal switches, these elements' non-linear characteristics were not considered in the simulation which led to different results.

Loading level variation and components manufacturing tolerance are two important factors that must be considered in a complete analysis of a filter design and installation problem. A sensitivity analysis should be carried out to give more insight on how these two parameters can affect the effectiveness of the proposed reactance one-port compensator.

7.6 Sensitivity analysis

In selecting a particular network from the many available, different criteria may be used. Usually, the selection is based on the economics of the construction of the filter circuit, though sometimes even these economic factors are not the most important consideration. The final decision may be entirely subjective. For example, the size and type of components happen to be in stock may dictate which network to choose.

Another factor that may determine which of the circuits to use is the sensitivity. When

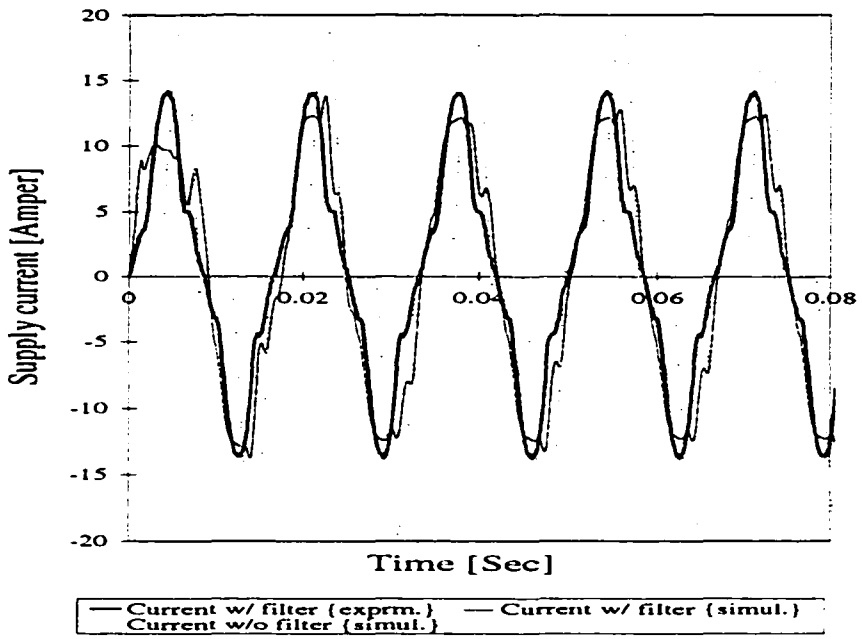

Figure 7.26: Supply current of circuit having DBR load before and after compensation, as obtained experimentally

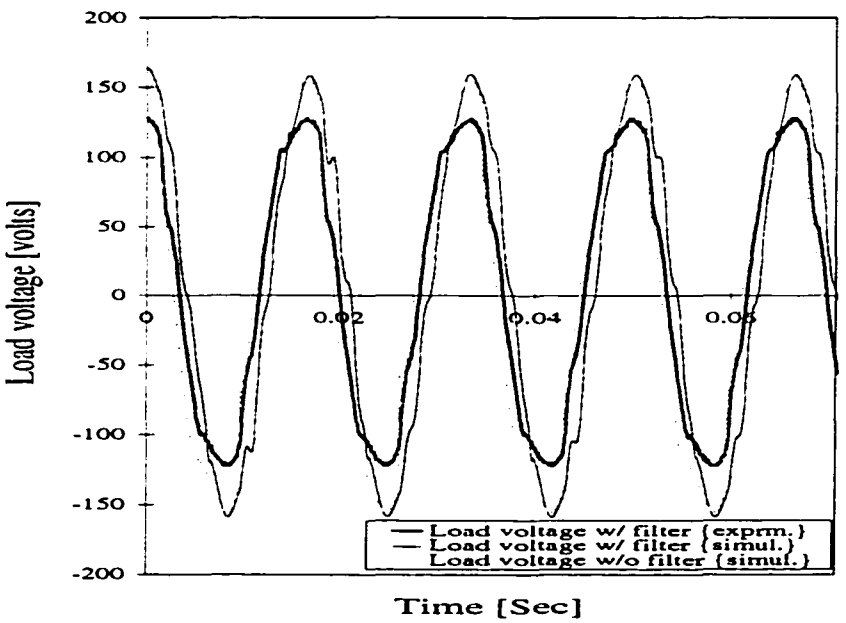

Figure 7.27: Load voltage of circuit having DBR load before and after compensation, as obtained experimentally

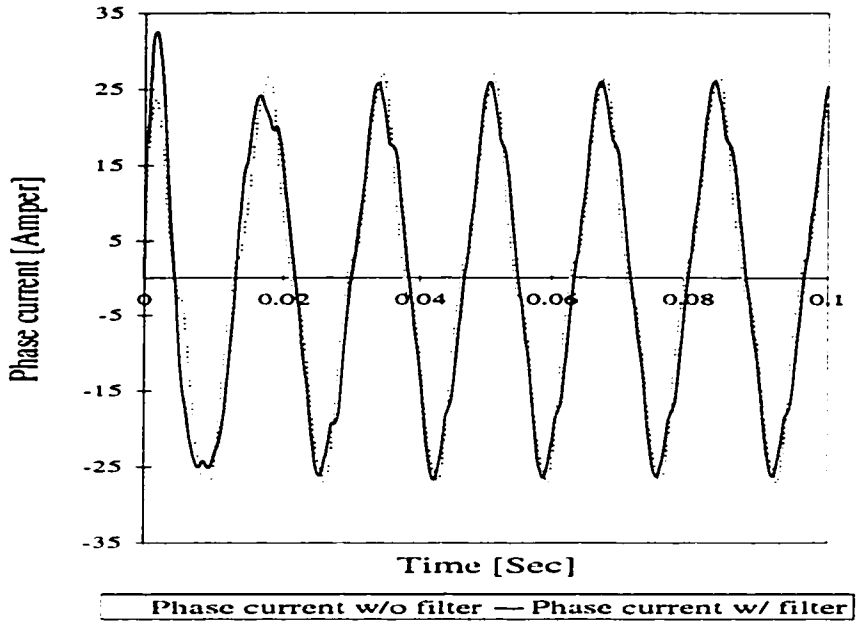

Figure 7.28: Phase current of three-phase circuit having DBR and CFL combination before and after compensation, as obtained experimentally

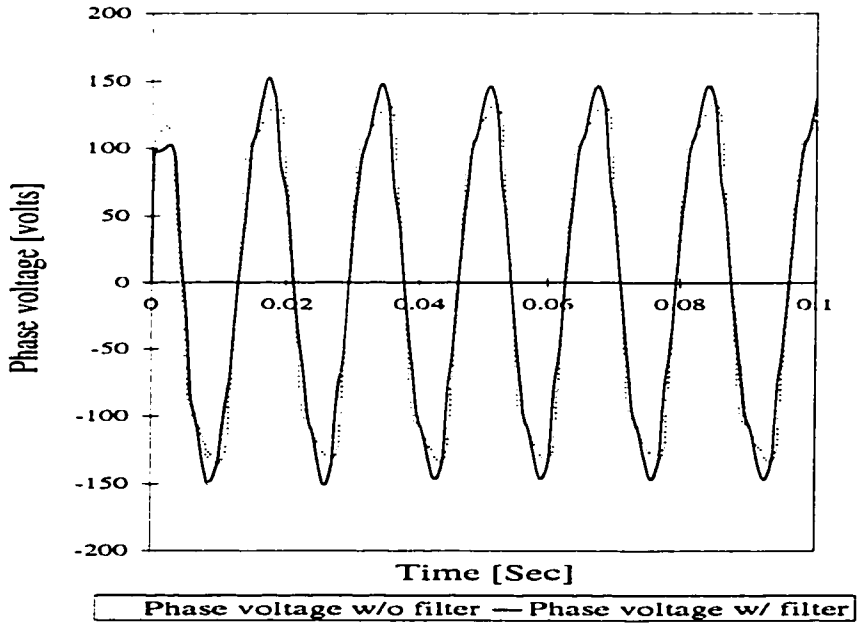

Figure 7.29: Phase voltage of three-phase circuit having DBR and CFL combination before and after compensation, as obtained experimentally

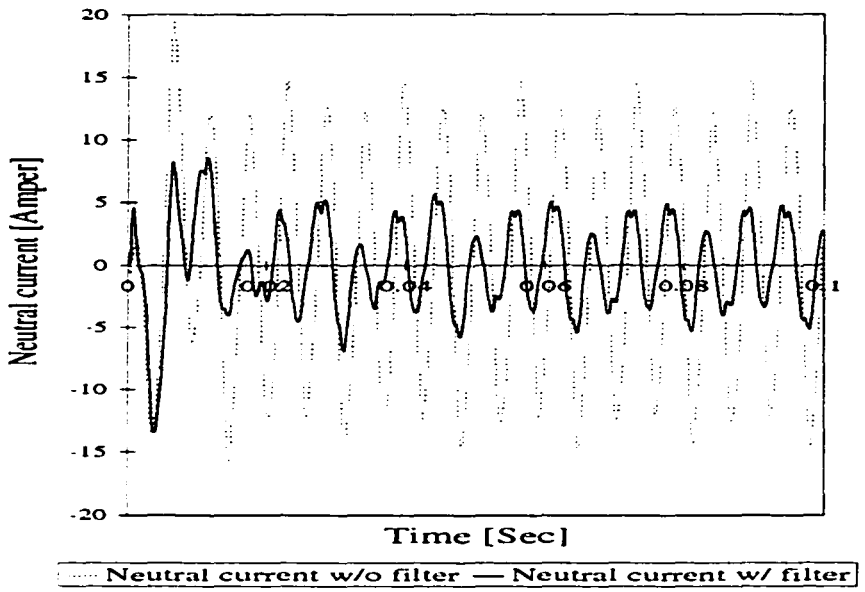

Figure 7.30: Neutral current of three-phase circuit having DBR and CFL combination before and after compensation, as obtained experimentally

a network is synthesized, its nominal component values can be obtained. If all components are not only accurate, but also remain constant under different ambient conditions throughout their lifetime, then there will be little difference in the filter performance. However, in practice, real components do deviate from their nominal values due to initial inaccuracy in fabrication, environmental factors such as temperature and humidity, and chemical and mechanical changes due to aging. The effect of component values deviation from their nominal values is an alteration of the filter performance. There are two different approaches to reduce this undesirable effect. One is to make the initial component values very accurate and subsequently endeavor to keep these values from fluctuating, but this approach is not only unnecessarily costly, but also impractical. The other approach is to select a network whose performance is least affected by the changes in its element values. Since distribution systems are dynamic in nature, the loading level and operating point variations can cause differences in the filter performance in addition to

the element values deviation. Therefore, checking the filter sensitivity to both elements' values variation and loading condition variation is one of the most important factors in selecting the desired filter.

The sensitivity of some performance measure y with respect to a network element value x is defined as:

$$S_x^y = \frac{x}{y} * \frac{dy}{dx}. \tag{7.23}$$

If y is a function of several variables $[y = f(x_1, x_2, ..., x_n)]$, then the sensitivity of y with respect to x_i is:

$$S_{xi}^y = \frac{x_i}{y} * \frac{\partial y}{\partial x_i}, \quad i = 1, 2, ..., n \tag{7.24}$$

The definition given in 7.23 is known as the differential, first-order, classical or relative sensitivity.

7.6.1 Sensitivity to filter elements variation

The first sensitivity study investigates how the deviation from nominal values of the compensator elements can affect the filter performance. To accomplish this task, all inductive and capacitive elements included in the compensator are allowed to vary within a certain tolerance. This tolerance is assumed to be either 3% or 5% depending on the economic considerations. In this study, the distribution system described in Figure 7.18 and its designed filter shown in Figure 7.21 were utilized. The variation of both THDI and THDV as a result of the 3% *or* 5% deviation of the compensator elements are given in Tables 7.2 and 7.3, respectively.

It is apparent from Tables 7.2 and 7.3 that, when all elements are allowed to deviate by 3% at the same time, both THDI and THDV remain within acceptable levels. The

Table 7.2: Current and voltage THD values corresponding to compensator inductive and capacitive elements variation of 3%.

Condition	L_1 mH	L_2 mH	L_3 mH	C_1 μF	C_2 μF	C_3 μF	THDI	THDV
Original	2.363	0.0965	0.199	2067.	4557.	552.	2.32	4.01
$L\uparrow$ $C\uparrow$	2.434	0.0994	0.205	2129.	4694.	568.6	6.17	6.19
$L\downarrow$ $C\downarrow$	2.292	0.0936	0.193	2005.	4420.	535.4	8.39	7.35
$L\uparrow$ $C\downarrow$	2.434	0.0994	0.205	2005.	4420.	535.4	2.38	4.06
$L\downarrow$ $C\uparrow$	2.292	0.0936	0.193	2129.	4694.	568.6	2.25	3.94
$L\uparrow$, $C = const$	2.434	0.0994	0.205	2067.	4557.	552.	4.31	5.04
$L\downarrow$ $C = const$	2.292	0.0936	0.193	2067.	4557.	552.	4.37	4.87
$L = const$, $C\uparrow$	2.363	0.0965	0.199	2129.	4694.	568.6	4.21	4.98
$L = const$, $C\downarrow$	2.363	0.0965	0.199	2005.	4420.	535.4	4.58	4.99

only exception is the worst case, where both inductive and capacitive elements increase or decrease together. In contrast, when all elements are allowed to deviate by 5%, a violation of the voltage total harmonic distortion resulted, except in cases with different direction of change for both inductors and capacitors (inductors increase and capacitors decrease or vice versa). These results reveal that for the cases studied, even if all the compensator elements deviate within the 3% tolerance range, both THDI and THDV will remain within acceptable standards. However, if the deviation exceeds the 3% limit, then, with the exception of few cases, both THDI and THDV will violate the limits. It is worth noting that if all the elements are not allowed to change at the same time, then the 5% range may be employed without violating the distortion levels.

Table 7.3: Current and voltage THD values corresponding to compensator inductive and capacitive elements variation of 5%.

Condition	L_1 mH	L_2 mH	L_3 mH	C_1 μF	C_2 μF	C_3 μF	THDI	THDV
Original	2.363	0.0965	0.199	2067.	4557.	552.	2.32	4.01
$L\uparrow$ $C\uparrow$	2.481	0.101	0.209	2170.	4785.	579.6	7.16	7.13
$L\downarrow$ $C\downarrow$	2.245	0.0917	0.189	1964.	4329.	524.4	12.5	10.8
$L\uparrow$ $C\downarrow$	2.481	0.101	0.209	1964.	4329.	524.4	2.49	4.09
$L\downarrow$ $C\uparrow$	2.245	0.0917	0.189	2170.	4785.	579.6	2.19	3.89
$L\uparrow$, $C = const$	2.481	0.101	0.209	2067.	4557.	552.	5.67	5.86
$L\downarrow$ $C = const$	2.245	0.0917	0.189	2067.	4557.	552.	6.86	6.3
$L = const$, $C\uparrow$	2.363	0.0965	0.199	2170.	4785.	579.6	5.45	5.7
$L = const$, $C\downarrow$	2.363	0.0965	0.199	1964.	4329.	524.4	7.32	6.62

7.6.2 Sensitivity to load level variation

The second sensitivity study investigated how deviating system operating points or loading conditions, from their nominal values, can affect the filter performance. The distribution system described in Figure 7.18 and its designed filter shown in Figure 7.21 were employed for this study. During this study the compensator elements remained constant at their nominal values and the only variable was the system loading level. Two factors are considered important in this investigation: the first is the percentage loading of the system; the second is the percentage sharing of each load type in the total system loading. The sharing of each load type is expressed as a percentage of its own nominal value. Starting with a system loading level equal to 100% and a specific load sharing,

each load type is assumed to be 100% of its own share. Increasing or decreasing a specific type of load will always be referred to its original share. The system loading will be allowed to decrease bellow or increase above its rated capacity. The change in both THDI and THDV in accordance with these loading level variations are listed in Table 7.4. The results presented in Table 7.4 show that the compensator performance will still be acceptable and the distortion levels for both voltage and current will remain within the acceptable levels, even if the loading level varies within ±20% of its rated value.

Table 7.4: Current and voltage THD values corresponding to loading level variation

System loading(%)	I_{RMS}	DBR load		CFL load		PAVC load		Linear load		THDI	THDV
		%	Amp.	%	Amp.	%	Amp.	%	Amp.		
117.8	241.7	116	134.5	96	37.3	164	65.3	97	39	1.87	4.1
107.5	220.5	119	137.4	98.5	38.2	100	39.9	99	39.7	2.26	4.1
100†	205.2	100	115.8	100	38.8	100	39.9	100	40.2	2.32	4.01
91.8	188.3	79	91.5	100	38.8	100	40.	100	40.2	2.67	4.27
88.7	182	71.1	82.35	100	38.9	100	40.1	100	40.3	2.74	4.21
87.05	178.6	70.5	81.6	100	38.8	100	39.9	110	44.2	2.75	4.13
84.4	173.2	71.7	83.1	102	39.5	76.7	30.6	101	40.7	2.98	4.2
83.4	171.2	56.8	65.8	102	39.5	101	40.4	101	40.7	2.9	4.13
83.5	171.3	71.6	82.9	102	39.5	101	40.6	74	29.7	2.84	4.1
79.25	162.6	71.4	82.6	76.5	29.6	101	40.6	74.5	29.9	3.2	4.29

† Full load condition.

Table 7.4 reveals that the reactance one-port compensator utilized is characterized by relatively low sensitivity to load variation. One of the reasons for this low sensitivity to load variation is that, as a rule, all elements in a passive filter circuit have comparable

effects on the network performance. Hence, the burden of accomplishing the filtering task is shared by all elements.

7.7 Assessment

In this chapter, a comprehensive study was performed to design and test a reactance one-port compensator capable of reducing both voltage and current harmonic distortions in systems loaded with different non-linear loads. In order to evaluate the effectiveness of such a compensator, different configurations ranging from simple single-phase circuits and ending up with some complex secondary distribution feeders were utilized. The results show that:

1. The reactance one-port compensators are capable of improving the distribution systems power quality by decreasing both voltage and current harmonic distortion levels, even if the system is heavily loaded with different non-linear loads.

2. The reactance one-port compensator is characterized by a relatively low sensitivity to the change in the loading levels and can tolerate changes up to $\pm 20\%$ of the nominal load.

3. The reactance one-port compensator can tolerate changes in its elements' values up to $\pm 3\%$ without damaging the compensation performance.

Chapter 8

Conclusions and Future Research

In this thesis, harmonic generation and propagation in distribution systems was thoroughly studied. The effects of both attenuation and the diversity phenomenon on distribution systems were investigated analytically as well as experimentally. This precise study led to more accurate information about the distribution systems behavior.

When it comes to reducing the distribution system harmonics, the active filtering, though characterized with the higher expense, is preferable to passive filtering since a lack of information can lead to inaccurate passive filter design. After the in-depth study carried out in this thesis, it becomes apparent that accurate system information can allow for the design of passive filters which can be utilized in achieving results comparable to those of the active filters.

A hybrid method was developed and tested for the use of reactance one-port compensators to improve distribution system power quality. This methodology was tailored to be applied both to non-linear and linear distribution systems. The proposed methodology was conducted according to a four-phase approach. The first phase, in this approach as presented in Chapter 4, identified the non-linear loads commonly used in distribution systems. These loads were grouped into three different categories depending on the com-

mon features in their current waveforms. The second phase, which was introduced in Chapter 4, investigated the effect of the load voltage and current harmonic interactions. These interactions, referred to the attenuation effect, were considered to be one of the crucial factors in obtaining accurate waveforms for both the supply current and the load voltage. The third phase, which was presented in Chapters 5 and 6, dealt with the investigation of the main system and load parameters that affect the harmonic performance of the non-linear loads identified in the first phase. The collective harmonic performance of these loads when connected in both single-phase and three-phase four-wire configurations were studied. Moreover, the dependence of the net harmonic currents produced by different load groups on those parameters were examined. The fourth phase, as presented in Chapter 7, introduced a new time-domain based technique to estimate the non-linear load susceptance at different harmonic frequencies. This was followed by the rigorous design and testing of the proposed reactance one-port compensator needed to decrease both voltage and current distortion levels. Finally, experimental verification was demonstrated in Chapters 4, 5, 6 and 7 as validation of the simulation results. The conclusions derived from the analysis conducted throughout this research are as follows:

1. The interaction between the load voltage and current harmonics (attenuation phenomenon) can not be neglected in any practical distribution system. These interactions lead to a reduction in the supply current distortion level, and neglecting this phenomenon could result in a significant overestimation of the system distortion levels.

2. The reduction in harmonic currents due to the attenuation effect increases significantly with the system loading.

3. Harmonic phase cancellation (diversity phenomenon) reduces the levels of net harmonic currents injected into the distribution systems. This phenomenon can be

experienced even if only identical loads are operating together.

4. Harmonic current magnitudes demonstrate a tendency to decrease with the increase of either the loading level of a single non-linear load or the number of loads connected to the same distribution feeder.

5. Harmonic current magnitudes are inversely proportional to the X/R ratio of the supply internal inductive impedance.

6. Harmonic reduction can be achieved by combining different types of non-linear loads together.

7. The level of each harmonic component changes with the interchange of the position of the harmonic producing device along the distribution feeder.

8. In balanced three-phase four-wire distribution feeders, the neutral current is composed of only triplen harmonics. Moreover, in unbalanced systems, the non-triplen harmonics contribute by not more than 40% of the neutral current.

9. Reactance one-port compensators can be implemented successfully in order to decrease the net harmonic distortion of both load voltage and supply current.

10. The compensator sensitivity to elements' values deviation can allow for at least ±3% tolerance if all compensator elements are to change simultaneously or ±5% if only some of these elements are changing.

11. The compensator sensitivity to loading level can tolerate changes in the operating point up to ±20%.

8.1 Contributions

The original contributions of the work done in this thesis can be summarized as follows:

1. An often-overlooked phenomenon, attenuation, was advanced as a major factor to be considered when estimating distortion levels or in the determination of voltage and current waveforms in any practical non-linear distribution system. Neglecting this phenomenon will result in a significant overestimation of the system distortion levels, and was therefore thoroughly investigated;

2. A time-domain based iterative approach capable of producing accurate voltage and current waveforms in systems loaded with different types of non-linear loads was developed. The proposed approach is proven to be superior to other non-linear frequency-domain approaches because it accurately accounts for the harmonic coupling as well as the system non-linearity and voltage dependency;

3. A time-domain based approach for estimating the non-linear load susceptances at different harmonic frequencies was developed. This approach is considered as a milestone for any passive filter design; and

4. This thesis implemented an innovative design for reactance one-port compensators in non-linear distribution systems. This filter prototype was developed and tested rigorously. It was found to satisfy the design criteria, that is, it reduced both current and voltage harmonic distortion levels to meet the recommended standreds. This is a significant contribution because comparable results were achieved with a relatively inexpensive passive filter as with a more expensive active filter. This represents a potential for a significant savings.

8.2 Future investigations

The research results presented in this thesis point to several issues where future investigation may be considered. Some of these issues are:

1. This research should be extended to include the effect of the daily load variation of the distribution system upon the filter performance. Different compensator stages should be designed to match these variations and an automated procedure should be utilized to achieve a proper switching process between different filter stages;

2. The designed compensator should be optimized to find the best available performance with the least cost and sensitivity; and

3. The effect of both magnitude and location of power factor capacitors upon the harmonic generation and the compensator design and performance should be investigated.

Appendix A

Instantaneous Power Components

Decomposition of source current into two components (in-phase and quadrature) will result in two components of instantaneous power as given in Figures A.1 and A.2.

$$p(t) = v(t) * i(t), \tag{A.1}$$

$$p(t) = VI\cos\phi\,[1 - \cos(2\omega_1 t)] + VI\sin\phi\,\sin(2\omega_1 t), \tag{A.2}$$

$$p(t) = P_p + P_q. \tag{A.3}$$

where

$$P_p = P(1 - \cos(2\omega_1 t)), \tag{A.4}$$

$$P = VI\cos\phi, \tag{A.5}$$

$$P_q = Q\sin(2\omega_1 t), \textit{and} \tag{A.6}$$

$$Q = VI\sin\phi. \tag{A.7}$$

The components P_p has an average value P and it is a unidirectional power fluctuating

between zero and $2P$. Where P is known as the real power, also called active or average power. The component P_q is an oscillation of power at double the supply frequency. This component transfers energy back and forth between the source and the linear load, what is called reciprocating flow of energy. The amplitude of this component is known as the reactive power Q and it is considered a useless loading of the source, which increases the source current rms value. In sinusoidal systems, the reactive power Q is an additive quantity which is not only considered to be a measure of the uselessly transmitted power, but it is also directly related to the compensating equipment ratings that can improve the source power factor.

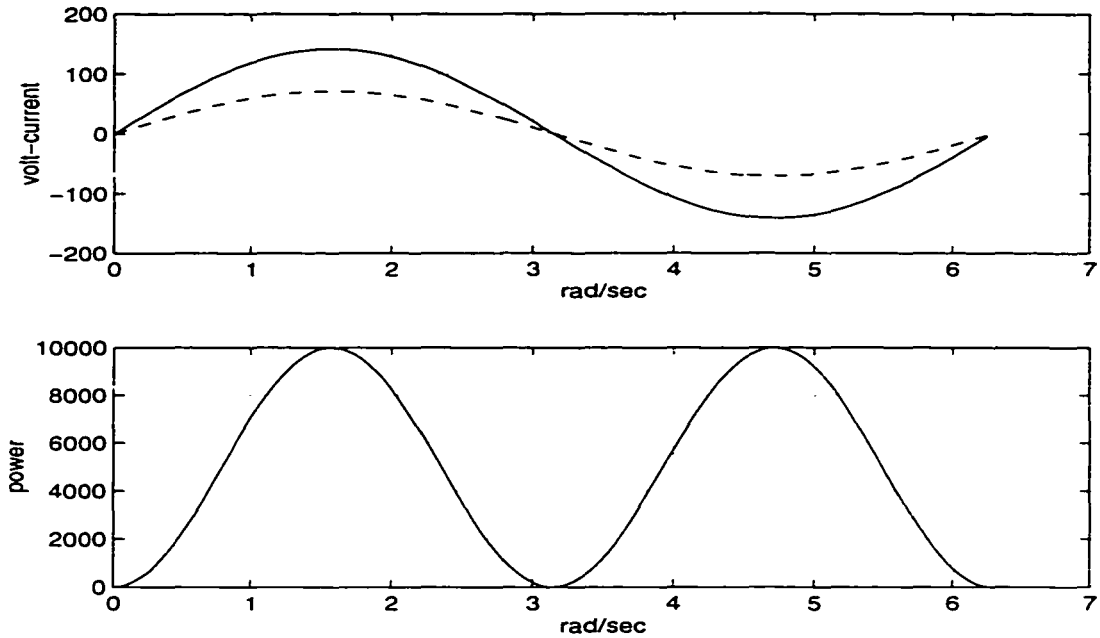

Figure A.1: In-phase current and the unidirectional power P_p

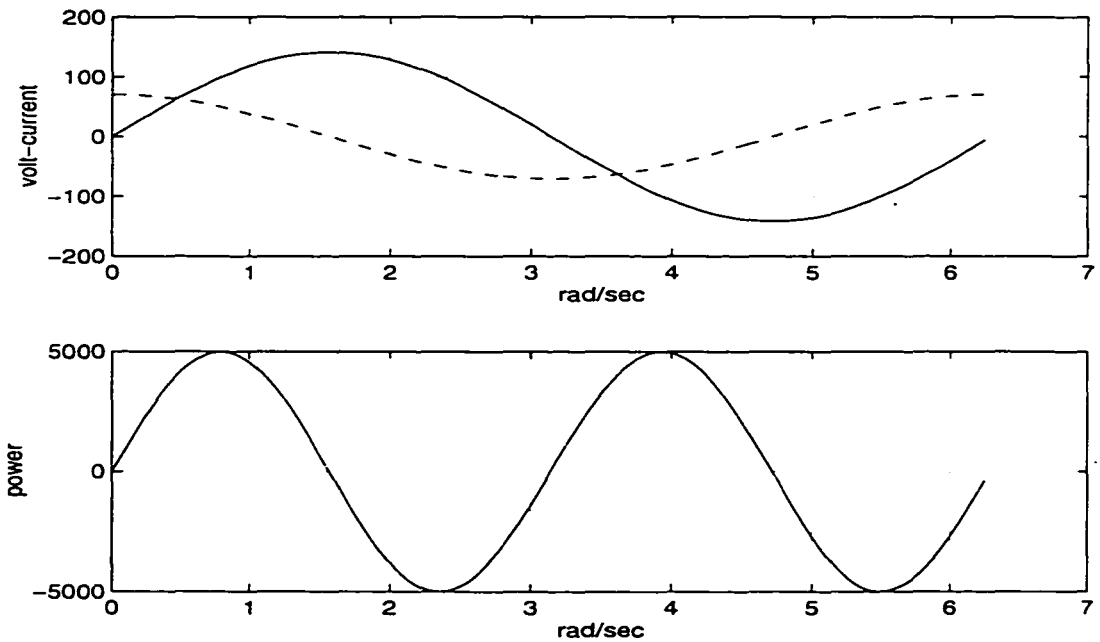

Figure A.2: Reactive current and the double frequency power oscillations

Appendix B

Experimental Setup

The equipment utilized in the laboratory in order to perform the experimental verifications are described as follows:

Digital Oscilloscope

- Model: Tektronix TDS 644A.
- Bandwidth selection: 20 MHz, 100 MHz, and Full (500 MHz).
- Input impedance selection: 1 MΩ.
- Range, sensitivity: 1 mv/div to 10 v/div.
- Accuracy: 1%.
- Range, sample-rate: 10 sample/sec to 2 Gsample/sec.
- Input voltage: ± 400 volts (DC + peak AC).
- Lower frequency: $\leq$ 10HZ when AC-1MΩ coupled.

Waveform Analyzer

- Model: Dranetz 658-406.
- Range: 0-600 v (RMS), 6120 volt-peak, 0-1000 Amp (RMS), 6000 Amp-peak.
- Frequency: 45-65 Hz, 310-445 Hz.
- Accuracy: Voltage $\pm 1\%$, current $\pm 2\%$.

Multimeter

- Model: Fluke 25 Digital electronic multimeter
- Voltage Range: 0.001 volt $\rightarrow$ 1000 volt.
- Current Range: 0.1μA $\rightarrow$ 10 Amp. (10A continuous or 20A for 30 sec. max.)
- Resistance Range: $0.1\Omega \rightarrow 32\text{M}\Omega$.
- Accuracy: V: $\pm(0.1\%+1)$, I: $\pm(0.75\%+2)$.

Computer

- Model: Pantium
- Frequency: 133 MHz.

Printer

- Model: HP Lazer jet III
- Memory: 4 MB

Diodes

- Model: 1N1206A.
- Rating: 12 Amp, 600 volt-DC

Fluorescent Lamps

- Type: General Electric.
- Model: F40CW-EX
- Power: 40 Watt.

Ballast

- Type: Philips.
- Model: R2S40-TPC-MARK III.
- Volt: 120 volts.
- Frequency: 60 Hz.
- Current: 0.73 Ampere.
- Sound Rated: A.
- P.F.: Above 0.9.

Appendix C

IEEE Recommended Standreds (IEEEstd-519)

The philosophy of developing harmonic limits is to:

1. Limit the harmonic injection from individual customers so that they will not cause unacceptable voltage distortion levels for normal system characteristics; and

2. Limit the overall harmonic distortion of the system voltage supplied by the utility.

Table C.1: Basis for harmonic current limits

SCR at PCC	Maximum Individual Frequency (%) Voltage Harmonic (%)	Related Assumption
10	2.5–3.0%	Dedicated system
20	2.0–2.5%	1–2 large customers
50	1.0–1.5%	A few relatively large customers
100	0.5–1.0%	5–20 medium customers
1000	0.05–0.1%	Many small customers

C.1 Current distortion limits

Table C.2: Current distortion limits for general distribution systems (120 V → 69 KV)

Maximum harmonic current distortion in percent of I_L						
Individual harmonic order (odd harmonics)						
I_{sc}/I_L	≤11	11≤h≤17	17≤h≤23	23≤h≤35	35≤h	TDD
≤20	4.0	2.0	1.5	0.6	0.3	5.0
20≤50	7.0	3.5	2.5	1.0	0.5	8.0
50≤100	10.0	4.5	4.0	1.5	0.7	12.0
100≤1000	12.0	5.5	5.0	2.0	1.0	15.0
≥1000	15.0	7.0	6.0	2.5	1.4	20.0

Where:

I_{sc} = *maximum short circuit current at PCC.*

I_L = *maximum demand load current (fundamental frequency component) at PCC.*

TDD = *Total Demand Distortion (harmonic current distortion in % of maximum demand load current.*

Even harmonics are limited to 25% of the odd harmonic above and current distortion that result in a dc offset, e.g., half-wave converters, are not allowed.

C.2 Limits on commutation notches

The notch depth, the total harmonic distortion factor (THD) and the notch area of the line-to-line voltage at PCC should be limited as shown in Table C.3.

Table C.3: Low-Voltage system classification and distortion limits

	Special Applications	General Systems	Dedicated Systems[§]
Notch depth	10%	20%	50%
THD (Voltage)	3%	5%	10%
Notch area[†](A_N)[‡]	16400	22800	36500

[§] A dedicated system is exclusively dedicated to the converter load.

[‡] The value A_N for other than 480 V systems should be multiplied by $V/480$.

[†] The value of A_N is in volt-microseconds at rated voltage and current.

C.3 Voltage distortion limits

The limits listed in Table C.4 should be used as system design values for the 'worst case' of normal operation (conditions lasting longer than one hour). For shorter periods, during start-ups or unusual conditions, the limits may be exceeded by 50%.

Table C.4: Voltage distortion limits

Bus voltage at PCC	Individual voltage Distortion %	Total voltage distortion $THD(\%)$
69 KV and bellow	3.0	5.0
69 KV→161 KV	1.5	2.5
161 KV and above	1.0	1.5

Appendix D

FILTER COMPONENTS

Table D.1: Components ratings and manufacturer

(a)Filter chocks

Model #	Manufacture	Inductance mH	Current Amp	Resistance Ω	Weight Lb
195G20	Hammond	5.0	20.0	0.03	9.3
195E20	Hammond	2.5	20.0	0.025	5.7
195C20	Hammond	1.0	20.0	0.013	2.5
195J20	Hammond	10.0	20.0	0.053	17.0
195M10	Hammond	20.0	10.0	0.13	10.0
159ZL	Hammond	2.5	10.0	0.044	2.75
157D	Hammond	1.0	10.0	0.038	1.0

(b)Filter capacitors

Model #	Manufacturer	Capacitance μF	voltage v
PSU54015B	Mallory	540→648	110/125
PSU40015	Mallory	400→480	110/125
PSU24315A	Mallory	243→292	110/125
PSU18915A	Mallory	189→227	110/125
PSU5315	Mallory	64→77	110/125
PSU6415	Mallory	53→64	110/125
Z97F9037	GE	$15\mu F$ $\pm 6\%$	440
Z97F9039	GE	$20\mu F$ $\pm 6\%$	440
Z97F9608	GE	$30\mu F$ $\pm 6\%$	440
RP3304	Mallory	$4\mu F$ $\pm 4\%$	330

Bibliography

[1] IEEE Working Group on Power System Harmonics, "Power system harmonics: An overview," *IEEE Transactions on Power Apparatus and Systems*, vol. PAS-102, no. 7, pp. 2455–2460, August 1983.

[2] A. Domijan, J.T. Heydt, A.P.S. Meliopoulos, S.S. Venkata, and S. West, "Directions of research on electric power quality," *IEEE Transactions on Power Delivery*, vol. 8, no. 1, pp. 429–436, January 1993.

[3] IEEE, "Recommended practices and requirements for harmonic control in electrical power systems," New York, 1984, IEEE Std. 519-1993.

[4] International Electrotechnical Commission Standered, "General guide on harmonics and interharmoincs measurements and instrumentations, for power supply systems and equipment," Tech. Rep. IEC 1000-4-7, 1996.

[5] K. Olejniczak and G.T. Heydt, "Basic mechanisms of generation and flow of harmonic signals in balanced and unbalanced three-phase power systems," *IEEE Transactions on Power Delivery*, vol. 4, no. 4, pp. 2162–2170, October 1989.

[6] E.F. Fuchs, D.J. Roesler, and F.S. Alshhab, "Sensitivity of electrical applications to harmonics and fractional harmonics of the power systems voltage, part I:," *IEEE Transactions on Power Delivery*, vol. 2, no. 2, pp. 437–4, April 1987.

[7] E.F. Fuchs, D.J. Roesler, and F.S. Alshhab, "Sensitivity of electrical applications to harmonics and fractional harmonics of the power systems voltage, part II:," *IEEE Transactions on Power Delivery*, vol. 2, no. 2, pp. 4–4, April 1987.

[8] T.H. Ortmeyer and T. Hiyama, "Harmonic characteristics of grouped and individual loads," in *International Conference on Power System Harmonics*, 1989, pp. 1–7.

[9] Task force on harmonic modeling and simulation, "Modeling and simulation of the propagation of harmonics in electric power network: Part I: concepts, models and simulation techniques," *IEEE Transactions on Power Delivery*, vol. 11, no. 1, pp. 452–465, January 1996.

[10] Task force on harmonic modeling and simulation, "Modeling and simulation of the propagation of harmonics in electric power network, part II: Sample systems and examples," *IEEE Transactions on Power Delivery*, vol. 11, no. 1, pp. 466–474, January 1996.

[11] A.M. Emanuel and M. Yang, "On harmonic compensation in nonsinusoidal systems," *IEEE Transactions on Power Delivery*, vol. 8, no. 1, pp. 393–399, January 1993.

[12] T.H. Ortmeyer and T. Hiyama, "Distribution system harmonic filter planning," *IEEE Transactions on Power Delivery*, vol. 11, no. 4, pp. 2005–2012, October 1996.

[13] D.A. Gonzalez and J.C. Mccall, "Design of filters to reduce harmonic distortion in industrial power systems," *IEEE Transactions on Industry Applications*, vol. 23, no. 3, pp. 504–511, June 1987.

[14] W.K. Chang and W.M. Grady, "Minimizing harmonic voltage distortion with multiple current-constrained active power line conditioner," *IEEE Transactions on Power Delivery*, vol. 12, no. 2, pp. 837–843, April 1997.

[15] J.W. Dixon, G. Venegas, and L.A. Moran, "A series active power filter based on a sinusoidal current-controlled voltage-source inverter," *IEEE Transactions on Industry Applications*, vol. 44, no. 5, pp. 612–620, October 1997.

[16] L.S. Czarnecki, "Scattered and reactive current, voltage and power in circuits with non-sinusoidal waveforms and their compensation," *IEEE Transactions on Instrumentations and Measurement*, vol. 40, no. 3, pp. 563–567, June 1991.

[17] A.E. Emanuel, J.A. Orr, and D. Cyganski, "Review of harmonic fundamentals and proposal for a standered terminology," in *International Conference on Power System Harmonics*, 1988, pp. 1–7.

[18] D.A. Dini, "Testing the rating of transformers for use with non-linear loads," in 2nd *International Conference on Power Quality*, September 1992, pp. 25–31.

[19] H.W. Dommel, A. Yan, and S. Wei, "Harmonics from transformer saturation," *IEEE Transactions on Power Systems*, vol. 1, no. 1, pp. 209–214, April 1986.

[20] J. Blommaert, R. de Vre, and R. Kniel, "Analysis of harmonics in low voltage distribution networks caused by television receivers," in *International Conference on Electricity Distribution*, 1977, pp. 8–12.

[21] A. Mansoor, W.M. Grady, A.H. Chowdhury, and M.J. Samotyj, "An investigation of harmonic attenuation and diversity among distributed single-phase electronic loads," *IEEE Transactions on Power Delivery*, vol. 10, no. 1, pp. 467–473, Jan. 1995.

[22] D.J. Pillegi, E.M. Gulachenski, C.E. Root, T.J. Gentile, and A.E. Emanuel, "The effect of modern compact fluorescent lights on voltage distortion," *IEEE Transactions on Power Delivery*, vol. 8, no. 3, pp. 1451–1459, July 1993.

[23] A. Mansoor, W.M. Grady, R.S. Thallan, M.T. Doyle, S.D. Krein, and M.J. Samotyj, "Effect of supply voltage harmonics on the input current of single-phase diode bridge rectifier loads," *IEEE Transactions on Power Delivery*, vol. 10, no. 3, pp. 1416–1422, July 1995.

[24] R. Yacamini and J.C. Oliveira, "Harmonics in multiple converter systems: A generalized approach," *IEE Proceeding*, vol. 127, no. 2, pp. 98–106, March 1980.

[25] B.R. Pelly, *Thyristor Phase Controlled Converters and Cycloconverters*, Wiley Interscience, New York, 1971.

[26] L. Gyugi and B.R. Pelly, *Static Power Frequency Changers*, Wiley Interscience, New York, 1976.

[27] J.P. Brozek, "The effects of harmonics on over-current protection devices," in *Proceedings of the 1990 IAS*, 1990, pp. 1965–1967.

[28] D.E. Rice, "Adjustable speed drive and power rectifier harmonics: Their effect on power system components," *IEEE Transactions on Industry Applications*, vol. 22, no. 1, pp. 161–177, Jan. 1986.

[29] W.F. Horton and S. Goldberg, "The effect of harmonics on the operating points of electro-mechanical relays," *IEEE Transactions on Power Apparatus and Systems*, vol. PAS-104, no. 5, pp. 1178–1186, May 1985.

[30] M.S. Hwang, W.M. Grady, and H.W. Sanders, "Distribution transformer winding losses due to non-sinusoidal currents," *IEEE Transactions on Power Delivery*, vol. 2, no. 1, pp. 140–146, January 1987.

[31] IEEE Working Group, "Power line harmonic effects on communication line interference," *IEEE Transactions on Power Apparatus and Systems*, vol. PAS-104, no. 9, pp. 2578–2587, September 1985.

[32] IEEE Task Force on the Effects of Harmonics on Equipment, "Effect of harmonics on equipment," *IEEE Transactions on Power Delivery*, vol. 8, no. 2, pp. 672–680, April 1993.

[33] G.R. Selmon, "Equivalent circuits for transformers and machines including non-linear effects," *Proceedings IEEE*, vol. 101, no. IV, pp. 129–143, 1953.

[34] O.R.H. Galloway et al, "Calculation of electrical parameters for short and long poly phase transmission lines," *IEE Proceeding*, vol. 111, no. 12, pp. 2051–2059, December 1964.

[35] G. Shackshoft, O.C. Symons, and J.G. Hadwick, "General purpose model of power system loads," *IEE Proceeding*, vol. 124, no. 8, pp. 851–856, August 1977.

[36] R.J. Hill and D.C. Carpenter, "Modeling of non-linear rail impedance in ac traction power systems," *IEEE Transactions on Power Delivery*, vol. 6, no. 4, pp. 1755–1761, October 1991.

[37] M.I. Semesima and E.M. Dias, "Frequency response analysis and modeling of measurement transformers under distorted current and voltage supply," *IEEE Transactions on Power Delivery*, vol. 6, no. 4, pp. 1762–1768, October 1991.

[38] D.A. Douglass and A.C. Cross, "Non-linear modeling of transformers," *IEEE Transactions on Industry Applications*, vol. 24, no. 3, pp. 434–438, May 1988.

[39] IEEE Task Force, "Load representation for dynamic performance analysis," *IEEE Transactions on Power Systems*, vol. 8, no. 2, pp. 472–482, May 1993.

[40] C. Lin, Y. Chen, C. Chiou, C. Huaug, H. Chiang, J. Wang, and L. Ahmed, "Dynamic load models in power systems using the measurement approach," *IEEE Transactions on Power Systems*, vol. 8, no. 1, pp. 309–315, February 1993.

[41] T. Dovan, T.S. Dillon, C.S. Berger, and K.E. Forward, "A microcomputer based on-line identification approach to power system dynamic load modeling," *IEEE Transactions on Power Systems*, vol. 2, no. 3, pp. 529–536, August 1987.

[42] G.P. Christoforidis and A.P. Meliopoulos, "Effects of modeling on the accuracy of harmonic analysis," *IEEE Transactions on Power Delivery*, vol. 5, no. 3, pp. 1598–1607, July 1990.

[43] A. Semlyen, J.F. Eggleston, and J. Arrillaga, "Admittance matrix model of a synchronous machine for harmonic analysis," *IEEE Transactions on Power Systems*, vol. 2, no. 3, pp. 833–840, November 1987.

[44] H.W. Dommel, A. Yan, and S. Wei, "Harmonics from transformer saturation," *IEEE Transactions on Power Delivery*, vol. 1, no. 2, pp. 209–214, April 1986.

[45] A. Medina and J. Arrillaga, "Simulation of multilimb power transformers in the harmonic domain," *IEE Proceeding*, vol. 139, no. 3, pp. 269–276, May 1992.

[46] A. Medina and J. Arrillaga, "Generalized modeling of power transformers in the harmonic domain," *IEEE Transactions on Power Delivery*, vol. 7, no. 3, pp. 1458–1465, July 1992.

[47] G. Carpinelli, F. Gagliardi, M. Russo, and D. Villacci, "Generalized converter models for iterative harmonic analysis in power systems," *IEE Proceeding*, vol. 141, no. 5, pp. 549–556, September 1994.

[48] W.W. Price, K.A. Wirgan, A. Murdoch, J.V. Mitsche, E. Vaahedi, and M.A. El-Kady, "Load modeling for power flow and transient stability computer studies," *IEEE Transactions on Power Systems*, vol. 3, no. 1, pp. 180–187, 1988.

[49] R. Yacamini and J.C. deOliveira, "Comprehensive calculation of converter harmonics with system impedances and control representation," *IEE Proceeding*, vol. 133, no. 2, pp. 95–102, March 1986.

[50] D. Xia and G.T Heydt, "Harmonic power flow studies, part I- formulation and solution," *IEEE Transactions on Power Apparatus and Systems*, vol. PAS-101, no. 6, pp. 1257–1265, June 1982.

[51] D. Xia and G.T Heydt, "Harmonic power flow studies, part II- implementation and practical application," *IEEE Transactions on Power Apparatus and Systems*, vol. PAS-101, no. 6, pp. 1266–1270, June 1982.

[52] W. Song and G.T. Heydt, "The integration of hvdc subsystems into the harmonic power flow algorithm," *IEEE Transactions on Power Apparatus and Systems*, vol. 103, no. 3, pp. 1953–1961, August 1984.

[53] W. Shephared and P. Zand, *Energy Flow and Power Factor in Nonsinusoidal Circuits*, Cambridge University Press, London, 1979.

[54] H.W. Dommel, *Electromagnetic Transient Program EMTP reference manual and theory book*, Bonneville power administration, Department of Electrical Engineering, University of British Colombia, August 1986.

[55] T.J Aprille and T.N. Trick, "Steady state analysis of non-linear circuits with periodic inputs," *IEEE Transactions on Power Apparatus and Systems*, vol. 60, pp. 108–114, January 1972.

[56] C.A. Gross, *Power System Analysis*, John Wiley & Sons, New York, 1986.

[57] L.S. Czarnecki, "Misinterpretation of some power properties of electric circuits," *IEEE Transactions on Power Delivery*, vol. 9, no. 4, pp. 1760–1769, October 1994.

[58] A.E. Emanuel, "Power in non-sinusoidal situations, a review of definitions and physical meaning," *IEEE Transactions on Power Delivery*, vol. 5, no. 3, pp. 1377–1389, July 1990.

[59] S. Sun and S. Huang, "On the meaning of non-sinusoidal active currents," *IEEE Transactions on Instrumentations and Measurement*, vol. 40, no. 1, pp. 36–38, February 1991.

[60] A.E. Emanuel, "Apparent and reactive powers in three-phase systems, in search of a physical meaning and a better resolution," *Europe Trans. on Electric Power Engineering, ETEP*, vol. 3, no. 1, pp. 7–14, 1993.

[61] P.S. Filipski, Y. Baghzouz, and M.D. Cox, "Discussion of power definitions contained in the ieee directory," *IEEE Transactions on Power Delivery*, vol. 9, no. 3, pp. 1237–1244, July 1994.

[62] A.E. Emanuel and L.S. Czarnecki, "Powers components in a system with sinusoidal and non-sinusoidal voltages and/or currents," *IEE Proceeding*, vol. 137, no. 3, pp. 194–196, May 1990.

[63] L.S. Czarnecki, "Comparison of power definitions for circuits with non-sinusoidal waveforms," *IEEE Transactions on Power Delivery*, vol. 5, no. 1, pp. 43–50, January 1990.

[64] L.S. Czarnecki, "Physical reasons of current rms value increase in power systems with non-sinusoidal voltage," *IEEE Transactions on Power Delivery*, vol. 8, no. 1, pp. 437–447, January 1993.

[65] C.I. Budeanu, "Reactive and fictitious powers," in *Romanian National Institute*, 1927, pp. 1–6.

[66] W. Shepherd and P. Zakikhani, "Suggested definitions of reactive power for non-sinusoidal systems," *IEE Proceeding*, vol. 119, no. 9, pp. 1361–1362, September 1972.

[67] L.S. Czarnecki, "Consideration on the reactive power in non-sinusoidal situations," *IEEE Transactions on Instrumentations and Measurement*, vol. 34, no. 3, pp. 399–404, September 1985.

[68] L.S. Czarnecki, "Powers in non-sinusoidal networks: Their interpretation, analysis and measurements," *IEEE Transactions on Instrumentations and Measurement*, vol. 39, no. 2, pp. 340–345, April 1990.

[69] L.S. Czarnecki, "Orthogonal decomposition of the currents in a three-phase non-linear asymmetrical circuits with a non-sinusoidal voltage source," *IEEE Transactions on Instrumentations and Measurement*, vol. 37, no. 1, pp. 30–34, March 1988.

[70] L.S. Czarnecki, "Power related phenomena in three-phase unbalanced systems," *IEEE Transactions on Power Delivery*, vol. 10, no. 3, pp. 1168–1176, July 1995.

[71] D. Sharon, "Reactive power definitions and power factor improvement in non-linear systems," *IEE Proceeding*, vol. 120, pp. 704–706, June 1973.

[72] D. Sharon, "Power factor definition and power transfer quality in non-sinusoidal situations," *IEEE Transactions on Instrumentations and Measurement*, vol. 45, no. 3, pp. 728–733, June 1996.

[73] S. Fryze, "Active, reactive and apparent powers in networks with nonsinusoidal waveforms of voltage and current," in *ETZ Electrotech*, 1932, pp. 596–599.

[74] N.L. Kuster and W.J.M. Moore, "On the definition of reactive power under non-sinusoidal situations," *IEEE Transactions on Power Apparatus and Systems*, vol. PAS-99, no. 3, pp. 1845–1854, September 1980.

[75] C.H. Page, "Reactive power in non-sinusoidal situations," *IEEE Transactions on Instrumentations and Measurement*, vol. 29, no. 2, pp. 420–423, December 1980.

[76] M. Depenbrock, "Active and fictitious power of periodic current in single-phase and poly-phase systems with periodic voltage of any waveshape," in *VDE Verlag*, 1980, pp. 17–59.

[77] L.S. Czarnecki, "What is wrong with the budeanu concept of reactive and distortion power and why it should be abandoned," *IEEE Transactions on Instrumentations and Measurement*, vol. 36, no. 3, pp. 834–837, September 1987.

[78] L.S. Czarnecki, "Some comments on capacitive and residual reactive powers in non-sinusoidal system," in *International Conference on Power System Harmonics*, 1984, pp. 238–243.

[79] L.S. Czarnecki, "Minimization of reactive power under non-sinusoidal conditions," *IEEE Transactions on Instrumentations and Measurement*, vol. 36, no. 1, pp. 18–22, March 1987.

[80] G.T. Heydt, *Electric Power Quality*, Stars in a Circle Publications, West Lafayette, Indiana, 1991.

[81] R.C. Dugan, M.F. McGranaghan, and H.W. Beaty, *Electric Power System Quality*, McGraw-Hill, New York, 1996.

[82] N. Mohan, H. Peterson, W. Long, G. Dreifuerst, and J. Vithayathil, "Active filters for ac harmonic suppression," in *IEEE Winter Power Meeting*, 1980, pp. 1–6.

[83] M. El-Sharkawy, M. Chen, S. Vedari, G. Fissal, and S. Venkata, "Development and field testing of a closed-loop adaptive power factor controller," *IEEE Transactions on Energy Conversion*, vol. 3, no. 2, pp. 235–239, June 1988.

[84] J. Arrillaga, D.A. Bradely, and P.S. Bodger, *Power System Harmonics*, John Wiley & Sons, New York, 1985.

[85] R.F. Chu, J. Wang, and H. chiang, "Strategic planning of lc compensators in nonsinusoidal distribution system," *IEEE Transactions on Power Delivery*, vol. 9, no. 3, pp. 1558–1563, July 1994.

[86] R.T. Saleh and A.E. Emanuel, "Optimum shunt capacitor for power factor correction at buses with lightly distorted voltage," *IEEE Transactions on Power Delivery*, vol. 2, no. 1, pp. 165–173, January 1987.

[87] R.K. Hartana and G.G. Richards, "Comparing capacitive and lc compensators for power factor correction and voltage harmonic reduction," *Electric Power System Research Journal*, vol. 17, pp. 57–64, 1989.

[88] W. Shepherd and P. Zakikhani, "Power factor correction in nonsinusoidal systems by the use of capacitance," *Journal of Physics*, vol. Part-D, pp. 1850–1861, 1973.

[89] G.G. Richards, P. Klinkhachorn, O.T. Tan, and R.K. Hartana, "Optimal lc compensators for non-linear loads with uncertain nonsiusoidal source and load characteristics," *IEEE Transactions on Power Systems*, vol. 4, no. 1, pp. 30–36, February 1989.

[90] A.E. Emanuel, "Suggested definition of reactive power in nonsinusoidal systems," *IEE Proceeding*, vol. 121, no. 7, pp. 705–706, July 1974.

[91] D.F. Tuttle, *Network Synthesis*, John Wiley & Sons, New York, 1958.

[92] W.H. Chen, *Linear Network Design and Synthesis*, McGraw-Hill, New York, 1964.

[93] G.C. Temes and J.W. Lapatra, *Circuit Synthesis and Design*, McGraw-Hill, New York, 1977.

[94] A.E. Emanuel, "Voltage distortion in distribution feeders with non-linear loads," *IEEE Transactions on Power Delivery*, vol. 9, no. 1, pp. 79–87, January 1994.

[95] R.S. Thallam, W.M. Grady, and M.J. Samotyj, "Estimating future harmonic distortion levels in distribution systems due to single-phase adjustable speed drive air-conditioners: A case study," in *International Conference on Power System Harmonics*, 1992, pp. 65–70.

[96] R.S. Wallace, "The harmonic impact of variable speed air-conditioners on residential power distribution," in *Proceedings of* 7th *annual Applied Power Electronic Conference*, 1992, pp. 23–27.

[97] V. Sharama, R.J. Fleming, and L. Niekamp, "An iterative approach for analysis of harmonic penetration in the power transmission networks," *IEEE Transactions on Power Delivery*, vol. 6, no. 4, pp. 1698–1706, October 1991.

[98] D.J. Pillegi, N.H. Chandra, and A. E. Emanuel, "Prediction of harmonic voltages in distribution systems," *IEEE Transactions on Power Apparatus and Systems*, vol. PAS-100, no. 59, pp. 1307–1315, March 1981.

[99] W.M. Grady and G.T. Heydt, "Prediction of power system harmonics due to gaseous discharge lighting," *IEEE Transactions on Power Apparatus and Systems*, vol. PAS-104, no. 4, pp. 554–561, March 1985.

[100] W. Xu, J.R. Marti, and H.W. Dommel, "A multiphase harmonic load flow solution technique," *IEEE Transactions on Power Systems*, vol. 6, no. 1, pp. 174–182, February 1991.

[101] E.F. El-Saadany and M.M.A. Salama, "Effect of interactions between voltage and current harmonics on the net harmonic current produced by single-phase non-linear loads," *Electric Power System Research Journal*, vol. 40, pp. 155–160, 1997.

[102] E.F. El-Saadany, M.M.A. Salama, and A.Y. Chikhani, "Investigation of system parameters affecting the harmonic distortion levels in distribution systems loaded with non-linear loads," in 29th *North American Power Symposium (NAPS'97)*, October, 1997, pp. 121–128.

[103] P. Crnosija, "Determination of voltage distortion factor for a network loaded with several dc motor drives," *IEE Proceeding*, vol. 131, no. 3, pp. 81–84, May 1984.

[104] A. Liew, "Excessive neutral currents in three-phase fluorescent lighting circuits," *IEEE Transactions on Industry Applications*, vol. 25, no. 4, pp. 776–782, August 1989.

[105] A.E. Emanuel, J. Janczak, D.J. Pileggi, E.M. Gulachenski, M. Breen, T.J. Gentile, and D. Sorensen, "Distribution feeders with non-linear loads in the northeast u.s.a: Part1- voltage distortion forecast," *IEEE Transactions on Power Delivery*, vol. 10, no. 1, pp. 340–347, January 1995.

[106] E.F. El-Saadany and M.M.A. Salama, "Reduction of the net harmonic current produced by single-phase non-linear loads due to attenuation and diversity," *International Journal of Electrical Power and Energy Systems*, 1998, currently in press.

[107] T.M. Gruzs, "A survay of neutral currents in three-phase computer power systems," *IEEE Transactions on Industry Applications*, vol. 26, no. 4, pp. 719–725, August 1990.

[108] United States Department of Agriculture, *Effect of Electric Voltage/Current on Farm Animals*, Washington D.C., 1990, United States Department of Agriculture Handbook #696.

[109] T.S. Key and J.S. Lai, "Comparison of standards and power supply design options for limiting harmonic distortion," *IEEE Transactions on Industry Applications*, vol. 29, no. 3, pp. 688–695, August 1993.

[110] T. Key and J.S. Lai, "Cost and benefits of harmonic current reduction for switch-mode power supplies in commercial building," in *IEEE-IAS Annual Meeting*, October, 1995, pp. 1101–1108.

[111] H. Akagi, A. Nabae, and S. Atoh, "Control strategy of active power filters using multiple-voltage source pwm converters," *IEEE Transactions on Industry Applications*, vol. 20, no. 2, pp. 460–265, May 1986.

[112] J. Nastran, R. Cajhen, M. Seliger, and P. Jereb, "Active power filters for non-linear ac loads," *IEEE Transactions on Power Electronics*, vol. 9, no. 1, pp. 92–96, January 1994.

[113] T.H. Ortmeyer and K. Zehar, "Distribution system harmonic design," *IEEE Transactions on Power Delivery*, vol. 6, no. 1, pp. 289–294, January 1991.

[114] Y. Baghzouz, "Effect of non-linear loads on optimal capacitor placement in radial feeders," *IEEE Transactions on Power Delivery*, vol. 6, no. 1, pp. 245–251, January 1991.

[115] E.F. El-Saadany, M.M.A. Salama, and A.Y. Chikhani, "Comparing reactance one-port and notch filters for voltage and current harmonic reduction in non-linear distribution systems," in *IEEE Canadian Conference on Electrical and Computer Engineering (CCECE'98)*, May, 1998.

[116] G.D. et al, "Hvdc-ac harmonic interaction: Part ii-ac system harmonic model with comparison of calculated and measured data," *IEEE Transactions on Power Apparatus and Systems*, vol. PAS-101, no. 3, pp. 709–718, March 1982.

[117] A. deOliveira, J.C. deOliveira, J.W. Resende, and M.S. Miskulin, "Practical approaches for ac system harmonic impedance measurement," *IEEE Transactions on Power Delivery*, vol. 6, no. 4, pp. 1721–1726, October 1991.

[118] T.H. Ortmeyer, M.S.A.A. Hammam, T. Hiyama, and D.B. Webb, "Measurement of the harmonic characteristics of radial distribution systems," *IEE Proceeding*, vol. 2, no. 3, pp. 163–172, May 1988.

[119] T. Hiyama, M.S.A.A. Hammam, and T.H. Ortmeyer, "Distribution system modeling with distributed harmonic sources," *IEEE Transactions on Power Delivery*, vol. 4, no. 2, pp. 1297–1304, April 1989.

[120] M. Etezadi-Amoli and T. Florence, "Voltage and current harmonic content of a utility system: A summary of 1120 test measurements," *IEEE Transactions on Power Delivery*, vol. 5, no. 3, pp. 1552–1557, July 1990.

[121] S.N. Govindarajan, M.D. Cox, and F.C. Berry, "Survay of harmonic levels on the southwestern electric power company system," *IEEE Transactions on Power Delivery*, vol. 6, no. 4, pp. 1869–1875, October 1991.

[122] A.E. Emanuel, J.A. Orr, D. Cyganski, and E.M. Gulachenski, "A survay of harmonic voltages and currents at distribution substations," *IEEE Transactions on Power Delivery*, vol. 6, no. 4, pp. 1883–1890, October 1991.

[123] A.E. Emanuel, J.A orr, D. Cyganski, and E.M. Gulachenski, "A survay of harmonic voltages and currents at the customer's bus," *IEEE Transactions on Power Delivery*, vol. 8, no. 1, pp. 411–421, January 1993.

[124] E.F. El-Saadany, M.M.A. Salama, and A.Y. Chikhani, "Minimization of harmonic current produced by single-phase non-linear loads using passive filters," in 59th *American Power Conference (APC'97)*, April, 1997, pp. 475–480.

[125] E.F. El-Saadany, M.M.A. Salama, and A.Y. Chikhani, "Passive filter design for harmonic reactive power compensation in single-phase circuits supplying non-linear loads," *IEEE Transactions on Power Delivery*, 1998, under review.

[126] E.F. El-Saadany, M.M.A. Salama, and A.Y. Chikhani, "New passive filter design for neutral current cancelation in balanced three-phase four-wire distribution systems with non-linear loads," *Electric Power System Research Journal*, 1998, under review.

[127] E.F. El-Saadany, M.M.A. Salama, and A.Y. Chikhani, "Reduction of voltage and current distortion in distribution systems with non-linear loads using hybrid passive filters," *IEE Journal, Generation, Transmission and Distribution*, 1998, currently in press.

IMAGE EVALUATION TEST TARGET (QA-3)

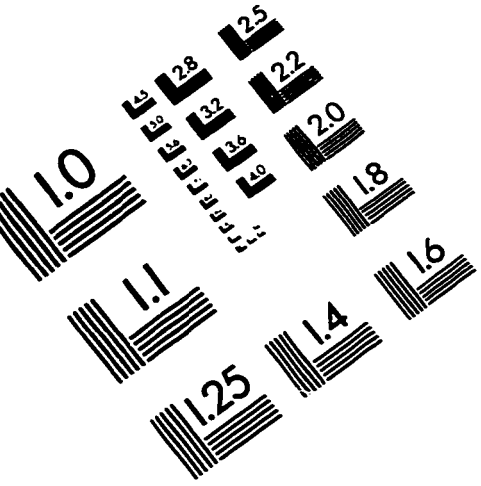

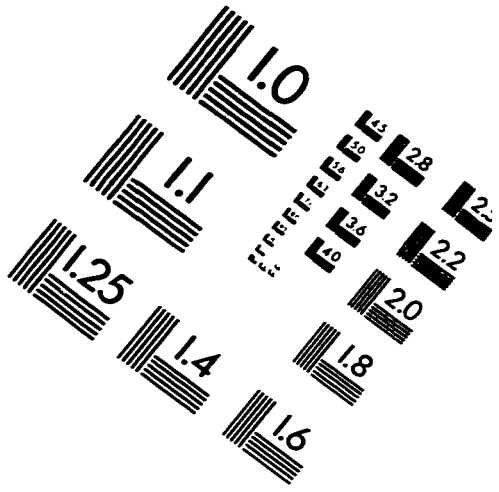

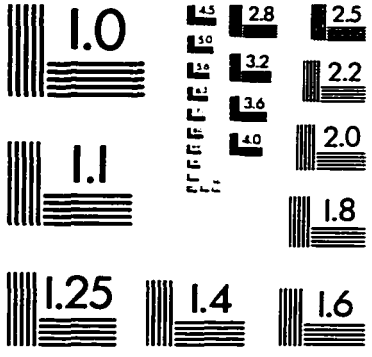

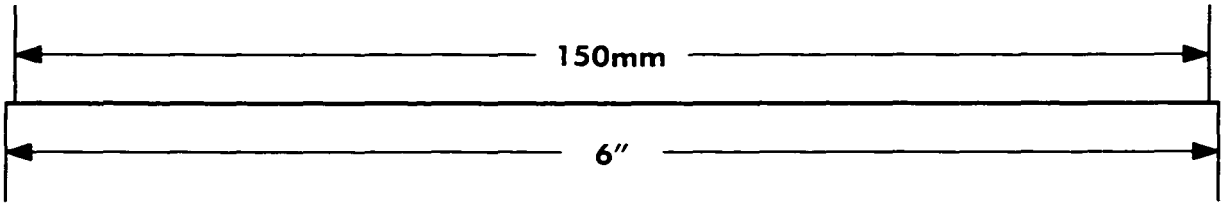

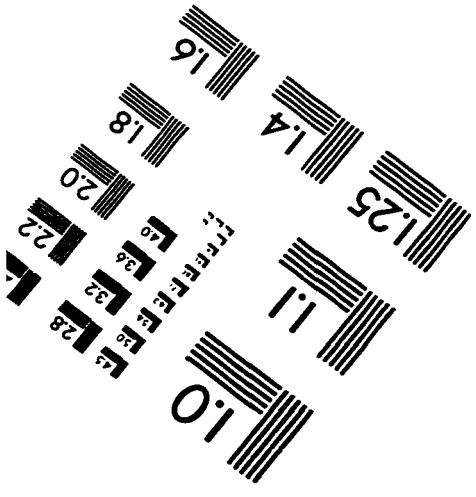

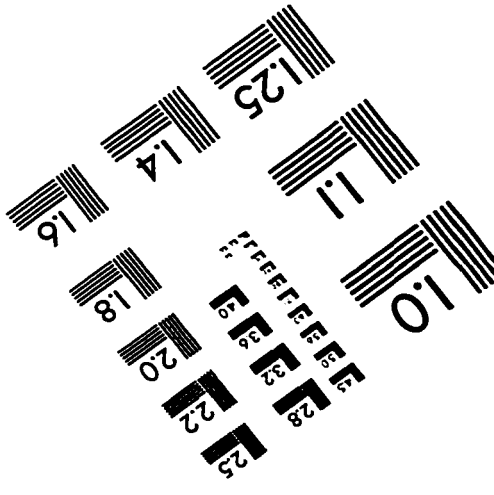

APPLIED IMAGE, Inc
1653 East Main Street
Rochester, NY 14609 USA
Phone: 716/482-0300
Fax: 716/288-5989

© 1993, Applied Image, Inc., All Rights Reserved